INFORMATION TO USERS

This dissertation was produced from a microfilm copy of the original document. While the most advanced technological means to photograph and reproduce this document have been used, the quality is heavily dependent upon the quality of the original submitted.

The following explanation of techniques is provided to help you understand markings or patterns which may appear on this reproduction.

1. The sign or "target" for pages apparently lacking from the document photographed is "Missing Page(s)". If it was possible to obtain the missing page(s) or section, they are spliced into the film along with adjacent pages. This may have necessitated cutting thru an image and duplicating adjacent pages to insure you complete continuity.

2. When an image on the film is obliterated with a large round black mark, it is an indication that the photographer suspected that the copy may have moved during exposure and thus cause a blurred image. You will find a good image of the page in the adjacent frame.

3. When a map, drawing or chart, etc., was part of the material being photographed the photographer followed a definite method in "sectioning" the material. It is customary to begin photoing at the upper left hand corner of a large sheet and to continue photoing from left to right in equal sections with a small overlap. If necessary, sectioning is continued again — beginning below the first row and continuing on until complete.

4. The majority of users indicate that the textual content is of greatest value, however, a somewhat higher quality reproduction could be made from "photographs" if essential to the understanding of the dissertation. Silver prints of "photographs" may be ordered at additional charge by writing the Order Department, giving the catalog number, title, author and specific pages you wish reproduced.

University Microfilms

300 North Zeeb Road
Ann Arbor, Michigan 48106

A Xerox Education Company

Downloaded from SHAREOK. Persistent Handle URL: https://hdl.handle.net/11244/3283

72-22,442

LAKE, Jerome Glen, 1932-
ON THE PROPAGATION OF AN INITIAL SPHERICAL DENSITY DISCONTINUITY IN A RAREFIED MEDIUM.

The University of Oklahoma, Ph.D., 1972
Aerospace Studies

University Microfilms, A XEROX Company, Ann Arbor, Michigan

THIS DISSERTATION HAS BEEN MICROFILMED EXACTLY AS RECEIVED.

THE UNIVERSITY OF OKLAHOMA

GRADUATE COLLEGE

ON THE PROPAGATION OF AN INITIAL SPHERICAL DENSITY DISCONTINUITY IN A RAREFIED MEDIUM

A DISSERTATION

SUBMITTED TO THE GRADUATE FACULTY

in partial fulfillment of the requirements for the

degree of

DOCTOR OF PHILOSOPHY

BY

JEROME GLEN LAKE

Norman, Oklahoma

1972

ON THE PROPAGATION OF AN INITIAL SPHERICAL

DENSITY DISCONTINUITY IN A RAREFIED MEDIUM

APPROVED BY

Maurice Rasmussen

Martin C. Jischke

Edward J. Blick

Daryl L. Harden

William N. Hugo

DISSERTATION COMMITTEE

PLEASE NOTE:

Some pages may have

indistinct print.

Filmed as received.

University Microfilms, A Xerox Education Company

ACKNOWLEDGEMENTS

This work was accomplished during a tour of duty with the Air Force Institute of Technology Civilian Institutions Program at the University of Oklahoma. Thanks are due to those who have made this program possible.

I am indeed grateful for the assistance of my advisory committee, especially the chairman Dr. Maurice Rasmussen. Without Dr. Rasmussen's patience, efforts, and suggestions as well as his encouragement and inspiration this work could not have been completed. The time and effort of Dr. Martin Jischke, Dr. Edward Blick, Dr. Darrel Harden, and Dr. William Huff are sincerely appreciated. Also my thanks are extended to Dr. Raymond Kaser who served on my committee prior to his sabbatical leave.

Above all I recognize and give humble thanks for the guidance and strength given to me by my Lord, Jesus Christ.

This work is dedicated to my wife, Claudette, and my children, Judy, Jay, and Chip, who provided their own special contribution.

ABSTRACT

The subject of spherical expansions has been of interest for over a century but remains of continuing concern, for the most part, in that an exact solution to the expansion of a uniform sphere of gas into another gas as a result of a density differential has not been obtained. This work presents several approximate solutions for spherical explosions and implosions into a rarefied gas. Two limiting cases are analyzed by means of two different theories of gas dynamics.

The kinetic theory of gases is used to find large Knudsen-number solutions. Further knowledge of multi-species kinetic theory is obtained by examining the effects when different species are inside and outside the sphere for a sphere initially at rest. The effects of diffusion and other transport properties are discussed. For a simplified case with both gases identical except for an initial density difference, the embryonic formation of a spherical shock wave is examined. The collisionless solutions are compared with solutions obtained from inviscid-acoustic theory. Also for large Knudsen-numbers a solution of the Boltzmann equation is formulated in order to obtain first-order collision effects.

For the limit of small knudsen numbers the problem is examined by means of a viscous acoustic solution from the linearization of the Navier-Stokes equations about a uniform ambient medium obtained by Laplace-transform techniques. Both short-time and long-time solutions are presented.

TABLE OF CONTENTS

		Page
ACKNOWLEDGMENTS		iii
ABSTRACT		iv
LIST OF ILLUSTRATIONS		vii
NOMENCLATURE		x
Chapter		
I.	INTRODUCTION	1
II.	THEORETICAL CONCEPTS	8
	Theory of Gases	8
	Kinetic Theory	10
	Statistical Concepts	11
	Flow Field Properties	14
	The Kinetic Equation	15
III.	EXPANSIONS FOR LARGE KNUDSEN NUMBERS	18
	Solution to the Collisionless Kinetic Equation	18
	Macroscopic Flow-Field Properties	20
	A Sample Calculation	24
	Behavior of Flow-Field Properties	28
	Transport Properties	39
	Non-Equilibrium Indicator	46
IV.	EMBRYONIC SPHERICAL SHOCK WAVE DEVELOPMENT	51
	Basis for Analysis	51
	Three-Dimensional Results	56
	Spherical Shock Analysis	57
	Inviscid Acoustics for Spherical Explosions	59
	Strong Explosions	64
	Strong Implosions	66
	H-Function and Entropy	67
V..	NEARLY FREE MOLECULE FLOW EXPANSIONS	70

TABLE OF CONTENTS (Cont'd.)

VI. EXPANSIONS FOR SMALL KNUDSEN NUMBERS. 78

The Viscous Acoustic Equation 79
The Laplace-Transform Solution. 81
Analytical Short-Time Solutions 85
The Long-Time Solution. 89

VII. CONCLUDING REMARKS. 92

REFERENCES. 95

OTHER SOURCES 96

APPENDICES

A. BASIC INTEGRAL RELATIONS. 98

B. ASYMPTOTIC VALUES OF FLOW-FIELD PROPERTIES. 101

C. ANALYTICAL EVALUATION OF $(\vec{g}\cdot\vec{e})\vec{e}$ 108

D. DERIVATION OF THE VISCOUS ACOUSTIC RELATIONS. . . . 111

LIST OF ILLUSTRATIONS

Figure		Page
1-1.	Initial Spherical Distribution.	1
3-1.	Spherical Coordinate System in Velocity Space	26
3-2.	Translated Spherical Coordinate System in Velocity Space.	27
3-3.	Case 1 Free-Molecule Variables for $\Delta = 0.1$ at $\tau_1 = 0.2$.	30
3-4.	Case 1 Free-Molecule Variables for $\Delta = 0.1$ at $\tau_1 = 1.0$.	30
3-5.	Case 1 Free-Molecule Variables for $\Delta = 10$ at $\tau_1 = 0.2$.	32
3-6.	Case 2 Density for $\Delta = 0.1$, $m_1/m_2 = 0.069$, and $\tau_1 = 0.2$	34
3-7.	Case 2 Velocity for $\Delta = 0.1$, $m_1/m_2 = 0.069$, and $\tau_1 = 0.2$	34
3-8.	Case 2 Temperature for $\Delta = 0.1$, $m_1/m_2 = 0.069$ and $\tau_1 = 0.2$	34
3-9.	Case 2 Heat Flux for $\Delta = 0.1$, $m_1/m_2 = 0.069$, and $\tau_1 = 0.2$	34
3-10.	Case 2 Radial Stress for $\Delta = 0.1$, $m_1/m_2 = 0.069$, and $\tau_1 = 0.2$	35
3-11.	Case 2 Angular Stresses for $\Delta = 0.1$, $m_1/m_2 = 0.069$, and $\tau_1 = 0.2$.	35
3-12.	Free-Molecule Variables for a Pressure Difference with $\Delta = 1.0$, $m_1/m_2 = 0.069$, and $T_{11}/T_{22} = 1.0$ at $\tau_1 = 0.2$	38
3-13.	Free-Molecule Variables for a Pressure Difference with $\Delta = 1.0$, $m_1/m_2 = 1.0$, and $T_{11}/T_{22} = 10.0$ at $\tau_1 = 0.2$	38
3-14.	Non-Equilibrium Indicator for $\Delta = 0.1$ at $\tau_1 = 0.2$ . . .	49

LIST OF ILLUSTRATIONS (Cont'd.)

4-1. Macroscopic Shock-Tube Phenomena in the x-t Diagram . . 53

4-2. Shock-Tube Density Profile for $\Delta^{-1} = 10$. 54

4-3. Shock-Tube Pressure Profile for $\Delta^{-1} = 10$. 54

4-4. Shock-Tube Temperature Profile for $\Delta^{-1} = 10$ 55

4-5. Shock-Tube Velocity Profile for $\Delta^{-1} = 10$. 55

4-6. Macroscopic Spherical Shock Phenomena in the r-t Diagram. 58

4-7. Regions of the Inviscid Acoustic Solution 62

4-8. Comparison of Kinetic and Acoustic Number Densities for $\Delta = 0.6$ and $\tau = 0.1$. 63

4-9. Comparison of Kinetic and Acoustic Velocities for $\Delta = 0.6$ and $\tau = 0.1$. 63

4-10. Comparison of Kinetic and Acoustic Temperature for $\Delta = 0.6$ and $\tau = 0.1$. 64

4-11. Comparison of Velocities for Strong Exploxions and Expansion into a Vacuum for $\tau = 0.05$ 65

4-12. Comparison of Temperatures for Strong Explosion and Expansion into a Vacuum for $\tau = 0.05$ 65

4-13. Velocity for a Strong Implosion with $\Delta = 10$ at $\tau = 0.05$ 66

4-14. Temperature for a Strong Implosion with $\Delta = 10$ at $\tau = 0.05$ 66

4-15. Non-Equilibrium Indicator for $\Delta = 10^{-5}$ and $\tau = 0.05$ . . 68

4-16. H-Function and Entropy Function for Free-Molecule Flow, $\Delta = 10^{-5}$, $\Delta = 0$, and $\tau = 0.05$. 68

5-1. Collision Plane 71

5-2. Orientation of Collision Plane. 71

5-3. Graphic Interpretation of Collisional Distribution Function 73

LIST OF ILLUSTRATIONS (Cont'd.)

6-1. Short-Time Density Profiles 88

6-2. Short-Time Velocity Profiles. 88

6-3. Short-Time Temperature Profiles 88

6-4. Long-Time Viscous Acoustic Temperature Profiles for Varying Reynolds Number. 90

6-5. Long-Time Viscous Acoustic Density Profiles for Varying Reynolds Number. 90

B-1. Minimum Temperature at R = 0 as a Function of the Initial Density Ratio. 106

B-2. The Time for the Minimum Temperature to Occur at R = 0 as a Function of the Initial Density Ratio 106

B-3. Temperature Profiles for $\Delta = 0.1$ and Increasing Times . 107

NOMENCLATURE

a	initial radius of given sphere of gas
a_o	isentropic speed of sound
b	impact parameter
C_p	specific heat at constant pressure
C_v	specific heat at constant volume
$\vec{c}$	peculiar velocity
e	specific internal energy of system $[\frac{3}{2}\ kT/m]$
$\hat{e}_j$	unit vector in j direction
$\hat{e}$	apse vector
F	collision interaction force law
f	molecular velocity distribution function
f_o	initial Maxwellian distribution function
$f^{(m)}$	mth order approximation of f
$\vec{g}$	relative velocity vector
$H(z)$	Heaviside unit step function
H	Boltzmann H-Function
$\bar{H}$	normalized Boltzmann H-Function
$J(\ )$	collision operator
J_{mn}	collision operator which denotes the net change of species m due to collisions with species n
K	conductivity coefficient; force constant (Chapter V)
Kn	Knudsen number

k	Boltzmann constant
L	characteristic length
$\vec{L}$	angular momentum vector
m	mass
N	non-dimensional number density
n	number density
n_{ii}	initial number density inside sphere, i = 1, or outside the sphere, i = 2
$n^{(m)}$	mth order approximation of number density
P	non-dimensional pressure
Pr	Prandtl number
p	pressure
p_{ii}	initial pressure inside sphere, i = 1, or outside sphere, i = 2
Q	non-dimensional radial heat flux
$\vec{q}$	heat-flux vector
R	non-dimensional radius
Rey	Reynolds number
$\vec{r}$	radius vector
$\vec{r}_o$	integration constant
r^*	distance between centers of molecules
S_o	non-dimensional entropy
S_{jj}	non-dimensional stress tensor component
s	entropy; Laplace transform variable (Chapter VI)
T	temperature
$\bar{T}$	non-dimensional temperature

T_{ii} initial temperature inside sphere, i = 1, or outside sphere, i = 2

t time

$\vec{U}_i$ non-dimensional diffusion velocity for ith species

$\vec{u}$ mass velocity

u radial velocity component

V non-dimensional radial velocity

x cartesian coordinate (Chapter IV)

α spherical coordinate in velocity space

$\beta^{-\frac{1}{2}}$ initial mean thermal speed of a molecule $[(\frac{2kT}{m})^{\frac{1}{2}}]$

γ ratio of specific heats

Δ initial density ratio

δ $(1-\Delta)/\Delta$

δ_{jk} delta function

$\bar{\varepsilon}$ positive constant that may be chosen as near zero as desired

$\vec{\vec{\varepsilon}}$ rate of strain tensor

ε angle between the collision plane and an arbitrary plane

$\vec{\xi}_o$ constant of integration

$\vec{\xi}$ molecule velocity (species implied by functional notation in a given equation)

ξ_j molecular velocity component

θ a spherical coordinate

λ average mean free path

μ viscosity coefficient

$\tilde{\mu}$ effective viscosity coefficient

ρ_{ii} initial density inside sphere, i = 1, or outside sphere, i = 2

$\bar{\rho}$ non-dimensional density

ρ density function

$\overleftrightarrow{\sigma}$ stress tensor

σ_{jk} stress tensor component

τ_{jk} viscous stress tensor component

τ non-dimensional time $[\frac{T}{a\beta^{\frac{1}{2}}}]$

τ_c non-dimensional time $[a_o \frac{t}{a}]$

Φ molecular property

ϕ spherical coordinate in velocity space, velocity potential

χ deflection angle

ψ spherical coordinate

ON THE PROPAGATION OF AN INITIAL SPHERICAL DENSITY DISCONTINUITY IN A RAREFIED MEDIUM

CHAPTER I

INTRODUCTION

This work is concerned with the propagation of an initial spherical density discontinuity in a rarefied medium. This problem contains both theoretical and practical implications pertaining to explosions and implosions in the atmosphere. It also pertains to certain problems of developing stars in intersteller space.

Conceptually we consider a physical model of a gas uniformly distributed inside an impermeable thin spherical shell of radius $r = a$ as illustrated in Figure 1-1. The gas with molecules of mass m_1 inside the sphere is in equilibrium at mass density ρ_{11}, pressure p_{11},

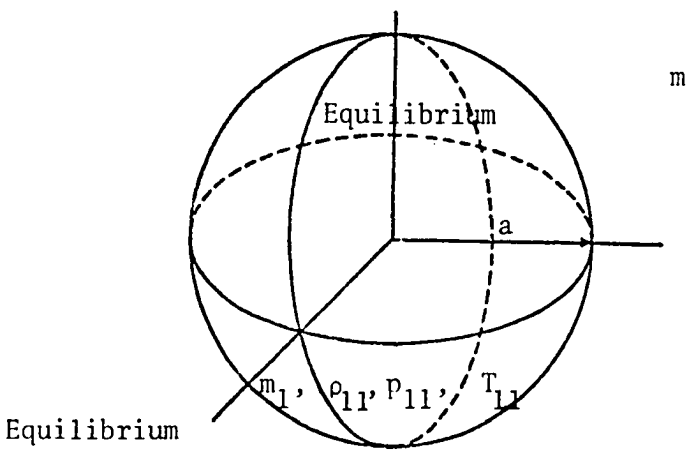


Figure 1-1. Initial Spherical Distribution

and temperature T_{11}. Outside the sphere the gas with molecules of mass m_2 is in equilibrium at ρ_{22}, p_{22}, and T_{22}. At time $t = 0$ the bounding sphere instantaneously vanishes and we are interested in describing the resulting flow field. External surfaces are assumed to play no significant part in this spherical problem.

If we consider the spherical case with $T_{11} = T_{22}$ and both gases the same, this problem is akin to the one-dimensional (shock tube) problem studied by Bienkowski (1965) and Yates and Karamcheti (1967). The spherical problem, however, has at least four aspects that make it different from and more interesting than the one-dimensional problem:

(1) The spherical problem is three-dimensional. This aspect makes the problem more useful from a practical point of view. In addition, three-dimensional problems have not been as thoroughly investigated as one-dimensional problems.

(2) The three-dimensional problem is not self-similar as is the one-dimensional problem. This makes the spherical problem more complicated to analyze, but at the same time introduces new features into the problem. For instance, the spherical problem has two characteristic lengths instead of the one present in the one-dimensional problem. The first is the initial radius of the sphere, $L = a$. The second characteristic length is the average distance a molecule travels, before undergoing a collision, after the diaphragm is removed, or $L = \beta_1^{-\frac{1}{2}}t$, where $\beta_1^{-\frac{1}{2}}$ is the initial mean thermal speed of the molecules inside the sphere. The rarefied kinetic problem is concerned with the limit of large Knudsen numbers, $Kn = \lambda/L \to \infty$, where λ is the average mean

free path of the molecules. The spherical kinetic problem, therefore, is concerned with sufficiently small sphere radii or sufficiently small times, whereas the one-dimensional problem is concerned only with sufficiently small times, that is with the embryonic development of shock tube flow.

(3) The spherical problem contains both explosions and implosions. Thus a new physical feature is involved.

(4) Another phenomenon present in the spherical problem but not in the one-dimensional problem is the secondary shock. This feature was studied by Friedman (1961) for the continuum limit, $Kn \to 0$.

For the given spherical model the effects of differing gases at differing temperatures can be examined. Other items of interest which can be investigated are the transport properties for collisionless flow.

Although such a generalized study of the spherical expansion problem has not been made, the treatment of spherical expansions has been the subject of many papers during the past century. Some of the earlier works considered the spherical propagation of sound waves. Such research was conducted by such well known fluid dynamicists as Lamb (1910) and Rayleigh (1896). Keller (1956) provided one of the first mathematical analysis of spherical gas flows utilizing Lagrangian variables.

With the advent of nuclear weapons and high yield conventional warheads there has been increased interest in the past fifteen years in spherical blast waves. The Russians, particularly Sedov (1957) and Stanukovich (1960), and Americans, such as Friedman (1961),

have done considerable work on spherical explosions in a continuum, obtaining various approximate solutions. An exact solution of the governing continuum regime equations for the spherical problem, whether we consider the Navier-Stokes equations or the Euler equations, is not in the literature. The non-linear, unsteady nature of the problem makes it an extremely difficult problem to solve.

Historically kinetic theory has been used to describe the collision dominated continuum regime as a limiting case by letting the Knudsen number go to zero. It would be natural to expect that we might find the continuum solution to the spherical explosion problem by this approach. The governing kinetic equation, however, is an integro-differential equation which is more difficult to solve than the continuum equations themselves. We find then that to obtain satisfactory solutions to the spherical problem one must make appropriate assumptions and rely on approximate analytical methods.

For the major part of this research effort we assume that we have a large Knudsen-number flow which allows us to obtain free-molecule solutions from the collisionless kinetic equation. A great deal of work has been done applying kinetic theory to continuum limit problems; very little on the other hand has been done with the free-molecule limit. Such topics as the Boltzmann H-Function and the transport properties have been limited to discussions involving collisions. This study examines these topics from the free-molecule flow notion. Also all the macroscopic moments of interest, including stresses and heat-flux are obtained by this approach. Density and velocity results have

been obtained previously, Molmud (1960) and Narashima (1962), but only for the special case of expansion into a vacuum.

In order to obtain a continuum-limit solution an approximate analytical approach is examined. The linearized Navier-Stokes equations are solved by means of Laplace-transform techniques. A short-time solution for the density, velocity, and temperature is obtained and its validity discussed.

In Chapter II a theoretical development of the theory of gases that governs the resulting flow field of a spherical expansion is given. The microscopic movement of the molecules is examined so as to better understand what occurs during the expansion. The place of kinetic theory in the theory of gas dynamics and the associated governing equations are discussed. To better understand what is meant by a mean value of a flow field variable a brief discussion of probability is included. From the theory of probability the molecular velocity distribution function is defined. The expected or mean values of the flow quantities follow from the distribution function which is obtained by solving the governing mathematical model, the kinetic equation.

In Chapter III the large Knudsen-number flow assumption based on small sphere radius and large mean free paths is applied. The general expansion problem is discussed with differing gases and differing temperatures. The free-molecule flow solutions are obtained from the collisionless kinetic equation. Free-molecule transport properties are found and compared with the familiar linear transport relations of continuum theory. A new indicator is introduced, the

non-equilibrium indicator, which is the absolute difference between the Boltzmann H-Function computed for free-molecule flow and the thermodynamic entropy, a continuum notion. This indicator provides a measure of the departure from equilibrium for the various types of spherical expansions considered in this work.

Chapter IV utilizes the characteristic length based on short time to establish the validity of the free-molecule flow solutions in the vicinity of the discontinuity. In the one-dimensional problem the exact Euler solution is available for comparison with the free-molecule results. An exact Euler solution is not available or easily obtained for the spherical expansion problem. For the purposes of qualitative comparison and for a basic understanding of the inviscid problem, a satisfactory approximate solution is easily obtained. This solution, the inviscid acoustic approximation, yields results which are compared with the free-molecule spherical expansion results. An interesting aspect of the problem that prevails for near vacuum conditions outside the sphere is presented. In the continuum limit the flow is isentropic when $\Delta = \rho_{22}/\rho_{11} = 0$ (vacuum) but involves a shock when $\Delta \neq 0$ no matter how small Δ is. The small time solutions in the large Knudsen-number limit are used to analyze embryonic shock structure.

Chapters V and VI present attempts at solving the collisional problem. In Chapter V the nearly free-molecule flow problem is discussed and its solution outlined. This is an attempt to obtain the first-order collisional effects by means of the full Boltzmann equation with external forces neglected. In Chapter VI the problem is examined by means

of the linearized Navier-Stokes equations. This solution is appropriate for the other end of the gas-dynamic spectrum, small Knudsen numbers.

CHAPTER II

THEORETICAL CONCEPTS

The Theory of Gases

It is of interest and basic to a more thorough understanding of the spherical expansion problem to examine the theory of gases as it relates to the expansion problem. The physical problem as posed in Chapter I is not restricted as to its number density, that is, how many molecules are in a given volume. Therefore, the physical model is applicable for a highly rarefied gas such as found 80 miles above the earth's surface as well as a denser gas such as that we breath. Also the choice of gas-dynamic theories ranges from the microscopic to the macroscopic.

By examining the motion of the molecules during a spherical expansion we can better appreciate the role of kinetic theory as it pertains to our problem. It is difficult, however, to imagine in our mind what is going on as far as each molecule is concerned during a spherical expansion. In order to simplify this, consider a billiards table which reduces the problem to a two-dimensional one. The cushions of the table are considered to be the walls of the container and the billiard balls the molecules. Since the container is assumed to have impermeable walls, we will assume that there are no pockets in our table. To idealize this model we will further assume that once the

balls on the table are set into motion it is a long time before friction and other passive forces destroy the motion.

Consider first that we have many balls on the table and impart a completely random motion to the balls initially. We will observe numerous collisions among the balls, sometimes several balls colliding together at one time. This special case would represent a dense gas.

A dilute gas would be modeled by reducing the number of balls such that when the balls are set into motion collisions involve only two balls at one time, or that only bi-molecular collisions occur. For the mathematical model used in this study, when collisions are involved, we assume such a gas. As we further reduce the number of balls on each successive trial we would observe that although there are still a significant number of balls on the table that they do not collide with one another but only with the cushions of the table. This would represent our major regime of interest, the large Knudsen-number regime.

To complete the two-dimensional model of the spherical expansion problem we further assume the billiards table under consideration is superimposed on an infinite table. The balls on the billiards table are all red and those on the infinite table are all white. All the balls are in random motion. The cushions of the billiards table are instantaneously removed at $t = 0$. We observe that the red balls now penetrate into the white ball area and the white balls penetrate into the red ball area. The mixing of the two kinds of colored balls is a diffusion phenomenon.

Another phenomenon that would be observed is that the velocities of the balls vary as collisions occur in the dilute gas case.

At one instant a ball may be brought completely to rest, while at another instant it will have a speed much in excess of the average speed of the various balls. For the collisionless case the variation in the velocity of the balls for a given region varies owing to the influx and efflux of balls with differing velocities. One of the problems we are faced with in describing the motion of a gas is finding how the velocities of the various molecules (balls) in a given space are distributed about the mean velocity.

Although the real problem has many complexities not covered by this simplified explanation it gives insight into the problem at hand. We will show that the key to the solution of the spherical expansion problem is the unknown function that describes the molecular velocity distribution. The flow quantities we shall present are diffusive in nature, that is, there are no discontinuities after $t = 0$.

Kinetic Theory

Now let us examine how kinetic theory fits into the various gas-dynamic theories. As previously pointed out, two general approaches for looking at spherical expansions are the macroscopic and the microscopic. Some theorists, e.g. Krook (1959), advance the concept that kinetic theory encompases the complete microscopic approach. Liboff (1969), on the other hand, looks upon kinetic theory as occupying middle ground between the macroscopic and microscopic approaches. Liboff's approach gives a clearer concept of the role of kinetic theory with respect to the following development of the kinetic equation.

The most precise study of gas flows is by the microscopic approach where we keep track of each molecule (billiards ball) as it

travels about, a formidable task to say the least since even at an altitude of 300 kilometers there are on the order of 10^9 molecules per cubic centimeter. This is compared to the order 10^{19} in the gas we breath. The microscopic approach can thus be considered as an n-body problem where n is a very big number. On the other hand, the macroscopic approach is less precise. It represents flow properties as an average over a certain volume, or area, or interval of time. The macroscopic approach describes the motion of all the molecules in the region of interest, not the individual molecules themselves.

The n-body problem is governed by the Liouville equation and the macroscopic problem by the familiar continuum conservation equations. The kinetic problem is governed by the so-called kinetic equation which has different names depending on the collision model used, the most famous being the Boltzmann equation.

The kinetic equation can be derived in a straightforward manner, e.g. Boltzmann (1964), or it can be obtained by starting with the Liouville equation and expanding a small subset of statistical mechanics theory. For a comprehensive study of various derivations starting with the Liouville equation see Liboff (1969).

From the kinetic equation we find the one-particle molecular velocity distribution function (one for each species present) which allows the calculation of the flow quantities such as mass density, pressure, mass velocity and temperature in a statistical sense.

Statistical Concepts

To understand what we mean by "statistical sense" a brief review of some concepts of probability are in order. The easiest example

to understand is that of tossing a coin and asking what the probability is of getting, say, a head. It is well known that the probability is one-half, but it is not as well known how this value is obtained.

First we must know that the probability of getting a certain event is between zero and unity. Experimentally the probability is obtained by conducting an experiment (flipping a coin) a large number of times and recording the outcomes (the number of times tails or heads appear). Doing this with the coin we find that there are two possible outcomes each with equal probability whose sum is unity. Most experiments have more than two outcomes, in fact, for a flow field property such as velocity the number of possible outcomes is infinite. We also find that the probability that any one velocity will be measured in an experiment is zero! This is true since with the coin we speak of discrete outcomes when we talk of getting a head or tail, but since velocity is a continuous function (at least for our collisionless problem) we can not speak of only one value. Instead of asking what the probability is of measuring a certain velocity we talk of the probability that the velocity measured in a spherical expansion will fall in a certain range, where the range is arbitrary. To describe this situation we must define a probability density function, $P(x)$, such that the sum (integral summation) is equal to unity. We write this as

$$\int_{-\infty}^{\infty} P(x)dx = 1 \quad . \tag{2.1}$$

In kinetic theory the molecular velocity distribution function is related to the probability density function defined above.

Designating $f(\vec{r},\vec{\xi},t)$ as the molecular velocity distribution function we can write the probable number of molecules in a small volume about a vector $\vec{r}$ with a velocity near $\vec{\xi}$ at time t by $fd\vec{r}d\vec{\xi}$. The number of molecules in a small volume about $\vec{r}$ irrespective of velocity is then

$$\int_{\text{all } \vec{\xi}} fd\vec{\xi}d\vec{r} = n(\vec{r},t)d\vec{r}$$

or

$$n = \int fd\vec{\xi} \tag{2.2}$$

where the integration is made over all values of $\vec{\xi}$ and $n(\vec{r},t)$ is the number density. From Equations (2.1) and (2.2) it is easily seen that the probability density function written in terms of f is $P = f/n$ or the probability of a molecule having a velocity between $\vec{\xi}$ and $\vec{\xi} + d\vec{\xi}$ is

$$\frac{f(\vec{r},\vec{\xi},t)d\vec{\xi}}{n(\vec{r},t)} .$$

The purpose in obtaining this function is to obtain by the theory of probability the expected value of the flow field properties. If we define Φ as a molecular property such as mass, velocity, or energy then we can write the expected value of Φ as

$$\langle\Phi\rangle = \frac{1}{n}\int \Phi f d\vec{\xi} .$$

This definition can be extended to the two-species spherical expansion problem by writing the expected value of a molecular property of the ith species as

$$\langle\Phi_i\rangle = \frac{1}{n_i}\int \Phi_i(\vec{\xi}) f_i d\vec{\xi} \tag{2.3}$$

where n_i and f_i are the number density and molecular velocity

distribution function of the ith species. The molecular velocity of each species will be designated by $\vec{\xi}$ without subscript or superscript notation, the specific species being understood by the subscript on the molecular property, the velocity distribution function, or as otherwise stated.

The molecular properties of interest are the mass m_i, momentum $m_i\vec{\xi}$, and energy $\frac{1}{2}m_i\xi^2$. The stress and heat-flux components are obtained from $\Phi_i = m_i\xi_j\xi_k$ and $\frac{1}{2}m_i\xi_j\xi^2$, respectively, where the spherical coordinates are given by the subscripts $j,k = r,\theta,\psi$ and the two species represented by the subscripts $i = 1,2$.

Flow-Field Properties

The expected value of the density and of the mass velocity can now be found from the following relations based on Equation (2.3):

$$\rho = \sum\rho_i = \sum n_i m_i = \sum m_i \int f_i d\vec{\xi} \tag{2.4}$$

and

$$\rho\vec{u} = \sum\rho_i\vec{u}_i = \sum m_i \int f_i \vec{\xi} d\vec{\xi} \tag{2.5}$$

where the summation is inferred over $i = 1,2$. The mass velocity $\vec{u}$ in this case is not the mean velocity of the molecules but a weighted mean giving to each molecule a weight proportional to its mass. The momentum of the gas per unit volume is the same as if every molecule moved with mass velocity $\vec{u}$.

From Equation (2.3) and by means of the notion of the peculiar velocity $\vec{c}_i = \vec{\xi} - \vec{u}$ which describes the random deviation of the ith species molecular velocity from the ordered motion with mass velocity $\vec{u}$, the expected values of the temperature, pressure, stress tensor,

and heat-flux vector are given by

$$\rho e = \frac{3}{2}nkT = \tfrac{1}{2}\sum m_i \int \xi^2 f_i d\vec{\xi} - \tfrac{1}{2}\rho u^2, \tag{2.6}$$

$$p = nkT ,$$

$$\sigma_{jk} = - \sum m_i \int \xi_j \xi_k f_i d\vec{\xi} + \rho u_j u_k , \tag{2.7}$$

and

$$q_j = \tfrac{1}{2}\sum \rho_i \int \xi^2 \xi_j f_i d\vec{\xi} - \tfrac{1}{2}\rho u^2 u_j + u_j \sigma_{jk} - u_j \rho e \tag{2.8}$$

where $j,k = r,\theta,\psi$ and $i = 1,2$.

The kinetic problem is then essentially that of finding the molecular velocity distribution function for each species and evaluating the various integrals to determine the flow field properties. In general this is still a complex problem. For the main area of interest of this study, free-molecule flow, the matter of finding f_i is greatly simplified.

The Kinetic Equation

The mathematical model appropriate for finding the molecular velocity distribution function valid for the full range of Knudsen numbers is the kinetic equation. The kinetic equations for two species, with external forces neglected, are

$$\frac{\partial f_1}{\partial t} + \vec{\xi} \cdot \frac{\partial f_1}{\partial \vec{r}} = J_{11} + J_{12}$$

and

$$\frac{\partial f_2}{\partial t} + \vec{\xi} \cdot \frac{\partial f_2}{\partial \vec{r}} = J_{21} + J_{22} \quad . \tag{2.9}$$

The symbol J_{mn} denotes the net change of species m due to collisions with species n. The collision operator varies according to the

particular collision model chosen. The Boltzmann collision operator is considered in Chapter V.

The initial conditions for the spherical problem as stated in Chapter I are given by

$$f_{o1} = n_{11}(\beta_1/\pi)^{3/2}\exp(-\beta_1\xi^2) \text{ for the gas inside the sphere} \qquad (2.10)$$

and

$$f_{o2} = n_{22}(\beta_2/\pi)^{3/2}\exp(-\beta_2\xi^2) \text{ for the gas outside the sphere}$$

where $\beta_i = m_i/2kT_{ii}$ and $n_{ii} = n_i(r,0)$ with $i = 1,2$.

Equation (2.9) can be rewritten as

$$\frac{Df_i}{Dt} = J_{i1} + J_{i2} \qquad (2.11)$$

where

$$\frac{Df_i}{Dt} = \frac{\partial f_i}{\partial t} + \vec{\xi}\cdot\frac{\partial f_i}{\partial \vec{r}} .$$

The differentiation in Equation (2.11) is carried out along the trajectory of a given molecule. By integration of Equation (2.11) we obtain the form of the general solution which is given by

$$f_i(\vec{r},\vec{\xi},t) = f_{oi}(\vec{r}_{oi},\vec{\xi}_o,0) + \int_o^t (J_{i1}+J_{i2})d\tau \qquad (2.12)$$

where $\vec{r}_{oi}$ and ξ_o are the constants of integration of the governing differential equations describing the trajectory of a molecule in 7-space with components, $\vec{r}$, $\vec{\xi}$, and t.

In Chapters III and IV the large Knudsen-number limit is considered; collisions among molecules are neglected. For this approximation the righthand side of Equation (2.11) is set equal to

zero and the general solution that follows is given by

$$f_i(\vec{r},\vec{\xi},t) = f_{oi}(\vec{r}_{oi},\vec{\xi}_o,0) \ . \tag{2.13}$$

CHAPTER III

EXPANSION FOR LARGE KNUDSEN NUMBERS

In this chapter the propagation of an initial spherical density discontinuity in a rarefied medium is examined based on large Knudsen number. It is assumed that the mean free path of each gas considered is large and that the initial sphere radius is sufficiently small to make the large Knudsen-number assumption valid.

Solution to the Collisionless Kinetic Equation

For the collisionless problem with $\rho_{11} \neq \rho_{22}$, $m_1 \neq m_2$ and $T_{11} \neq T_{22}$ we can consider the spherical problem from the standpoint of the inner gas of molecules with mass m_1 at $\rho_{11}, p_{11}, T_{11}$ exploding into a vacuum and the outer gas with molecules of mass m_2 at ρ_{22}, p_{22}, T_{22} imploding into a vacuum. The respective distribution functions are found from the collisionless kinetic equation

$$\frac{Df_i}{Dt} = 0 \tag{3.1}$$

where the left side is given by Equation (2.11) and for our 2-species problem $i = 1,2$. The initial conditions for this large Knudsen-number approximation are

$$f_{o1} = n_{11}(\beta_1/\pi)^{3/2}\exp(-\beta_1\xi^2)H(a-r)$$

and (3.2)

$$f_{02} = n_{22}(\beta_2/\pi)^{3/2}\exp(-\beta_2\xi^2)H(r-a)$$

with

$$H(z) = \begin{cases} 0 \text{ for } z < 0 \\ 1 \text{ for } z > 0 \end{cases},$$

the unit Heaviside step function.

The general solution to Equation (3.1) is given by Equation (2.13) which expresses f_i as a constant on a base characteristic curve, or on the trajectory of a molecule in a 7-space with components $\vec{r}$, $\vec{\xi}$ and t. The constants of integration $\vec{r}_o$ and $\vec{\xi}_o$ are obtained from the differential equations describing the trajectory. These differential equations are obtained by considering an 8-space with components f_i, $\vec{r}$, $\vec{\xi}$, and t. In terms of a scalar parameter ζ along the characteristic curve, f_i is expressed as:

$$f_i(\zeta) = f[\vec{r}(\zeta), \vec{\xi}(\zeta), t(\zeta)] \ .$$

Then taking the derivative of f_i with respect to ζ we obtain the total differential equation

$$\frac{df_i}{d\zeta} = \frac{dt}{d\zeta}\frac{\partial f_i}{\partial t} + \frac{d\vec{r}}{d\zeta} \cdot \frac{\partial f_i}{\partial \vec{r}} + \frac{d\vec{\xi}}{d\zeta} \cdot \frac{\partial f_i}{\partial \vec{\xi}} = 0 \qquad (3.3)$$

which states that f_i is a constant on a characteristic curve and agrees with Equation (3.1) when:

$$\frac{dt}{d\zeta} = 1 \ , \qquad (3.4)$$

$$\frac{d\vec{r}}{d\zeta} = \vec{\xi} \ , \qquad (3.5a)$$

and

$$\frac{d\vec{\xi}}{d\zeta} = 0 \ . \qquad (3.5b)$$

For simplicity, from Equation (3.4), set $\zeta = t$. Then t can be used as the parameter. The characteristic Equations (3.3) and (3.5)

become

$$df_i = 0 \ ,$$

$$\frac{d\vec{r}}{dt} = \vec{\xi} \ , \tag{3.6a}$$

and

$$d\vec{\xi} = 0 \ . \tag{3.6b}$$

The constants of integration for Equation (3.6) can be expressed as:

$$\vec{\xi}_o = \vec{\xi}$$

and

$$\vec{r}_o = \vec{r} - \vec{\xi}t \ . \tag{3.7}$$

Since $r_o = |\vec{r}_o|$, using spherical coordinates we write Equation (3.7) as

$$r_o = (r^2 - 2r\xi_r t + \xi^2 t^2)^{\frac{1}{2}} \ . \tag{3.8}$$

Now the molecular velocity distribution function $f_i(\vec{r},\vec{\xi},t)$ becomes, by combining the initial conditions given by Equation (3.1) and Equation (2.13),

$$f_1 = n_{11}(\beta_1/\pi)^{3/2}\exp(-\beta_1\xi^2)H(a-r_o) \tag{3.9a}$$

and

$$f_2 = n_{22}(\beta_2/\pi)^{3/2}\exp(-\beta_2\xi^2)H(r_o-a) \tag{3.9b}$$

where r_o is given by Equation (3.8). With f_i we have complete knowledge about the spherical problem. In order to put this knowledge into meaningful variables, the flow quantities, we substitute the f_i into expressions (2.4) through (2.8) and evaluate the integrals.

Macroscopic Flow Field Properties

The macroscopic flow-field properties are found to be functions of R, τ_1, and τ_2 and are dependent on the given mass and initial temperature ratios. Unlike the one-dimensional problem the spherical problem

is not a self-similar problem, that is, it is not a function of a similarity variable. A complete non-dimensional description of the flow field is given below by Equations (3.10) through (3.15), with

$$R = r/a,$$

$$\tau_i = t/a\beta_i^{\frac{1}{2}} ,$$

$$\Delta = \rho_{22}/\rho_{11},$$

$$Z_{1i} = (1+R)/\tau_i$$

and

$$Z_{2i} = (1-R)/\tau_i \quad .$$

Number Density

$$N \equiv n_1/n_{11} + n_2/n_{11} = \frac{1}{2\pi^{\frac{1}{2}}} \frac{\tau_1}{R} (e^{-Z_{11}^2} - e^{-Z_{21}^2}) + \tfrac{1}{2}(\mathrm{erf}Z_{11} + \mathrm{erf}Z_{21})$$

$$+\Delta \frac{m_1}{m_2}[1 - \frac{1}{2\pi^{\frac{1}{2}}} \frac{\tau_2}{R} (e^{-Z_{12}^2} - e^{-Z_{22}^2}) - \tfrac{1}{2}(\mathrm{erf}Z_{12} + \mathrm{erf}Z_{22})]$$

where n_1 is the number density of molecules of type 1, n_2 is the number density of molecules of type 2, and

$$\mathrm{erf}z = (2/\pi^{\frac{1}{2}}) \int_0^z \exp(-x^2)dx \ .$$

Density

$$\bar{\rho} \equiv \rho/\rho_{11}$$

$$= \frac{1}{2\pi^{\frac{1}{2}}} \frac{\tau_1}{R} (e^{-Z_{11}^2} - e^{-Z_{21}^2}) + \tfrac{1}{2}(\mathrm{erf}Z_{11} + \mathrm{erf}Z_{21})$$

$$+ \Delta[1 - \frac{1}{2\pi^{\frac{1}{2}}} \frac{\tau_2}{R} (e^{-Z_{12}^2} - e^{-Z_{22}^2}) - \tfrac{1}{2}(\mathrm{erf}Z_{12} + \mathrm{erf}Z_{22})] \ . \qquad (3.10)$$

Mass Velocity

$$V \equiv u_r \beta_1^{\frac{1}{2}}$$

$$= \frac{1}{2\pi^{\frac{1}{2}}\bar{\rho}} \left\{ [A_{11} e^{-Z_{11}^2} - A_{21} e^{-Z_{21}^2}] - \Delta \left(\frac{\beta_1}{\beta_2}\right)^{\frac{1}{2}} [A_{12} e^{-Z_{12}^2} - A_{22} e^{-Z_{22}^2}] \right\} \quad (3.11)$$

where

$$A_{1i} = \tau_i^2/2R^2 + 1/R$$

and

$$A_{2i} = \tau_i^2/2R^2 - 1/R \ .$$

The mass velocity as given by Equation (3.11) is in the radial direction. Owing to the spherical symmetry in the spherical expansion problem the mass velocities in the angular directions θ and ψ are zero.

Temperature

$$\bar{T} \equiv T/T_{11}$$

$$= \frac{1}{3\pi^{\frac{1}{2}}N} [B_{11} e^{-Z_{11}^2} - B_{21} e^{-Z_{21}^2}] + \frac{1}{2N} [\mathrm{erf}Z_{11} + \mathrm{erf}Z_{21}]$$

$$+ \frac{\Delta\beta_1}{N\beta_2} \left[1 - \frac{1}{3\pi^{\frac{1}{2}}} (B_{12} e^{-Z_{12}^2} - B_{22} e^{-Z_{22}^2}) - \tfrac{1}{2}(\mathrm{erf}Z_{12} + \mathrm{erf}Z_{22})\right]$$

$$- \frac{2\bar{\rho}V^2}{3N} \quad (3.12)$$

where

$$B_{1i} = 2\tau_i/R + 1/R\tau_i + 1/\tau_i$$

and

$$B_{2i} = 2\tau_i/R + 1/R\tau_i - 1/\tau_i \ .$$

Radial Stress

$$S_{RR} \equiv \sigma_{rr}/p_{11}$$

$$= -\left\{\frac{1}{\pi^{\frac{1}{2}}}\left(C_{11}e^{-Z_{11}^2}-C_{21}e^{-Z_{21}^2}\right) + \tfrac{1}{2}(\mathrm{erf}Z_{11}+\mathrm{erf}Z_{21})\right.$$

$$\left. + \Delta\,\frac{\beta_1}{\beta_2}\left[1-\frac{1}{\pi^{\frac{1}{2}}}\left(C_{12}e^{-Z_{12}^2}-C_{22}e^{-Z_{22}^2}\right) - \tfrac{1}{2}(\mathrm{erf}Z_{12}+\mathrm{erf}Z_{22})\right]\right\}$$

$$+ 2\bar{\rho}V^2 \qquad (3.13)$$

where

$$C_{1i} = \tau_i^3/2R^3 + 1/R\tau_i + \tau_i/R + 1/\tau_i + \tau_i/R^2$$

and

$$C_{2i} = \tau_i^3/2R^3 + 1/R\tau_i + \tau_i/R - 1/\tau_i - \tau_i/R^2 \ .$$

Angular Stresses

$$S_{AA} \equiv \sigma_{\theta\theta}/p_{11} = \sigma_{\psi\psi}/p_{11}$$

$$= -\left\{\frac{1}{\pi^{\frac{1}{2}}}\left(D_{11}e^{-Z_{11}^2}-D_{21}e^{-Z_{21}^2}\right) + \tfrac{1}{2}(\mathrm{erf}Z_{11}+\mathrm{erf}Z_{21})\right.$$

$$\left. + \Delta\,\frac{\beta_1}{\beta_2}\left[1-\frac{1}{\pi^{\frac{1}{2}}}\left(D_{12}e^{-Z_{12}^2}-D_{22}e^{-Z_{22}^2}\right)-\tfrac{1}{2}(\mathrm{erf}Z_{12}+\mathrm{erf}Z_{22})\right]\right\} \qquad (3.14)$$

where

$$D_{1i} = \tau_i/R - \tau_i^3/2R \ - \tau_i/R^2$$

and

$$D_{2i} = \tau_i/R - \tau_i^3/2R^3 + \tau_i/R^2 \ .$$

All other terms of the stress tensor are zero.

Heat Flux

$$Q \equiv q_r\beta_1^{\frac{1}{2}}/p_{11}$$

$$= \frac{1}{2\pi^{\frac{1}{2}}}\left\{\left(E_{11}e^{-Z_{11}^2}-E_{21}e^{-Z_{21}^2}\right) - \Delta\left(\frac{\beta_1}{\beta_2}\right)^{3/2}\left(E_{12}e^{-Z_{12}^2}-E_{22}e^{-Z_{22}^2}\right)\right\}$$

$$- \bar{\rho}V^3 + VS_{RR} - \frac{3}{2}\,NV\bar{T} \qquad (3.15)$$

where

$$E_{1i} = \tfrac{1}{2} + 2/\tau_i^2 + 3\tau_i^2/2R^2 + 1/2R^2 + 3/R + 1/R\tau_i^2 + R/\tau_i^2$$

and

$$E_{2i} = \tfrac{1}{2} + 2/\tau_i^2 + 3\tau_i^2/3R^2 + 1/2R^2 - 3/R - 1/R\tau_i^2 - R/\tau_i^2 \ .$$

The heat flux given by Equation (3.15) is in the radial direction. The angular heat fluxes are zero because of spherical symmetry.

A Sample Calculation

So that the reader may understand the method used to obtain the results given by Equations (3.10) through (3.15), the integration scheme for the density will be outlined. The other results follow from an analogous approach.

The density for the spherical expansion problem is found by integrating the expression obtained by substituting the relation for f_i given by Equation (3.9) into Equation (2.4) which gives us:

$$\rho = m_1 n_{11} (\beta_1/\pi)^{3/2} \int \exp(-\beta_1 \xi^2) H(a-r_o) d\vec{\xi} + m_2 n_{22} (\beta_2/\pi)^{3/2} \int \exp(-\beta_2 \xi^2) H(r_o - a) d\vec{\xi} \ . \qquad (3.16)$$

By means of the Heaviside function definition given by Equation (3.2), Equation (3.16) can be written as:

$$\rho = K_1 \int_{r_o<a} \exp(-\beta_1 \xi^2) d\vec{\xi} + K_2 \int_{r_o>a} \exp(-\beta_2 \xi^2) d\vec{\xi} \qquad (3.17)$$

where

$$K_i = m_i n_{ii} (\beta_i/\pi)^{3/2}, \quad i = 1,2 \ .$$

The second integral in Equation (3.17) can be expressed as an integral over all space minus an integral over $r_o<a$, or

$$\int_{r_o>a} f d\vec{\xi} = \int f d\vec{\xi} - \int_{r_o<a} f d\vec{\xi}$$

where

$$f = m_2 n_{22} (\beta_2/\pi)^{3/2} \exp(-\beta_2 \xi^2) \ .$$

From the definition of the number density given by Equation (2.3) with $\Phi_2 = m_2$ it follows that

$$\int_{r_o>a} f d\vec{\xi} = \rho_{22} - \int_{r_o<a} f d\vec{\xi}$$

where $\rho_{22} = m_2 n_{22}$. Now Equation (3.17) can be rewritten as:

$$\bar{\rho} = \Delta + (\beta_1/\pi)^{3/2} \int_{r_o<a} \exp(-\beta_1 \xi^2) d\vec{\xi} - \Delta(\beta_2/\pi)^{3/2} \int_{r_o<a} \exp(-\beta_2 \xi^2) d\vec{\xi} \qquad (3.18)$$

where $\Delta = \rho_{22}/\rho_{11}$ and $\rho_{11} = m_1 n_{11}$.

In order to integrate Equation (3.18) we use the fact that the unit Heaviside step function changes value at $r_o = a$. Setting $r_o = a$, substituting the value for r_o given by Equation (3.8), squaring both sides, and dividing by t^2, we obtain the relation

$$a^2/t^2 = (r/t - \xi_r)^2 + \xi_\theta^2 + \xi_\psi^2, \qquad (3.19)$$

in spherical coordinates, where

$$\xi^2 = \vec{\xi} \cdot \vec{\xi} = \xi_r^2 + \xi_\theta^2 + \xi_\psi^2 \qquad (3.20)$$

In velocity space Equation (3.19) describes a sphere whose center is a (r/t,0,0) as shown in Figure 3-1.

It is convenient to transform Equation (3.20) to new coordinates by means of a simple translation so that the center of the sphere

in velocity space is at (0,0,0). From the vector relations shown in Fig. 3-1 we can express $\vec{\xi}$ as the sum of two vectors:

$$\vec{\xi} = (r/t)\hat{e}_r + \vec{\xi}' \ .$$

Then Equation (3.20) can be rewritten as:

$$\xi^2 = r^2/t^2 + 2r\xi_r'/t + \xi'^2. \tag{3.21}$$

The results of the translation to the new coordinate system is shown in Fig. 3-2 from which the following relations are obtained:

$$\xi_r' = \xi'\cos\alpha \ , \tag{3.22a}$$

$$\xi_\theta' = \xi_\theta = \xi'\sin\alpha\cos\phi \ , \tag{3.22b}$$

$$\xi_\psi' = \xi_\psi = \xi'\sin\alpha\sin\phi \ , \tag{3.22c}$$

$$d\vec{\xi}' = d\vec{\xi} = \xi'^2\sin\alpha d\alpha d\phi d\xi \ . \tag{3.22d}$$

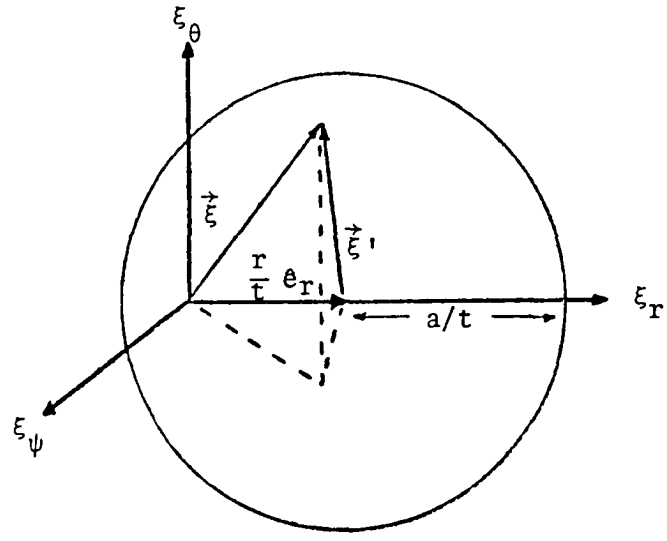


Fig. 3-1. Spherical Coordinate System in Velocity Space.

These are spherical coordinates in the translated system.

Substituting the value for ξ_r' from Equation (3.22) into Equation (3.21) we obtain:

$$\xi^2 = r^2/t^2 + (2r\xi'\cos\alpha)/t + \xi'^2 = \Gamma'$$

in terms of the new coordinates. The dummy variable Γ' will be used for convenience in writing arguments of exponentials. Substituting Γ' for ξ^2, $d\xi'$ from Equation (3.22) and the appropriate limits of integration into Equation (3.18) and dropping the primes, we obtain

$$\bar{\rho} = \Delta + (\beta_1/\pi)^{3/2} \int_0^{a/t} \int_0^{\pi} \int_0^{2\pi} d\xi d\alpha d\phi \xi^2 \sin\alpha \exp(-\beta_1\Gamma)$$
$$+ \Delta(\beta_2/\pi)^{3/2} \int_0^{a/t} \int_0^{\pi} \int_0^{2\pi} d\xi d\alpha d\phi \xi^2 \sin\alpha \exp(-\beta_2\Gamma) \ .$$

The result given by Equation (3.10) follows after straight foreward

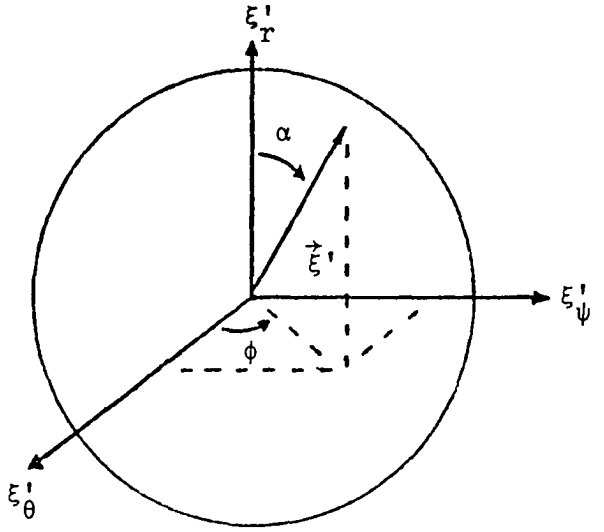


Fig. 3-2. Translated Spherical Coordinate System in Velocity Space.

integration over α and ϕ and integrating over ξ by means of the Equations (A-1) and (A-2), integral relations found in Appendix A.

Behavior of Flow-Field Properties

In order to discuss the behavior of the flow-field properties of Equations (3.10) through (3.15) the results are plotted for various values of initial density ratios and various times as a function of distance from the center of the initial sphere of gas. Three cases will be examined.

The first case, with $T_{11} = T_{22}$ and $m_1 = m_2$, will be used as a standard to investigate the behavior of explosions and implosions with respect to radius and time for a given initial density discontinuity. By further specializing this case by lettering $\Delta = 0$, we obtain the problem examined by Molmud (1960) and Narashima (1962), expansion of an initially uniform spherical gas cloud into a vacuum. The result obtained herein for the number density was obtained by Molmud and Narashima. Narashima also obtained a velocity expression but it can be shown to be in error in that it does not go to zero as $R \to 0$. In Chapter IV we again consider this special case for analyzing embryonic shock structure.

The second case of interest considers a weak explosion in a rarefied atmosphere with a mass ratio of $m_1/m_2 = 0.069$ and various temperature ratios. The mass ratio is based on an expansion of hydrogen gas into the atmosphere.

The third case considers a high temperature ratio and a mass ratio of 0.5. This case represents the expansion of a dissociated gas into the same gas in the undissociated state.

Case 1.

For Case 1 we consider a spherical expansion with the gases inside and outside the sphere being the same and at the same temperature. This gives $\beta_1 = \beta_2$ and $\tau_1 = \tau_2$. Since we do not have a self-similar problem the plot of the flow quantities must be made for a given initial density discontinuity at a specified time or τ. For the purposes of illustration we consider an initial density discontinuity of $\Delta = n_{22}/n_{11} = 0.1$ at $\tau = 0.2$. In order to observe the effect of time on the expansion we look at a later time $\tau = 1.0$. The results for the flow quantities of interest are shown in Figs. 3-3 and 3-4 for $\tau = 0.1$ and 1.0. For Case 1 since $m_1 = m_2$ the mass density Equation (3.10) represents the number density, or $\bar{\rho} = N = n/n_{11}$.

The compressive wave propagating outward and the expansion wave propagating inward for the explosion case are illustrated by the behavior of the temperature profile in Fig. 3-3. Also the diffuse nature of a kinetic expansion is shown by the number density curve in that there are no discontinuities. The heat flux curve suggests a relation between this curve and the temperature profile which will be considered mathematically later in this chapter. The velocity is observed to be large near R = 1 where the molecules have undergone the largest perturbation and decrease rapidly to zero at short distance from R = 1. For this case we will show in the next section that there is a mathematical relation between the velocity and the stresses.

The perturbation aspect of the problem is suggested by the profiles in Fig. 3-4. Noticeable is the spreading out of the number density and the weakening of the other quantities with time as they propagate

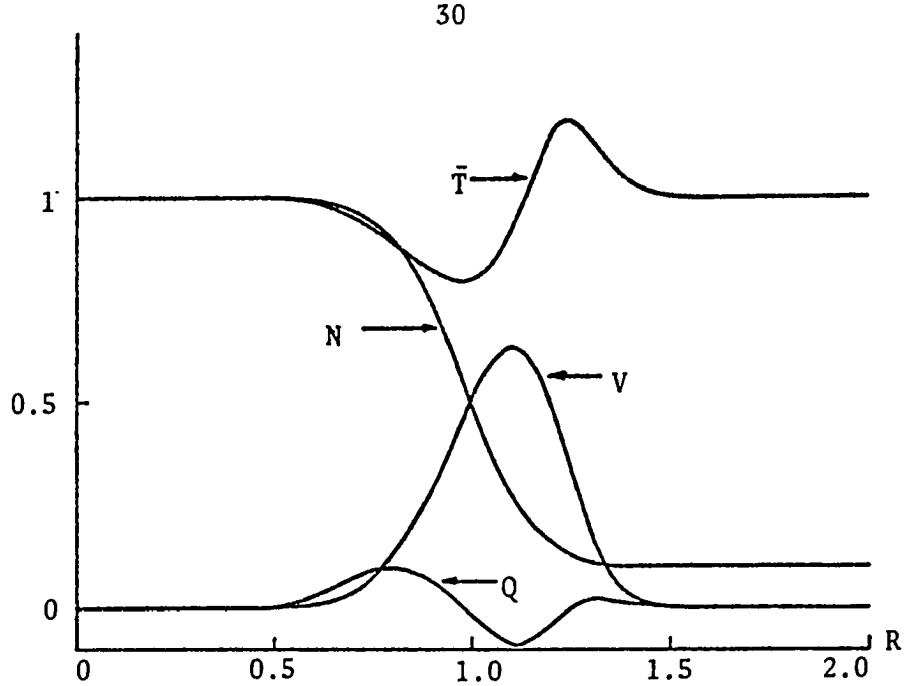


Fig. 3-3. Case 1 Free-Molecule Variables for $\Delta = 0.1$ at $\tau = 0.2$.

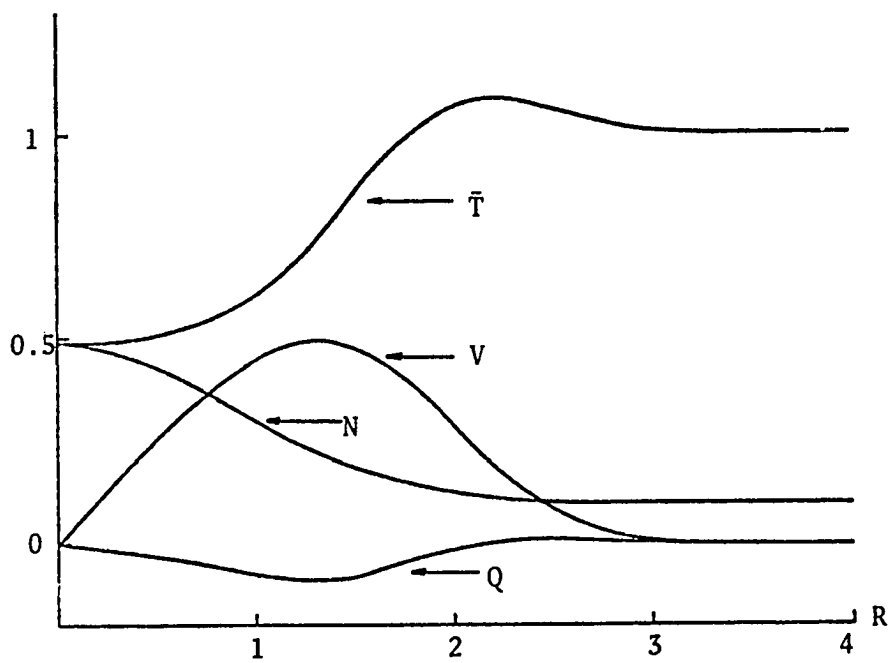


Fig. 3-4. Case 1 Free-Molecule Variables for $\Delta = 0.1$ at $\tau = 1.0$.

outward from R = 1. The perturbation behavior is further reflected by the temperature for increasing time as shown in Fig. B-3 (see Appendix B).

The behavior of the disturbance as $R \to 0$ and $R \to \infty$ can be demonstrated mathematically by considering the asymptotic expansions of the solutions. Expressions for the number density and temperature at R = 0 are found to be

$$N(0,\tau) = \Delta - \frac{2(1-\Delta)e^{-1/\tau^2}}{\pi^{\frac{1}{2}}\tau} + (1-\Delta)\mathrm{erf}(1/\tau) \tag{3.23}$$

and

$$\bar{T}(0,\tau) = 1 - \frac{4(1-\Delta)e^{-1/\tau^2}}{3\pi^{\frac{1}{2}}N(0,\tau)\tau^3} . \tag{3.24}$$

These relations are necessary in the evaluation of the Boltzmann H-Function to be introduced later in this chapter. A complete study of other pertinent asymptotic values is included in Appendix B.

The results for free-molecule flow given by Equations (3.10) through (3.15) are also valid for implosions, that is, when the initial density ratio is greater than unity (except for implosions into a vacuum, which requires renormalization). Typical results are shown in Fig. 3-5 for $\Delta = 10$ at $\tau = 0.2$ (the right hand scale applies only to the number density). Again these profiles reflect the diffuse nature of the kinetic problem as well as the perturbation effect. In this case the compression wave of the higher-density exterior gas propagates inward.

Case 2.

For Case 2 we consider a 2-species expansion with $m_1 \neq m_2$ and $T_{11} \neq T_{22}$. This model considers a weak explosion of hydrogen gas into the surrounding atmosphere. Thus we let $m_1/m_2 = 2/29 \simeq 0.069$ and select for discussion two temperature ratios $T_{11}/T_{22} = 1$ and 10. The

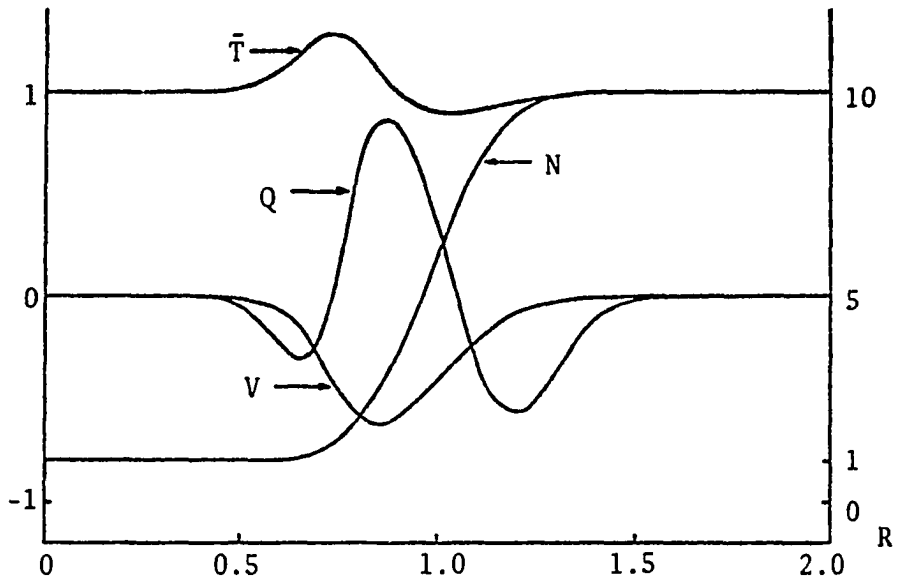


Fig. 3-5. Case 1 Free-Molecule Variables for a Compression Ratio of $\Delta = 10$ at $\tau = 0.2$ (Right Scale for Number Density Only)

same compression ratio $\Delta = 0.1$ and time $\tau_1 = 0.2$ is used as for Case 1. In this case the time t is non-dimensionalized based on initial conditions inside the sphere. The flow variables of interest are given in Figs. 3-6 through 3-11.

The free-molecule variables for Case 2 are observed to vary from the smooth profiles of Case 1 given in Fig. 3-5, although they are still diffusive in nature. For the special case of a 2-species expansion with the initial temperatures equal, the variations are induced by the $\Delta = m_2 n_{22}/m_1 n_{11}$ and $\tau_2 = \tau_1 (m_1/m_2)^{\frac{1}{2}}$ terms in Equations (3.10) through (3.15). With differing initial temperatures the Δ term remains the same but the time term becomes $\tau_2 = \tau_1 (m_1 T_{22}/m_2 T_{11})^{\frac{1}{2}}$. Also the components of Equations (3.11) through (3.15) which correspond to the i = 2 species (in this case the heavier species air) are multiplied by various ratios of β_1/β_2 or β_2/β_1, that is, by a product of the initial mass and temperature ratios.

The density shown in Fig. 3-6 and the mass velocity shown in Fig. 3-7 illustrate the weak influence of a 2-species expansion when the initial temperature ratio is unity. These profiles vary only slightly from the profiles given in Fig. 3-3. The variation becomes accentuated when the two species have different initial temperatures as can be observed in Figs. 3-6 and 3-7 for $T_{11}/T_{22} = 10$. The density and velocity profiles become steeper in the region $.93<R<.98$, the density decreasing faster than the 1-species expansion of Case 1 and the velocity increasing faster. In the vicinity of R = 1 both profiles flatten out with the density obtaining a greater value than the Case 1 result. The density then decreases at a faster rate as it goes to its large R value of Δ. The velocity continues to rise to a higher maximum value than for Case 1 with the maximum occurring in the vicinity of R = 1.1 as in Case 1. The lighter molecules inside the sphere at higher temperature reach a higher speed while propagating outward than if both species had the same mass and temperature.

The temperature of Case 2 reflects the same characteristic expansion wave propagating inward and compression wave propagating outward for a spherical expansion; however, the temperature in the expansion region goes to a lower temperature and that in the compression region goes to a higher temperature than observed for Case 1. The asymptotic limit of Equation (3.12) for large R is T_{22}/T_{11} (the derivation of this limit as well as all others for Case 2 is given in Appendix B). The location of the maximum temperature in the compression wave is observed to occur for a larger value of R than the maximum for Case 1.

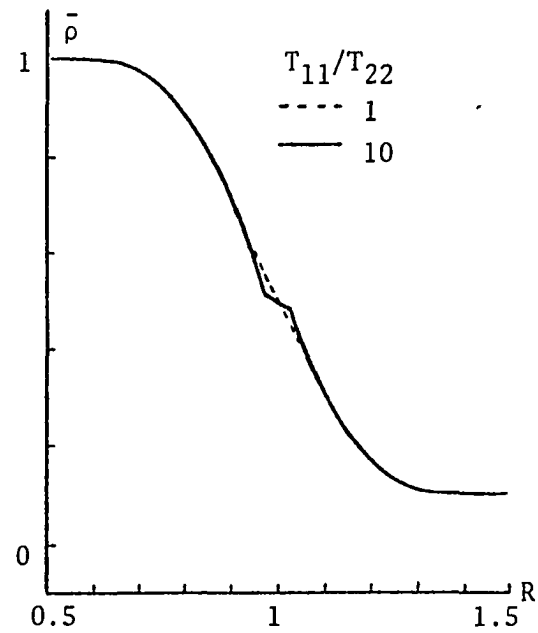


Fig. 3-6. Case 2 Density for Δ=0.1, m_1/m_2 = 0.069, and τ_1 = 0.2.

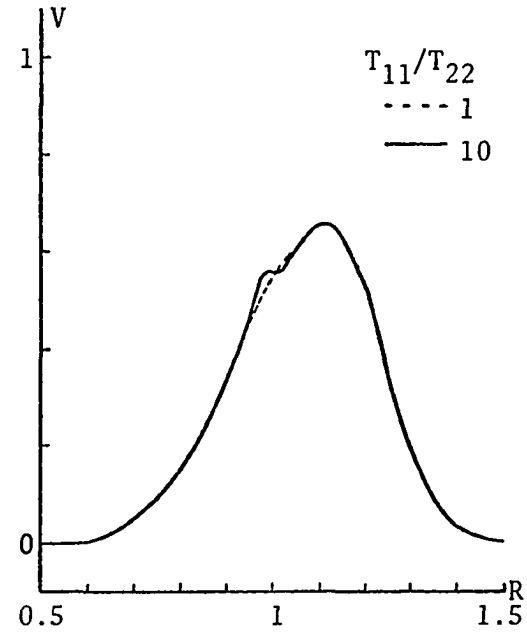


Fig. 3-7. Case 2 Velocity for Δ=0.1, m_1/m_2 = 0.069, and τ_1 = 0.2.

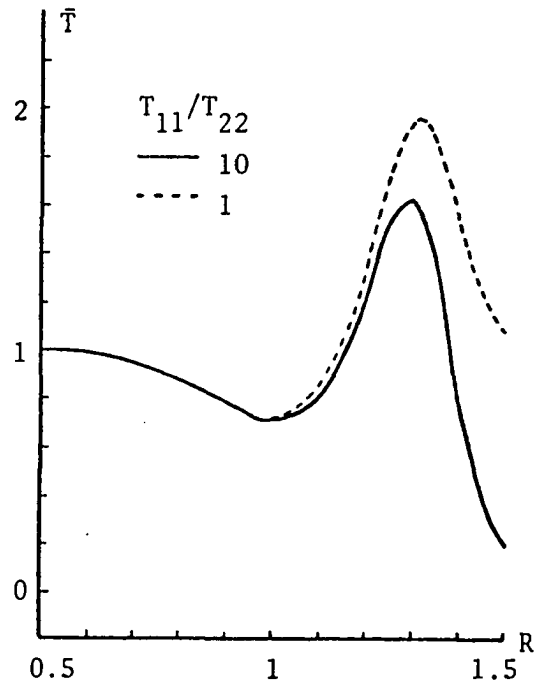


Fig. 3-8. Case 2 Temperature for Δ=0.1, m_1/m_2=0.069, and τ_1=0.2.

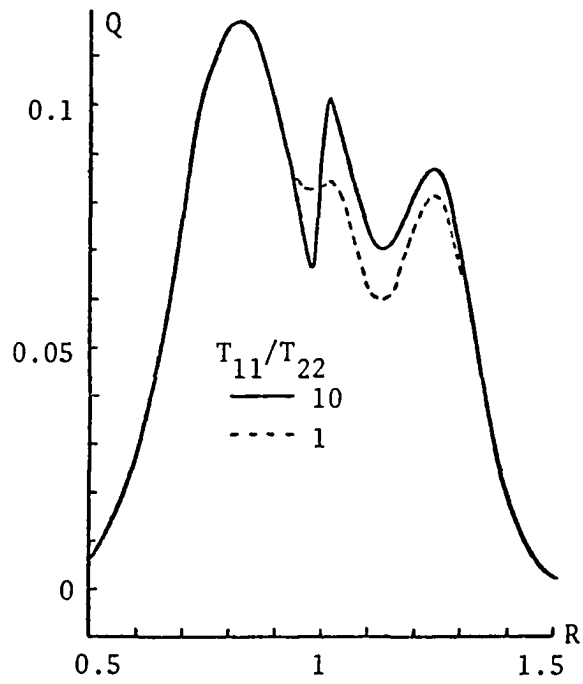


Fig. 3-9. Case 2 Heat Flux for Δ=0.1, m_1/m_2=0.069, and τ_1=0.2.

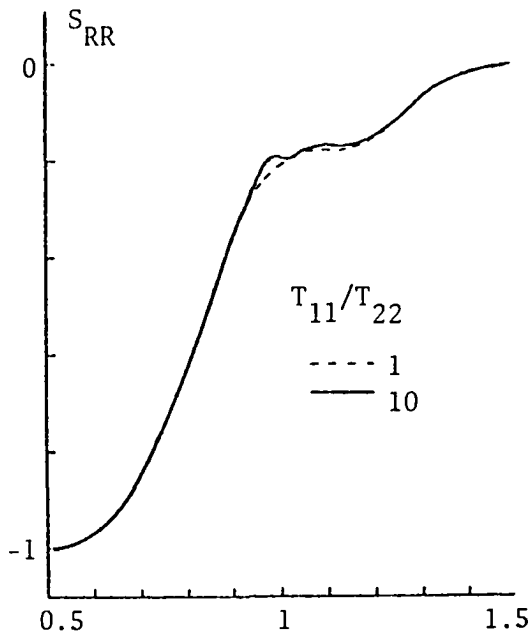


Fig. 3-10. Radial Stress for Δ=0.1, m_1/m_2 = 0.069, and τ_1 = 0.2.

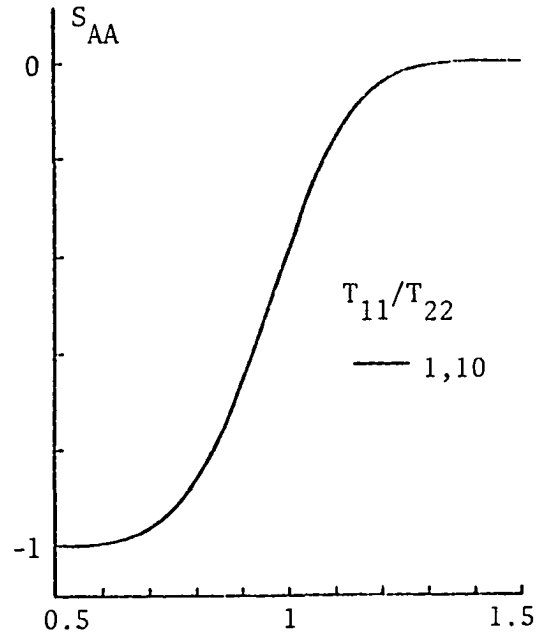


Fig. 3-11. Angular Stresses for Δ=0.1, m_1/m_2 = 0.069, and τ_1 = 0.2.

Thus for the 2-species expansion, with or without differing initial temperatures, the influx of lighter molecules into the R > 1 compression region is greater than the efflux of the heavier molecules from this region. The greater density of molecules at a higher speed causes the temperature to be higher in the compression region than found in Case 1. The efflux of the lighter molecules is greater than the influx of heavier molecules in the compression region, causing a decrease in density in this region. Also the lighter molecules depart at a faster rate. The combined effect is that the temperature is lower than for Case 1 in this region.

The Case 2 heat-flux results shown in Fig. 3-9 are observed to vary significantly from the Case 1 results. This could be anticipated

from macroscopic theory for the heat flux in that for multi-species problems a diffusion-flux term is added to the heat-flux equation. For Case 1 this diffusion flux is not a factor as will be shown in the next section.

For the density and the velocity the behavior of the heavier i = 2 molecules is governed by the initial density ratio in Equations (3.10) and (3.11). The initial pressure ratio, however, is the governing influence on the i = 2 terms in the temperature, stress tensor, and heat flux expressions since $\Delta(\beta_1/\beta_2) = P_{22}/P_{11}$. This influence shows up in the limiting values of the stress components.

For Case 1 the asymptotic limit of the stress tensor components for large R is $S_{RR} = S_{AA} = -\Delta$, the initial density ratio, whereas the limit for a 2-species expansion with varying initial temperatures is $S_{RR} = S_{AA} = -P_{22}/P_{11}$. The numerical value of the angular stresses for the initial temperature ratios 1 and 10 differ only slightly from one another so only one profile is given in Fig. 3-11. The radial stress profiles for both temperature ratios are given in Fig. 3-10. The Case 1 results for the stress components are qualitatively similar to those for Case 2 when the initial temperature ratio is unity and are therefore not included in Fig. 3-3. The effect of the differing initial temperatures on the radial stress occurs in the same region that we observed changes in the velocity gradient, $.93<R<1.1$.

Insight into the effects of 2-species expansions with differing initial temperatures can be obtained by considering two special cases, both resulting in a pressure difference contributing the essential driving force to the mixing action. In the first special case the

pressure difference arises because of a mass difference between the molecules initially inside the sphere and those outside. We assume that $\rho_{11} = \rho_{22}$, $T_{11} = T_{22}$, $m_1/m_2 = 0.069$, and $\tau_1 = 0.2$. Figure 3-12 reflects the density, velocity and temperature results for this special case. We observe that there is a decrease in density for $R < 1$ and an increase for $R > 1$. This effect is observed in Fig. 3-6. The velocity result in Fig. 3-7 is seen to rise and fall corresponding to the rise and fall of the velocity result shown in Fig. 3-12 for $R < 1$.

The second special case consists of a pressure difference due to an initial temperature difference. This 1-species expansion has $m_1 = m_2$, $\rho_{11} = \rho_{22}$, $T_{11}/T_{22} = 10$, and $\tau_1 = 0.2$. The results of interest are shown in Fig. 3-13. It is obvious that the density and velocity are qualitatively the same as the results in Fig. 3-12.

Two other special cases were examined to gain insight into the effects observed in the Case 2 expansion. We examined the effects of a density difference ($\Delta = 14.5$) with equal pressures, differing masses, and equal initial temperatures. The results correspond qualitatively with those shown in Fig. 3-12. Also a 1-species expansion was examined for differing temperatures, $T_{11}/T_{22} = 10$, and a density discontinuity of $\Delta = 0.1$ at $\tau_1 = 0.2$. Results similar to those of Case 2 with $m_1/m_2 = 0.069$ and $T_{11} = T_{22}$ were obtained.

The various special cases indicate that the causes of the variations noted for Case 2 with respect to Case 1 are not easily identifiable. When, however, there is both a difference in the mass of the molecules inside and outside the sphere and $T_{11} \neq T_{22}$, for a given initial density discontinuity, the variations are greater than if either

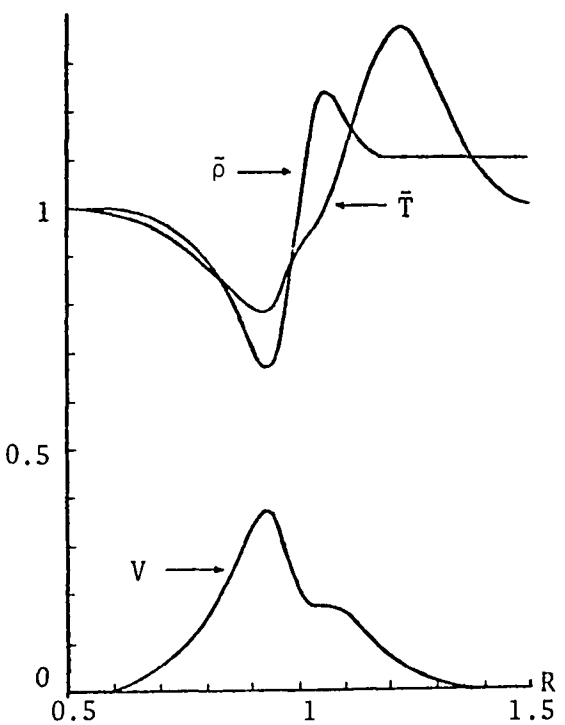


Fig. 3-12. Free-Molecule Variables for a Pressure Difference with $\Delta = 1$, $m_1/m_2 = 0.069$, and $T_{11}/T_{22} = 1^2$ at $\tau_1 = 0.2$.

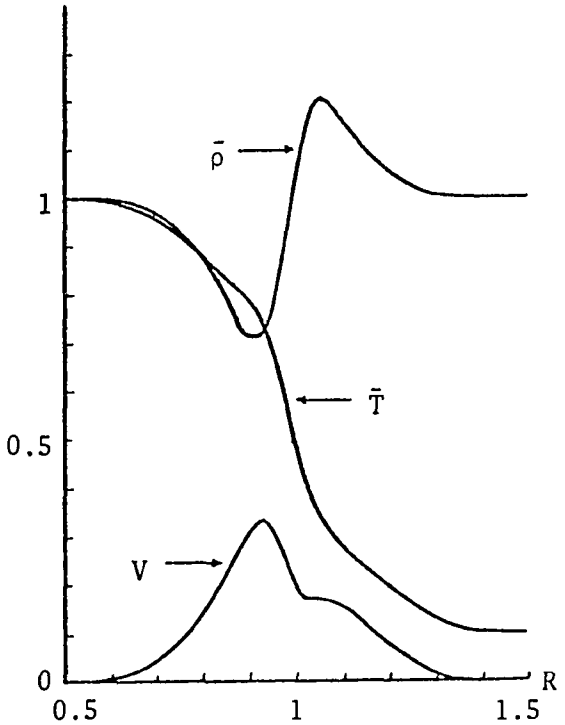


Fig. 3-13. Free-Molecule Variables for a Pressure Difference with $\Delta = 1$, $m_1/m_2 = 1$, and $T_{11}/T_{22} = 10$ at $\tau_1 = 0.2$.

a mass difference or a temperature difference exists alone.

Case 3.

The third case considered represents a stronger explosion with initial temperature ratios of $T_{11}/T_{22} = 10$ and 50 such that dissociation takes place inside the sphere but not ionization. For this case the mass ratio is $m_1/m_2 = 0.5$ and we select the same density ratio of $\Delta = 0.1$ and time $\tau_1 = 0.2$ examined in Cases 1 and 2 above.

Rather than presenting a plot of these results it is sufficient for our discussion to refer to Figs. 3-6 through 3-11 for Case 2. Specifically, results for both temperature ratios considered in Case 3 fall in between the profiles plotted for Case 2, the Case 3 temperature

ratio of 50 results lying closer to the Case 2 temperature ratio of 10 results. Thus the same description of the propagation of the molecules after the bounding surface is removed apply to Case 3 as was given in the Case 2 analysis.

The results obtained for Cases 2 and 3 give an envelope for a wide range of both initial temperature differences and mass differences with application to a wide variety of 2-species spherical expansion problems.

Transport Properties

In a fluid dynamics problem the mechanics of transport is interpreted in terms of the mean free path. A molecule traveling a distance of one mean free path is in effect transporting a certain amount of momentum, energy, and mass through a distance of the mean free path. In our collisionless problem of this chapter the mean free path is considered infinite or at least very large in comparison with the initial radius of the sphere. Therefore the transport phenomena of viscosity, heat conductivity, and mass diffusivity may be considered invalid for our discussion since these are generally considered as collision dominated phenomena. Also the transport phenomena above are processes of energy dissipation or irreversible processes and the collisionless expansion is a reversible process.

However, if we consider the equations of change obtained by multiplying both sides of the kinetic Equation (2.9) by the first three values of $\Phi_i(\vec{\xi})(m_i, \vec{\xi}, \frac{1}{2}m_i\xi^2)$, one at a time, and integrating over $d\vec{\xi}$ we find that we can obtain five equations (the conservation equations of mass, momentum and energy) which contain the mass flux, stress tensor

and heat flux vector. Burger (1969) obtained the collisionless 13-moment approximation by considering Equation (3.1) and multiplying the collisionless kinetic equation by higher powers of $\vec{\xi}$, thus obtaining the higher moments. The 13-moment approximation gives thirteen unknown flow quantities which include the mass flux, stress tensor and heat flux vector. These equations, the equations of change and the 13-moment approximation equations, could be considered as expressions of purely kinematic effects which show how the density flux, stress components and heat flux components arise from velocity, concentration, and temperature gradients as a result of the mixing process due to the whole spectrum of particle velocities in each element of volume. But it is of interest also to see if the explicit expressions for the components obtained in Equations (3.10) and (3.13) through (3.15) yield a simplified relation between the free-molecule variable and a combination of the gradients of concentration, pressure, velocity, and temperature. An additional purpose in this is to find the associated transport coefficients where possible and compare them to the collisional transport coefficients.

Transport of Momentum

From continuum gas-dynamic notions we let σ_{jk} represent that part of the momentum flux owing to the direct transfer of momentum with the mass of the moving fluid. Also we let $\sigma_{jk} + p\delta_{jk}$ be the viscous stress tensor τ_{jk} which represents the process of internal friction resulting from different fluid particles moving with different velocities so that there is a relative motion between various parts of the fluid. The viscous stress tensor thus depends on velocity gradients.

When the velocity gradients are small we know from continuum theory that the momentum transfer due to viscosity depends on the first derivative of velocity. From continuum theory the phenomenological expression for the viscous stress component in the radial direction, written in non-dimensional form, is

$$\tau^*_{RR} = \frac{4\mu_o}{3}\left[\frac{\partial V}{\partial R} - \frac{V}{R}\right] \tag{3.25}$$

where $\mu_o = \mu/ap_{11}\beta_1^{\frac{1}{2}}$ is an effective viscosity coefficient.

The kinetic radial viscous stress component is given by

$$\tau_{RR} = S_{RR} + P \tag{3.26}$$

where $P = N\bar{T}$. It is of interest then to see how τ_{RR} and τ^*_{RR} are related and if they are equal for a special case.

If we use the free-molecule result of Equation (3.11) in evaluating the right-hand side of Equation (3.25), we find that

$$\tau^*_{RR} = \frac{2\mu_o}{\tau_1}\frac{4}{3}\left\{-\frac{3\tau_1}{2R}\bar{\rho}V - \frac{R}{\tau_1}\left[\bar{\rho}_1 V_1 + \frac{\beta_1}{\beta_2}\bar{\rho}_2 V_2\right] - \frac{1}{2R\tau_1\pi^{\frac{1}{2}}}\left[E_1 - \Delta\left(\frac{\beta_2}{\beta_1}\right)^{\frac{1}{2}}E_2\right]\right.$$
$$\left. + V\left[\bar{\rho}_1 V_1 + \frac{\beta_2}{\beta_1}\bar{\rho}_2 V_2\right]\right\} \tag{3.27}$$

where

$$E_{1,2} = \exp(-A^2) - \exp(-B^2)\ ,$$
$$\bar{\rho}_1 = \rho_1/\rho_{11}\ ,$$
$$\bar{\rho}_2 = \rho_2/\rho_{11}\ ,$$
$$V_{1,2} = \langle\xi_r\rangle\beta_1^{\frac{1}{2}}$$

with

$$A = (1+R)/\tau_{1,2}$$

and

$$B = (1-R)/\tau_{1,2} .$$

If we let $\mu_o = \tau_1/2$ in Equation (3.27) we find that

$$\tau_{RR} = \tau^*_{RR} + (1- \frac{\beta_1}{\beta_2})[\bar{\rho}_2 V_2\{\frac{3\tau_1}{2R} + (\frac{R}{\tau_1} - V)\frac{\beta_2}{\beta_1}\} - \frac{\Delta(\frac{\beta_2}{\beta_1})^{\frac{1}{2}}}{2\pi^{\frac{1}{2}}R\tau_1} E_2] . \qquad (3.28)$$

We observe for two special cases that $\tau_{RR} = \tau^*_{RR}$. Special case (1) is when $m_1 = m_2$ and $T_{11} = T_{22}$, or Case 1 above. Special case (2) is when $m_1/m_2 = T_{11}/T_{22}$. It is obvious that (2) would be impossible for Case 3 and for Case 2 it is of little interest.

The viscosity coefficient applicable when $\mu_o = \tau_1/2$ is

$$\mu = \frac{\rho k t T_{11}}{2m_1} . \qquad (3.29)$$

For Case 1 with $m_1 = m_2$ this result corresponds to the viscosity coefficient found by Yates and Karamcheti (1967) in their one-dimensional, 1-species, short-time expansion study.

Transport of Mass

For the 2-species spherical expansion the diffusion-flux $\vec{i}$ is only unbalanced in the radial direction. In general the diffusion flux is influenced by the concentration gradient, temperature gradient, and the pressure gradient. For 2-species $\vec{i}_1 = -\vec{i}_2$ so we can write the non-dimensional form of the radial component of the diffusion flux [see Landau and Lifshitz (1959)] as

$$I^*_1 = -\bar{\rho}[D_M \frac{\partial C_1}{\partial R} + D_T \frac{\partial \ell n \bar{T}}{\partial R} + D_P \frac{\partial \ell n P}{\partial R}] \qquad (3.30)$$

where

$C_1 \equiv \bar{\rho}_1/\bar{\rho}$ is the concentration of the 1-molecule species,

$D_M \equiv \beta_1^{\frac{1}{2}} D/a$,

$D_T \equiv \beta_1^{\frac{1}{2}} DK_T/a$,

$D_P \equiv \beta_1^{\frac{1}{2}} DK_P/a$,

D is the mass transfer coefficient,

K_T is the thermal diffusion ratio,

and

K_P is the baro-diffusion ratio.

The diffusion flux is defined as the amount of the component transported through a unit area per unit time. For the kinetic problem we write this as

$$I_1 = \bar{\rho}_1 U_1 \tag{3.31}$$

where

$U_1 = V_1 - V$ is a diffusion velocity component in the radial direction.

The diffusion velocity of species 1 is the relative velocity of type 1 molecules with respect to the mass average velocity of the gas.

Working out the terms on the right-hand side of Equation (3.30) we obtain

$$I_1^* = \frac{2D_M}{\tau_1}\left[\bar{\rho}_1 V_1 - \bar{\rho}_1 \frac{(\bar{\rho}_1 V_1 + \frac{\beta_2}{\beta_1}\bar{\rho}_2 V_2)}{\bar{\rho}} + \frac{2\bar{\rho}}{3P}(K_T+K_P)\Theta + \bar{\rho}K_P(\bar{\rho}_1 V_1 + \frac{T_{11}}{T_{22}}\bar{\rho}_2 V_2)\right] \tag{3.32}$$

where

$$\Theta = -\frac{3}{4} N\tau_1 \frac{\partial \bar{T}}{\partial R} .$$

If we let $D_M = \tau_1/2$ in Equation (3.32) then we can write

$$I_1 = I_1^* - C_1\bar{\rho}_2 V_2[\frac{\beta_1}{\beta_2} - 1] - \frac{2}{3}\frac{\bar{\rho}}{P}(K_T+K_P)\Theta - \bar{\rho}K_P(\bar{\rho}_1 V_1 + \frac{T_{11}}{T_{22}}\bar{\rho}_2 V_2) \ .$$

Thus we find that $I_1 = I_1^*$ if $\beta_1 = \beta_2$, and $K_P = K_T = 0$. This special case corresponds to Fick's law, or the diffusion flux is linearly proportional to the concentration gradient alone.

For $D_M = \tau_1/2$ we find the diffusion coefficient to be

$$D = \frac{tkT_{11}}{m_1} \ . \tag{3.33}$$

The Transport of Energy

It is well known that heat will flow from hotter regions to colder regions so as to dissipate the gradient in the temperature (that the heat never flows in the opposite direction is the second law of thermodynamics). For a 2-species problem there is also a transport of energy due to the diffusion flux. If the concentration and thermal gradients are small we can write the heat flux [see Landau and Lifshitz (1959)] as

$$Q^* = C_o I_1^* - K_o \frac{\partial \bar{T}}{\partial R} \tag{3.34}$$

where

$K_o = \beta_1^{\frac{1}{2}} K/an_{11}k$ is a conductivity coefficient

and

$$C_o = \frac{\beta_1^{\frac{1}{2}}}{P_{11}}\{K_T(\frac{\partial \mu_s}{\partial C_1})_{P,T} - T(\frac{\partial \mu_s}{\partial T})_{P,C_1} + \mu_s\}$$

with μ_s the chemical potential which is a function of pressure, temperature, and concentration. The free-molecule heat flux for the 2-species

expansion is given by Equation (3.15)

By taking the derivative of the temperature with respect to R and letting I_1^* represent the right hand side of Equation (3.32) we can write Equation (3.34) as

$$Q^* = K_o \frac{4}{3N\tau_1} \{\bar{\rho}V(2+ \frac{1}{\tau_1^2} - 2\frac{\tau_1}{R}V)+[\bar{\rho}_1V_1+ \frac{\beta_2}{\beta_1} \bar{\rho}_2V_2] (\frac{R^2}{\tau_1^2} + V^2-2 \frac{R}{\tau_1} V)$$

$$+ \frac{1}{\pi^{\frac{1}{2}}} [E_1-\Delta(\frac{\beta_2}{\beta_1})^{\frac{1}{2}}E_2] (\frac{1}{\tau_1^2} - \frac{V}{R\tau_1}) - \frac{3}{2} \bar{T}[\bar{\rho}_1V_1+ \frac{T_{11}}{T_{22}} \bar{\rho}_2V_2]\} + C_oI_1^* \tag{3.35}$$

with $E_{1,2}$ given by Equation (3.27).

If we let $K_o = 3N\tau_1/4$ in Equation (3.35) we derive the following relation:

$$Q = Q^* -(1- \frac{\beta_1}{\beta_2}) \{\bar{\rho}_2V_2[3-2 \frac{\tau_1}{R} V+ \frac{\beta_2}{\beta_1} (\frac{R^2}{\tau_1^2} - 2V \frac{R}{\tau_1} + V^2)$$

$$- \frac{\Delta(\frac{\beta_2}{\beta_1})^{\frac{1}{2}}}{2\pi^{\frac{1}{2}}} (\frac{1}{\tau_1^2} - \frac{V}{R\tau_1})E_2]$$

$$+ \bar{\rho}_2V[1-(\frac{\beta_1}{\beta_2})^{\frac{1}{2}}] - \frac{3}{2} \bar{T}[NV-(\bar{\rho}_1V_1+ \frac{T_{11}}{T_{22}} \bar{\rho}_2V_2)] - C_oI_1^* . \tag{3.36}$$

It is easily seen from Equation (3.36) that $Q = Q^*$ when $m_1 = m_2$, $T_{11} = T_{22}$, and $C_o = 0$. For this case we have the thermal flux proportional to the temperature gradient.

For $K_o = 3N\tau_1/4$ we find the conductivity to be given by

$$K = \frac{3nk^2tT_{11}}{2m_1} . \tag{3.37}$$

For Case 1 with $m_1 = m_2$ and $T_{11} = T_{22}$ this expression for the conductivity corresponds to the conductivity found by Yates and Karamcheti

for the shock tube problem.

The transport coefficients given by Equations (3.29), (3.33), and (3.37) grow linearly with time. It is interesting to observe that when t is set equal to the upper limit for free-molecule flow, $\lambda/\bar{c}$, (where $\bar{c}$ is the mean speed of a molecule) that $\mu = \frac{\pi}{16}\rho\lambda\bar{c}$, $D = \frac{\pi}{8}\lambda\bar{c}$, and $K = 2\mu C_v$. These are the same relations, except for the numerical constants, as given by Vincenti and Kruger (1965) in their macroscopic study of the transport properties. The Prandtl number, $C_p\mu/K$, based on free-molecule results is 5/6 whereas the above mentioned macroscopic study gives 2/3.

We have shown in this section that although it is not apriori reasonable to expect a linear relation between the transport properties and the various gradients mentioned above we obtained a meaningful linear relation for each of the transport properties when $m_1 = m_2$ and $T_{11} = T_{22}$, Case 1. In the next section we shall see that Case 1 is more nearly in equilibrium than the expansions for Cases 2 and 3, possibly the underlying reason for the linear relations being valid for Case 1.

The Non-Equilibrium Indicator

In addition to the free-molecule flow quantities already found in this chapter it is of interest to consider two other integral properties of the collisionless problem, (1) the Boltzmann H-Function and (2) the thermodynamic entropy.

In kinetic theory the production of the H-Function comes about entirely because of collisions. In free-molecule flow the production of H is zero because there are no collisions. There are, however, H fluxes so changes in H are non-zero for the general collisionless problem.

The production of entropy does not rely entirely on collisions and therefore is non-zero. The production of entropy comes from terms such as $\overleftrightarrow{\tau}:\overleftrightarrow{\varepsilon}$, where $\overleftrightarrow{\tau}$ is the viscous stress tensor and $\overleftrightarrow{\varepsilon}$ is the rate of strain tensor, and $-(\vec{q}\cdot\nabla T)/T^2$, where $\vec{q}$ is the heat flux vector and T is the temperature. Thus, as Equations (3.25) and (3.34) indicate, there is entropy production in free-molecule flow even though there is no H production, and in this sense the flow is irreversible. It is legitimate to question here what the meaning of entropy is in the free-molecule situation where the flow is very far from thermodynamic equilibrium. The interested reader can pursue this question in Truesdell (1969).

The absolute difference between the H-Function H_o and an appropriately defined entropy function S_o introduces a measure of the degree of non-equilibrium present in the flow field. For regions of equilibrium we would expect

$$|H_o - S_o| = 0$$

and as the flow departed from equilibrium this difference would be expected to vary from zero, the maximum occurring in the region of maximum non-equilibrium.

For the general expansion problem with differing gases at differing temperatures we define the H-Function as:

$$\rho H(r,t) = \sum \rho_i H_i , \qquad i = 1,2$$

with

$$n_i H_i = \int f_i \ell n f_i \, d\vec{\xi} .$$

The H_i are then normalized by introducing an appropriately defined H-Function, or:

$$n_i\bar{H}_i = \int f_i \ln(f_i/f_{ref})d\vec{\xi}$$

where

$$f_{ref} = n_{11}(\beta_1/\pi)^{3/2}\exp(-C)$$

with C some unknown function which is eliminated from the calculation by further non-dimensionalizing $\bar{H}$. The dimensionless H-Function is written as:

$$H_o = \frac{\bar{H}(R,\tau) - \bar{H}(R\to\infty,\tau)}{\bar{H}(R\to 0,\tau) - \bar{H}(R\to\infty,\tau)}$$

so that $H_o(R\to\infty,\tau)$ goes to zero and $H_o(R\to 0,\tau)$ goes to 1.

For mathematical illustration the H-Function equation is presented only for Case 1 ($m_1 = m_2$ and $T_{11} = T_{22}$) but the general result is included in Fig. 3-14 for a qualitative comparison. The Case 1 solution is given by:

$$H_o = \frac{3\bar{T}/2 + V^2 - 3/2 + \ln\Delta[(N-\Delta)/(1-\Delta)]/N}{3\bar{T}(0,\tau)/2 - 3/2 + \ln\Delta[(N(0,\tau)-\Delta)/(1-\Delta)]/N(0,\tau)} \qquad (3.38)$$

where all variables and their limits have been previously defined in Equations (3.10), (3.12), (3.23) and (3.24).

The entropy function, S_o, is derived from Gibbs equation by appropriate normalization and non-dimensionalizing so that $S_o(R\to 0,\tau)$ goes to one and $S_o(R\to\infty,\tau)$ goes to zero. The Case 1 mathematical expression is given by:

$$S_o = \frac{(3/2)\ln\bar{T} - \ln N + \ln\Delta}{(3/2)\ln\bar{T}(0,\tau) - \ln N(0,\tau) + \ln\Delta} \; . \qquad (3.39)$$

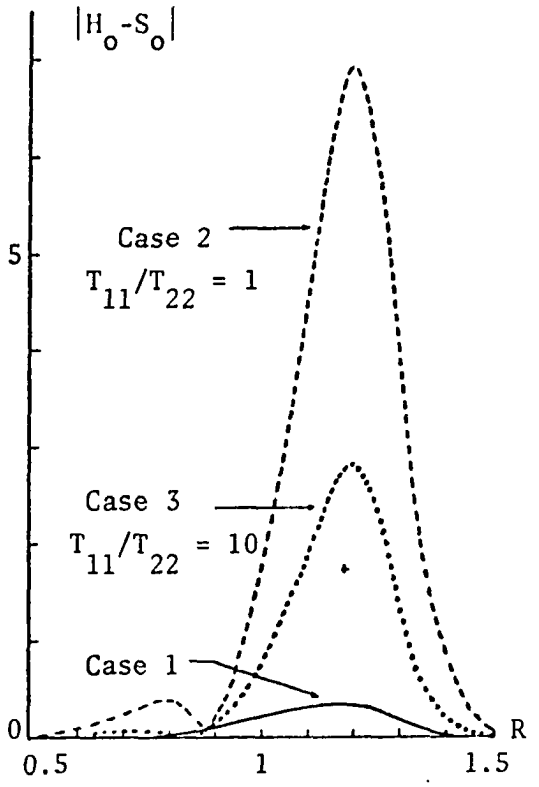


Fig. 3-14. Non-Equilibrium Indicator for $\Delta = 0.1$ at $\tau_1 = 0.2$.

The non-equilibrium indicator, $|H_o-S_o|$, is shown in Fig. 3-14 for each case considered in the previous sections. Case 1 is seen to be more nearly in equilibrium than Cases 2 and 3. Also of interest is the significant effect of the mass ratio on non-equilibrium as compared with the temperature ratio, in fact the non-equilibrium indicator is less with $T_{11}/T_{22} = 50$ for $m_1/m_2 = 0.5$ than it is with $T_{11}/T_{22} = 10$. The maximum for $T_{11}/T_{22} = 50$ is indicated by (+) on Fig. 3-14.

The smaller maximum shown for Cases 2 and 3 for $R \approx .8$ could be due to a mixing non-equilibrium phenomenon associated with diffusion of differing species since this maximum does not occur for Case 1. Justification for the transport properties being linearly proportional to flow property gradients for Case 1 and not Cases 2 or 3 may be derived

from this effect as well as the fact that Case 1 is more nearly in equilibrium. In Chapter IV we find another interesting application of the non-equilibrium indicator in conjunction with a discussion of embryonic shock structure.

CHAPTER IV

EMBRYONIC SPHERICAL SHOCK WAVE DEVELOPMENT

The solutions obtained in Chapter III for the study of the propagation of an initial spherical density discontinutiy in a rarefied medium based on a large Knudsen-number approximation are also valid for the study of embryonic shock wave development. For this chapter we still assume a large Knudsen number but instead of basing it on the characteristic length L = a, the initial radius of the sphere, we use a length based on the initial mean thermal speed of the molecules inside the sphere, $L = \beta_1^{-\frac{1}{2}}t$ where $\beta_1^{-1} = 2kT_{11}/m_1$. Thus for the purposes of this chapter we are examining the spherical expansion in the vicinity of the initial discontinuity for short times, that is, prior to the first collisions among the molecules initially inside and outside the sphere.

Since we are interested in discussing the embryonic shock wave formation and not the effects of differing gases at differing temperatures this chapter assumes that $m_1 = m_2$ and $T_{11} = T_{22}$. In essence, then, we are considering Case I as defined in Chapter III.

Basis for Analysis

A three-dimensional analysis of embryonic shock wave formation was motivated by studies made by Bienkowski (1965) and Yates and Karamcheti (1967) on one-dimensional (shock-tube type) expansions.

For a better understanding of the three-dimensional results the one-dimensional problem will be discussed first. This is a convenient starting place since the inviscid exact solutions are available for comparison with the free-molecule results.

In the one-dimensional shock-tube problem the pertinent characteristic length is the distance traveled by a molecule having a mean thermal speed $\beta^{-\frac{1}{2}} = (2kT/m)$ in the time t measured from the instant a diaphragm is burst, that is $L = \beta^{-\frac{1}{2}}t$. Thus the Knudsen number will be large in this case when the time is sufficiently short (and the distance from the diaphragm correspondingly small).

The region of validity for the short-time kinetic solution is best understood by examining a long-time x-t diagram as is given by Fig. 4-1. This diagram is made up of a line representing the shock wave, a contact surface line separating the fluid that has been shocked from the fluid that has not been shocked and an expansion fan. Since the shock itself is a collisional phenomenon and the large Knudsen-number solutions are based on a collisionless assumption, the time of observation by necessity must be short and the distance from the diaphragm correspondingly small. We are restricted then to a study of the region near $x = 0$ and $t = 0$ on Fig. 4-1.

The one-dimensional results of interest obtained by Yates and Karamcheti are shown in Figs. 4-2 through 4-5. The inviscid solution is shown by the dashed profiles with the regions of the x-t diagram clearly evident in the density profile of Fig. 4-2 and the temperature profile of Fig. 4-4. The horizontal axis in these figures represents the similarity parameter x/t. The one-dimensional free-molecule

solutions are shown by the solid line profiles. The compression ratio for this example is 10, or the driver gas is ten times more dense than the driven gas.

It is obvious from Figs. 4-2 and 4-3 that the free-molecule solutions do not exhibit the discontinuities of the inviscid solutions; instead they are spread out and look more like diffusion phenomena. From the billiard-ball analysis of Chapter II this analogy is obvious. Qualitatively, however, the similarity of the inviscid solution, which is valid for small-Knudsen numbers and long times, and the free-molecule solution, valid for large Knudsen numbers and short times, is striking. Even more striking is the comparison of the inviscid and free-molecule results of Figs. 4-4 and 4-5. In Fig. 4-4 the temperature in the free-molecule case is already showing the inviscid collisional distribution. This is also true for the velocity shown in Fig. 4-5. The effects of collisions can be thought of as steepening these gradients until a discontinuity is produced in the density and pressure. The free-molecule results are thus the first approximation to a systematic iterative scheme for the Boltzmann equation. This notion will be

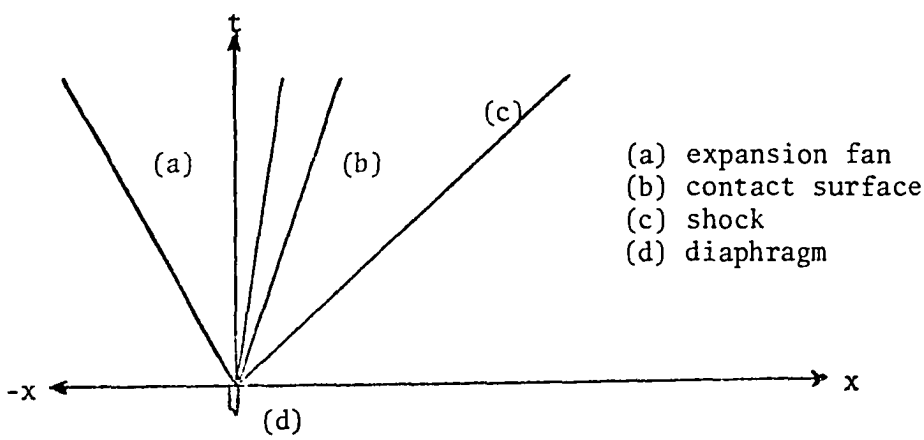


Fig. 4-1. Macroscopic Shock-Tube Phenomena in the x-t Diagram.

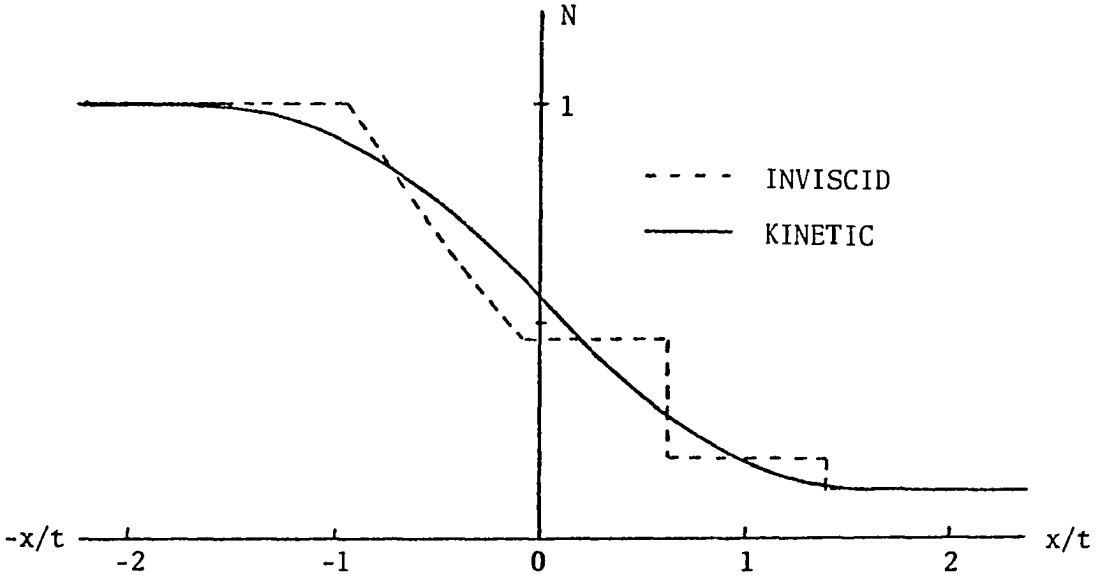


Fig. 4-2. Shock-Tube Density Profiles for $\Delta^{-1} = 10$.

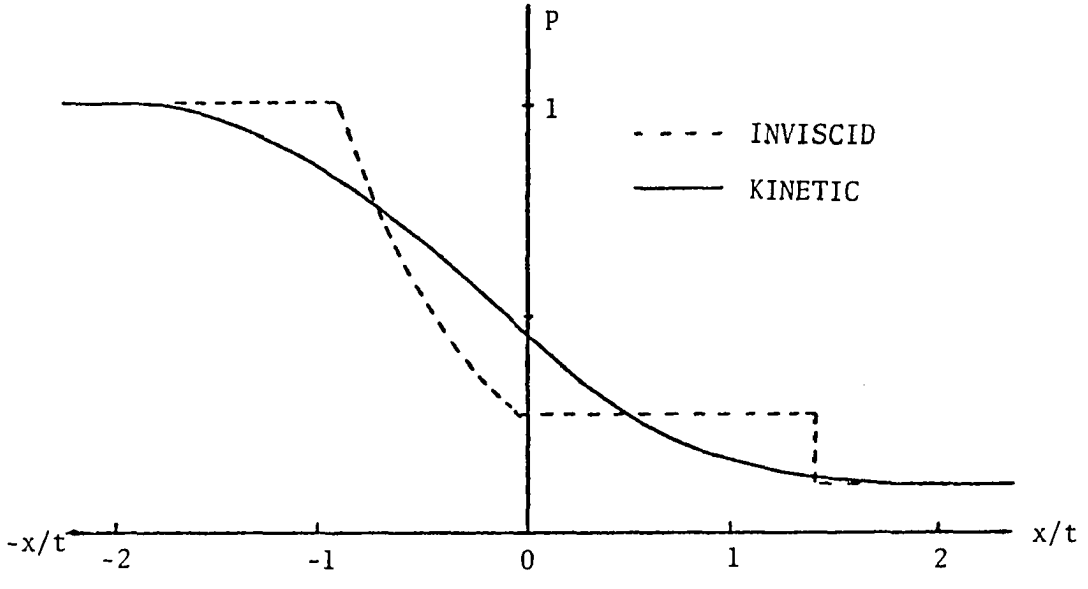


Fig. 4-3. Shock-Tube Pressure Profiles for $\Delta^{-1} = 10$.

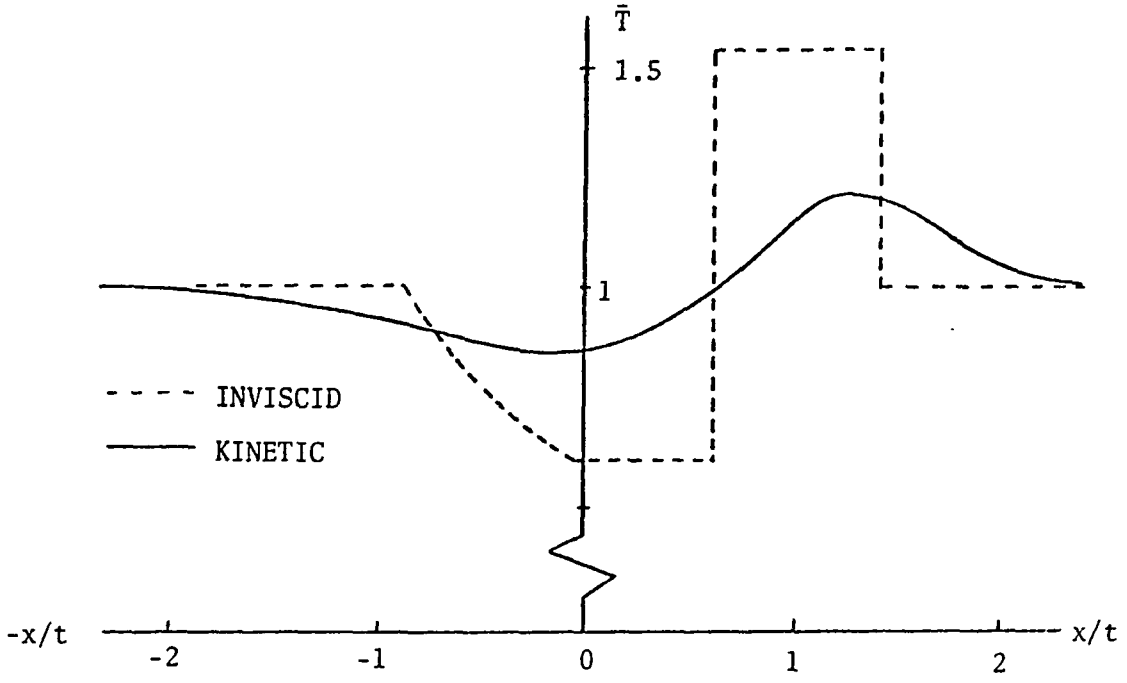


Fig. 4-4. Shock-Tube Temperature Profiles for $\Delta^{-1} = 10$.

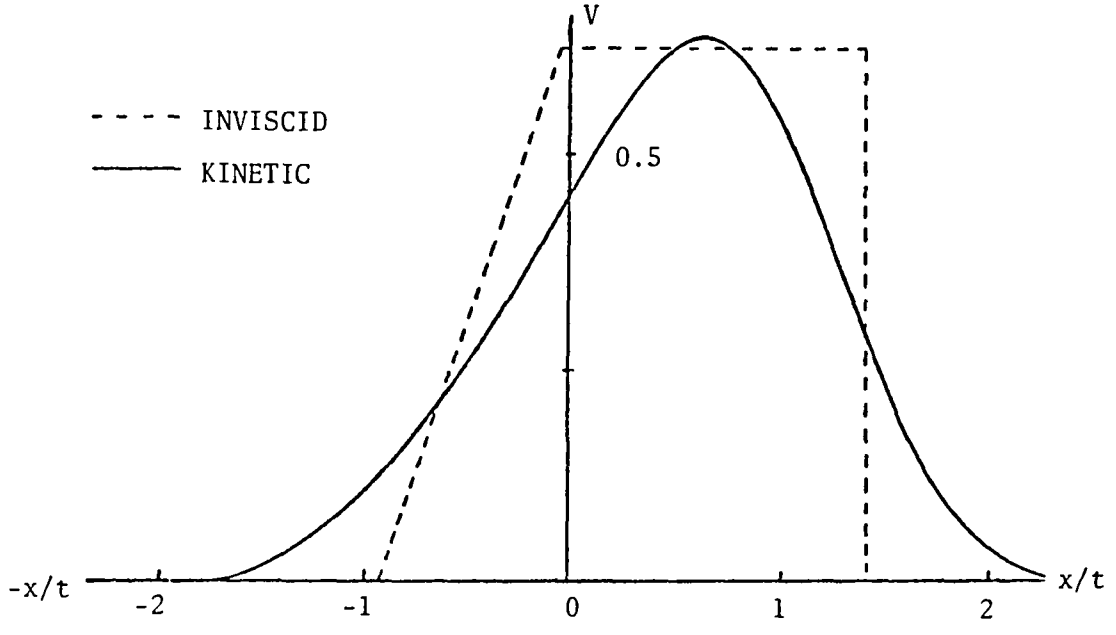


Fig. 4-5. Shock-Tube Velocity Profiles for $\Delta^{-1} = 10$.

pursued in Chapter V in our investigation of nearly free-molecule flow. From this discussion we can perceive the description of the embryonic shock wave development by means of free-molecule solutions.

Three-Dimensional Results

With the assumption that $m = m_1 = m_2$ and $T_{11} = T_{22}$ the relations given by Equations (3.10) through (3.15) may be written in a more convenient and simpler form. If we let

$$R \equiv r/a$$

$$\tau \equiv t/a\beta^{\frac{1}{2}}$$

$$A \equiv (1+R)/\tau$$

$$B \equiv (1-R)/\tau$$

with

$$\beta \equiv m/2kT_{11}$$

the non-dimensional flow variables can be written as

Number Density

$$N = \Delta + \frac{(1-\Delta)}{2}\left\{\frac{\tau}{\pi^{\frac{1}{2}}R}\left[e^{-A^2}-e^{-B^2}\right] + [\mathrm{erf}A+\mathrm{erf}B]\right\} \tag{4.1}$$

Radial Velocity

$$V = \frac{(1-\Delta)}{2\pi^{\frac{1}{2}}N}\left[\left(\frac{\tau^2}{2R^2}+\frac{1}{R}\right)e^{-A^2}-\left(\frac{\tau^2}{2R^2}-\frac{1}{R}\right)e^{-B^2}\right] \tag{4.2}$$

Temperature

$$\bar{T} = 1 + \frac{(1-\Delta)}{3\pi^{\frac{1}{2}}NR\tau}\left[e^{-A^2}-e^{-B^2}\right] + \frac{2}{3}\left[\frac{R}{\tau}V - V^2\right] \tag{4.3}$$

Radial Stress

$$S_{RR} = -N\left[1-2V^2 + 2V\left(\frac{\tau}{R}+\frac{R}{\tau}\right)\right] - \frac{(1-\Delta)}{\pi^{\frac{1}{2}}R\tau}\left[e^{-A^2} - e^{-B^2}\right] \tag{4.4}$$

Angular Stress

$$S_{\Theta\Theta} = S_{\Psi\Psi} = - N(1- \frac{\tau}{R}V) \tag{4.5}$$

Radial Heat Flux

$$Q = \frac{(1-\Delta)}{\pi^{\frac{1}{2}}\tau^2} [e^{-A^2} - e^{-B^2}] + NV[3-V^2 + \frac{(1+R^2)}{\tau^2}] - \frac{3N\bar{T}V}{2} + VS_{RR} \tag{4.6}$$

Other velocity, stress and heat-flux components are zero.

Spherical Shock Analysis

In contrast to the analogous one-dimensional problem, the spherical problem is not self-similar. Hence the flow variables given by Equations (4.1) through (4.6) cannot be represented, for a given density ratio Δ, by a single curve for all times and spacial positions. As in the one-dimensional problem the pertinent characteristic length is the distance traveled by a molecule having a thermal speed $\beta^{-\frac{1}{2}} = (2kT_{11}/m)^{\frac{1}{2}}$, or $L = \beta^{-\frac{1}{2}}t$.

There is an analogous r-t diagram for the spherical problem as for the one-dimensional problem given by Fig. 4-1. Friedman (1961) by means of characteristics produced the r-t diagram given by Fig. 4-6. A noticeable difference between Figs. 4-1 and 4-6 is the inclusion of a secondary shock wave which occurs in the continuum limit. The shock waves and contact surface are no longer straight lines in the r-t diagram. This reflects the influence of the distribution of the energy of the outward propagating shock over a larger surface area as the wave propagates outward.

The physical reason for the secondary shock formation is that the gas in the expansion region has been expanded to a lower pressure than that reached in the one-dimensional problem. This is due to the increase in volume of the sphere of gas as it propagates outward. The pressures at the tail of the expansion wave are less than the pressures transmitted by the leading shock; hence a shock is inserted to connect the two phases.

The region of interest for the spherical analysis is for time slightly greater than t = 0 and for radius near r = a. For this region sufficient time has not elapsed for the secondary shock to form. The free-molecule results, therefore, will not give us insight in to its embryonic development. It would be necessary to consider a higher order approximation than free-molecule flow before the secondary shock would be detected.

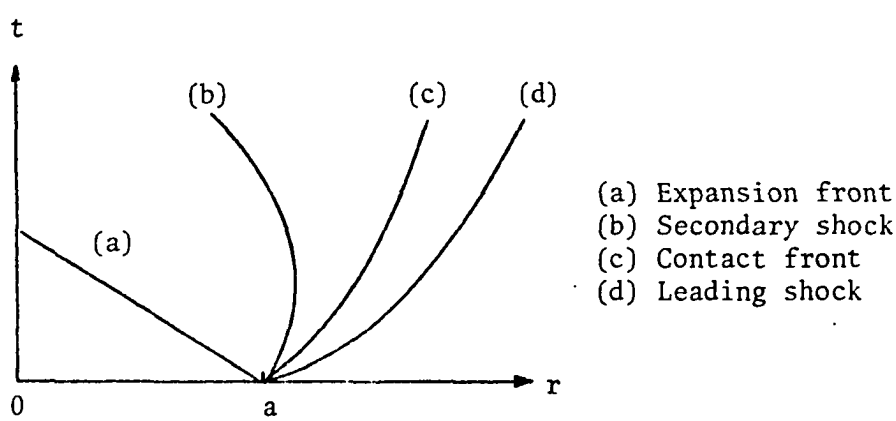


Fig. 4-6. Macroscopic Spherical Shock Phenomena in the r-t Diagram.

Inviscid Acoustics for Spherical Explosions

An exact continuum-theory solution for the spherical problem is not available as it is for one-dimensional expansions. An inviscid acoustic description of the equivalent continuum problem can, however, be easily obtained and is adequate for a qualitative comparison with the kinetic results. The inviscid acoustic approximation is valid for small Knudsen numbers ($\lambda/a \to 0$) and long times, whereas the free-molecule solution is valid for large Knudsen numbers ($\lambda/a \to \infty$) or short times.

The linearized versions of the inviscid Euler equations are:

$$\frac{\partial \rho}{\partial t} + \rho_{22} \operatorname{div} \vec{u} = 0 \tag{4.7a}$$

$$\rho_{22} \frac{\partial \vec{u}}{\partial t} = -\nabla p \tag{4.7b}$$

and

$$\frac{\partial s}{\partial t} = 0 \ . \tag{4.7c}$$

This gives a set of linear, first-order, partial differential equations. Integration of the energy equation gives

$$s = s(r) \ . \tag{4.8}$$

From the equation of state we have $\rho = \rho(p,s)$ so we can obtain the relation

$$\frac{\partial \rho}{\partial t} = \frac{1}{a_o^2} \frac{\partial p}{\partial t} \tag{4.9}$$

where $a_o = \left(\gamma \frac{k}{m} T_{22}\right)^{\frac{1}{2}}$ is the ambient speed of sound and γ is the ratio of specific heats. Substitution of Equation (4.9) into Equation (4.7a), differentiating with respect to time and combining with Equation (4.7b)

gives

$$\frac{\partial^2 p}{\partial t^2} - a_o^2 \nabla^2 p = 0 \ . \tag{4.10}$$

Since the flow is irrotational we can write the velocity in terms of a velocity potential, ϕ, or $\vec{u} = \nabla\phi$. Then from Equation (4.7b) we obtain

$$p - p_{22} = - \rho_{22} \frac{\partial \phi}{\partial t} \tag{4.11a}$$

and from Equation (4.10)

$$\phi_{tt} - a_o^2 \nabla^2 \phi = 0 \ ,$$

the acoustic equation. In spherical coordinates, for the spherical explosion problem, we have

$$r\phi_{tt} - a_o^2 (r\phi)_{rr} = 0 \ . \tag{4.11b}$$

For the initial conditions $u(r,0) = 0$ and $p(r,0) = p_{22} + \frac{1-\Delta}{\Delta} p_{22} H(a^2-r^2)$, the potential is found from Equation (4.11b) to be

$$\phi(r,t) = \frac{a_o}{4\gamma r} \left(\frac{1-\Delta}{\Delta}\right) [\zeta^2 H(a^2-\zeta^2) + a^2 H(\zeta^2-a^2) - \eta^2 H(a^2-\eta^2) - a^2 H(\eta^2-a^2)] \tag{4.12}$$

where $\zeta = r - a_o t$ and $\eta = r + a_o t$. From the velocity potential the non-dimensional radial velocity is found to be

$$V = \frac{\phi_r}{a_o} = \frac{1-\Delta}{4\gamma\Delta} \left\{ \left(1 - \frac{\tau_c^2}{R^2}\right) [H(1-\bar{\zeta}^2) - H(1-\bar{\eta}^2)] - \frac{1}{R^2} [H(\bar{\zeta}^2-1) - H(\bar{\eta}^2-1)] \right\} \tag{4.13}$$

where $\tau_c = \frac{a_o t}{a}$, $\bar{\zeta} = R - \tau_c$ and $\bar{\eta} = R + \tau_c$.

The non-dimensional pressure follows from Equation (4.11a):

$$P = \frac{1-\Delta}{2} \left[\left(1 - \frac{\tau_c}{R}\right) H(1-\bar{\zeta}^2) + \left(1 + \frac{\tau_c}{R}\right) H(1-\bar{\eta}^2) \right] + \Delta. \tag{4.14}$$

In order to determine the density and temperature we let

$$p = p_{22}(1+p')$$
$$\rho = \rho_{22}(1+\rho') \qquad (4.15)$$
$$T = T_{22}(1+T')$$

and

$$s' = (s-s_{22})/C_v$$

where the primed quantities are much less than unity and C_v is the specific heat at constant volume. From Gibbs equation we obtain the relation

$$s' = T' - (\gamma-1)\rho' \ . \qquad (4.16)$$

The thermal equation of state is written as

$$p' = \rho' + T' \ . \qquad (4.17)$$

From Equations (4.16) and (4.17) and the initial conditions

$$s'(r,0) = -(\gamma-1)\frac{1-\Delta}{\Delta} H(a^2-r^2)$$

the non-dimensional forms of the density and temperature are found to be:

$$N = \frac{1}{\gamma} P + \frac{\gamma-1}{\gamma}[\Delta+(1-\Delta)H(1-R^2)] \qquad (4.18a)$$

and

$$\tilde{T} = 1 + \frac{\gamma-1}{\gamma\Delta}[P-\Delta-(1-\Delta)H(1-R^2)] \ . \qquad (4.18b)$$

The acoustic solutions given by Equations (4.13) and (4.18) are discontinuous, with an outward propagating compression wave and for $a_o t/a<1$ an inward propagating expansion wave. A contact surface exists at R = 1. The various regions of the solutions are shown in Fig. 4-7, a r-t diagram.

The outward propagating compression wave represents a weak shock wave. The contact surface exists due to the initial variation in entropy. Although the acoustic problem is isentropic it is not homentropic since $s' = s'(r) = -(\gamma-1)\frac{1-\Delta}{\Delta} H(a^2-r^2)$. The contact surface remains at r = a since the entropy is initially discontinuous at r = a and does not vary with time or radius.

The density, velocity, and temperature relations of Equations (4.13) and (4.18), with the pressure term from Equation (4.14), are plotted in Figs. 4-8 through 4-10 for $\tau = (2/\gamma)^{\frac{1}{2}}\tau_c = 0.1$, $\Delta = 0.6$ and $\gamma = 5/3$ for monatomic molecules. The corresponding free-molecule results from Equations (4.1) through (4.3) are shown on the same figures for comparison.

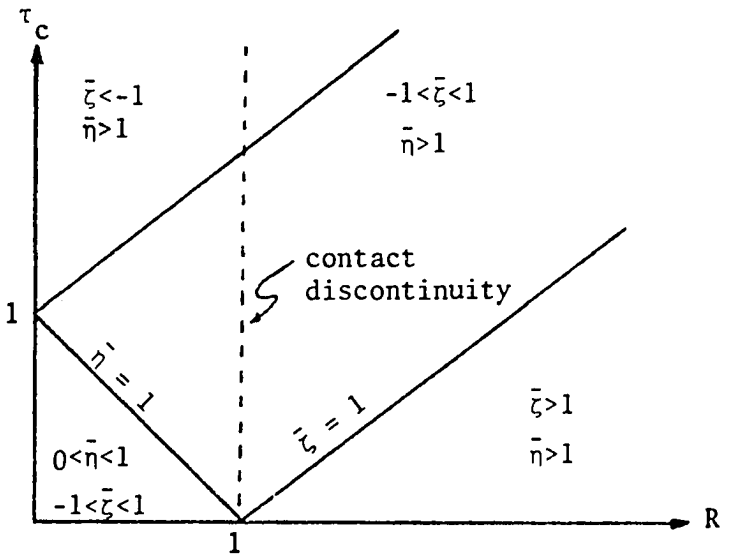


Fig. 4-7. Regions of Inviscid Acoustic Solution.

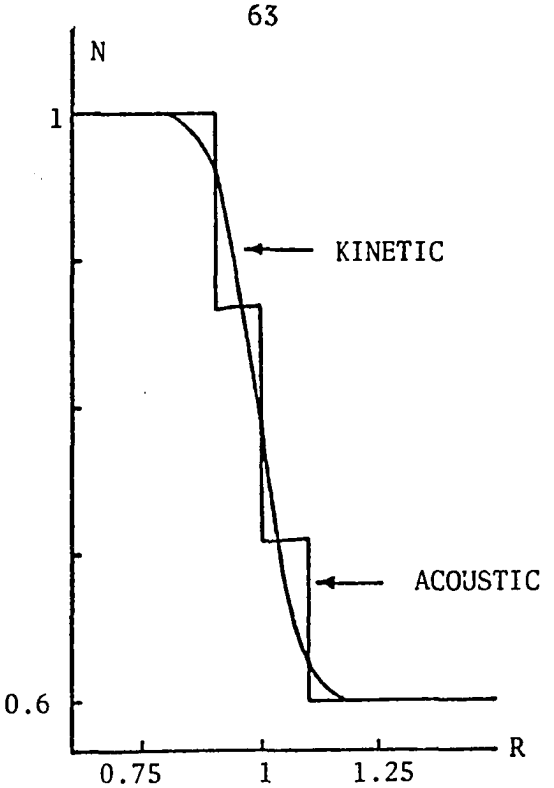


Fig. 4-8. Comparison of Kinetic and Acoustic Number Density for $\Delta = 0.6$ at $\tau = 0.1$.

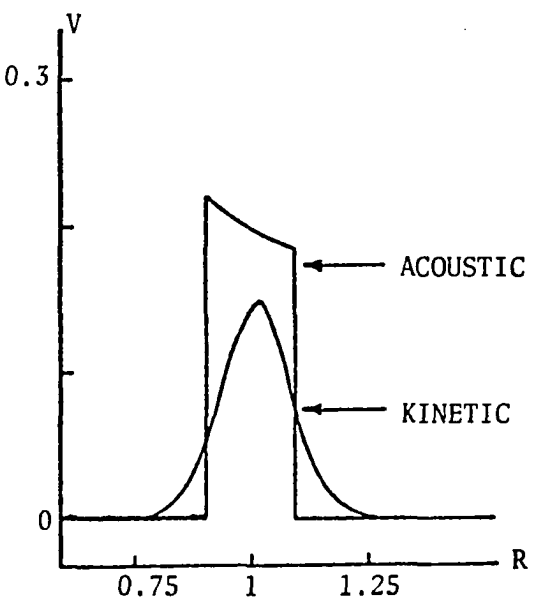


Fig. 4-9. Comparison of Kinetic and Acoustic Velocities for $\Delta = 0.6$ at $\tau = 0.1$.

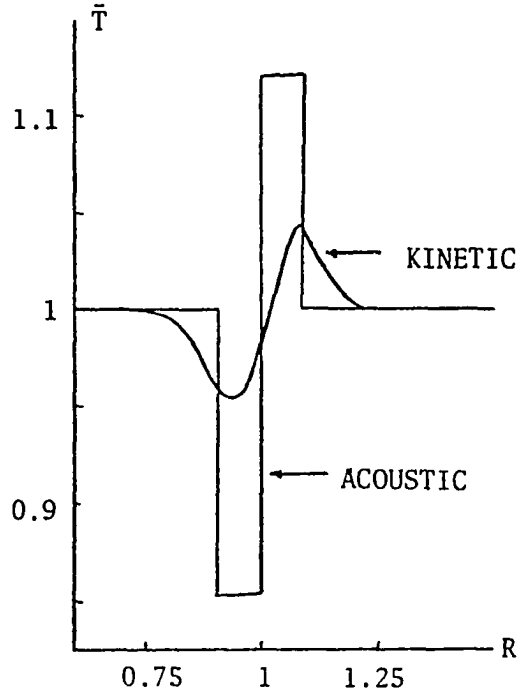


Fig. 4-10. Comparison of Kinetic and Acoustic Temperatures for $\Delta = 0.6$ at $\tau = 0.1$.

The free-molecule results give a smoothed out version of the acoustic results. The velocity and temperature reflect the same behavior in both cases, with the free-molecule results developing much less in magnitude than the corresponding linear acoustic results. The effects of collisions would be to steepen the front of the kinetic curves so that they would develop into a steep shock front. In this respect, as it was seen for the one-dimensional expansion, the free-molecule results describe the embryonic development of the outward propagating shock.

Strong Explosions

Strong explosions occur when the compression ratio Δ^{-1} is very large. It is interesting to compare the case of a strong explosion $\Delta = 10^{-5}$ with the limiting case of expansion into a vacuum, $\Delta = 0$.

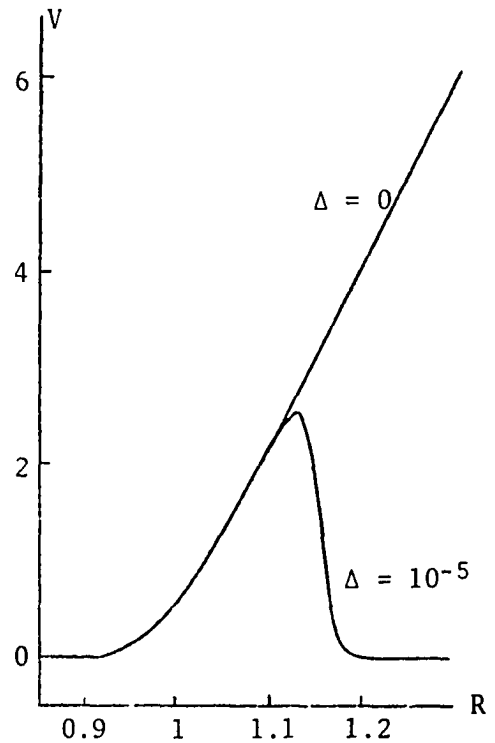


Fig. 4-11. Comparison of Velocities for Strong Explosion and Expansion into a Vacuum for $\tau = 0.05$.

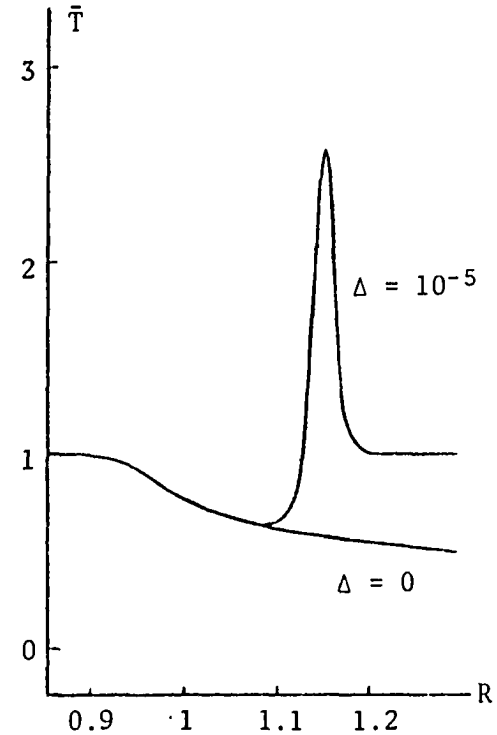


Fig. 4-12. Comparison of Temperatures for Strong Explosion and Expansion into a Vacuum for $\tau = 0.05$.

For $\tau = 0.05$ the free-molecule velocity profiles for $\Delta = 10^{-5}$ and $\Delta = 0$ are shown in Fig. 4-11 and the corresponding curves for temperature are shown in Fig. 4-12. A steep velocity gradient is noted for the outward propagating velocity front for the strong explosion and a very strong temperature rise is found only for the strong explosion, $\Delta = 10^{-5}$. For $\Delta = 0$, an asymptotic expansion for large $X \equiv (R-1)/\tau$ shows that the velocity grows asymptotically like X whereas the temperature decreases asymptotically like 2/3R, which reflects the result that more fast molecules escape the spherical region than slow ones. In the continuum limit the Euler equations would yield isentropic solutions for expansion into a vacuum. Thus smoothed-out shock wave behavior would be

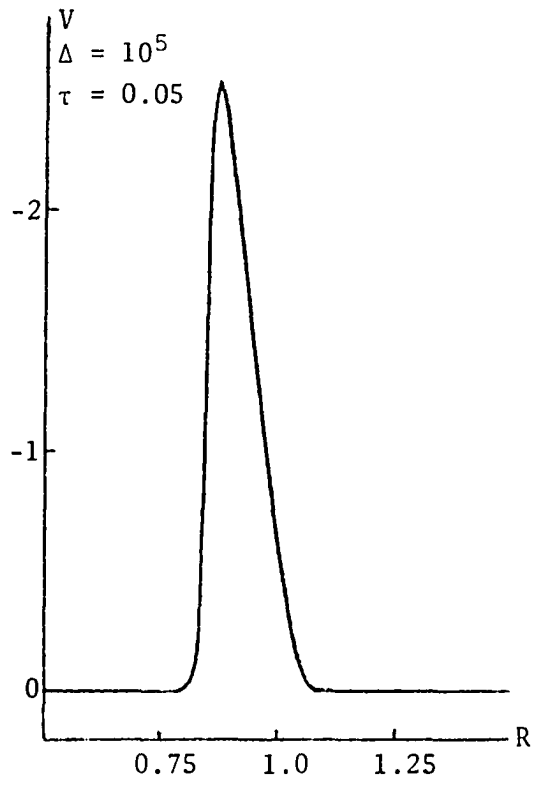


Fig. 4-13. Velocity for a Strong Implosion with $\Delta = 10^5$ at $\tau = 0.05$.

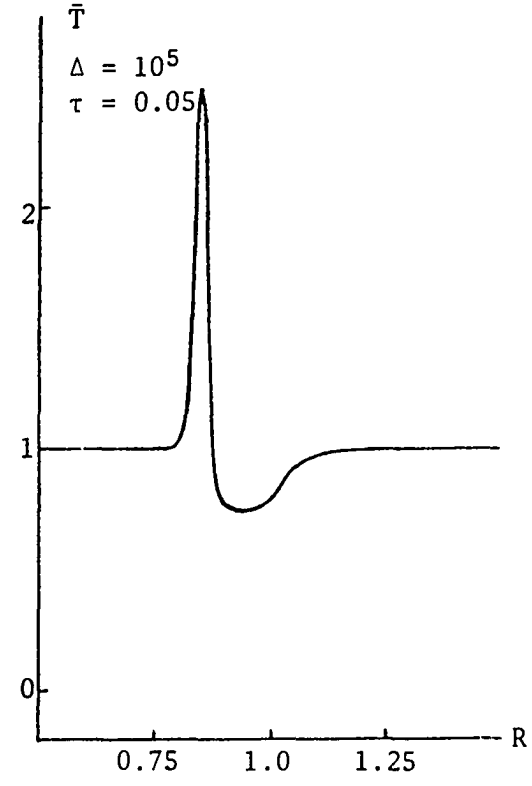


Fig. 4-14. Temperature for a Strong Implosion with $\Delta = 10^5$ at $\tau = 0.05$.

expected for strong explosions, but not for expansions into a vacuum. The expansion behind the steep temperature rise in the strong explosion is also typical of the flow that develops behind a shock wave in a shock tube. Thus as in the one-dimensional study by Yates and Karamcheti, the free-molecule flow represents the embryonic formation of the shock wave.

Strong Implosion

The spherical problem also allows for strong implosions. In Figs. 4-13 and 4-14 the large density ratio results for velocity and temperature are shown for $\Delta = 10^5$ and $\tau = 0.05$. In this case the compression wave of the higher density exterior gas propagates inward and the steep velocity and temperature gradients reflect the initial development of an inward propagating shock wave.

H-Function and Entropy

The non-equilibrium indicator, $|H_o-S_o|$, discussed in Chapter III has a more significant application in this chapter. Since a shock wave is a highly non-equilibrium phenomena we would expect the non-equilibrium indicator to reflect the presence of the embryonic shock wave. For the strong explosion case with $\Delta = 10^{-5}$ and $\tau = 0.05$, Fig. 4-15 presents the non-equilibrium indicator profile. It is obvious that the maximum difference between the H-Function and the entropy function occurs at $R \simeq 1.15$ which we label macroscopically as the region of maximum non-equilibrium. That is, the gradients of macroscopic quantities are maximum there.

The behavior of the normalized H-Function H_o and the entropy S_o is plotted in Fig. 4-16 for $\Delta = 10^{-5}$, $\Delta = 0$, and $\tau = 0.05$. For $\Delta = 10^{-5}$, the two curves are qualitatively the same, being slightly greater than unity in the colder expansion region and slightly negative in the hotter compression region. The entropy curve, however, shows a much larger negative dip in the compression region. For expansion into a vacuum, $\Delta = 0$, both curves are unity; the non-equilibrium indicator being zero everywhere indicating the absence of a region of non-equilibrium.

A further study of the non-equilibrium indicator for $\Delta = 10^{-5}$ and $\tau = 0.01$, 0.03, and 0.07 shows that the maximum value is approximately the same as that given in Fig. 4-15 and moves outward linearly from R = 1 at a speed $V_{n-e} = 3(\frac{2}{\gamma})^{\frac{1}{2}} a_o$. For air ($\gamma$=7/5) the speed of a one-dimensional shock wave in a shock tube with a compression ratio of

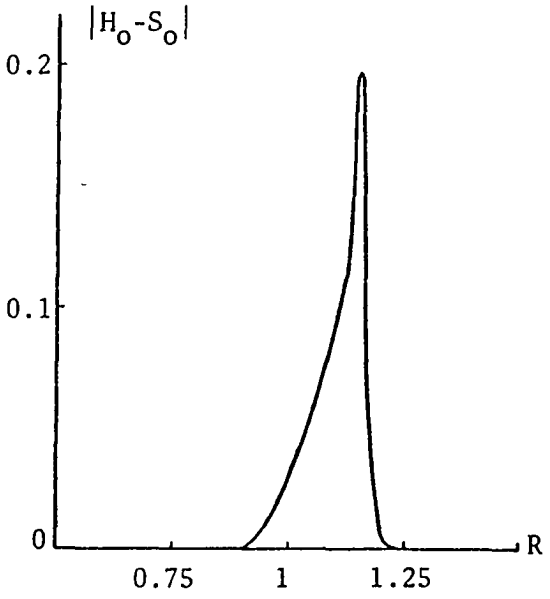


Fig. 4-15. Non-Equilibrium Indicator Profile for $\Delta = 10^{-5}$ at τ=0.05.

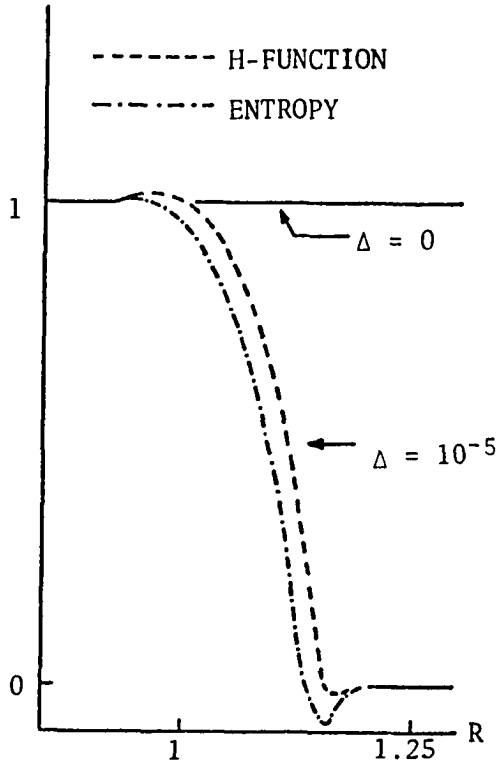


Fig. 4-16. H-Function and Entropy Function for Free-Molecule Flow, $\Delta = 10^{-5}$, $\Delta = 0$, and $\tau = 0.05$.

10^5 [see Fig. 3.9 Liepmann and Roshko (1957)] is approximately $V_s = 4.6a_o$. The region of maximum non-equilibrium seemingly propagates outward slower than the one-dimensional shock. Possibly this could be anticipated in that the free-molecule values of velocity and temperature are less than the inviscid-acoustic values as shown in Fig. 4-9 and Fig. 4-10. We conclude that the non-equilibrium indicator locates the region of embryonic shock wave formation and supports the concepts developed in this chapter that by the analysis of collisionless kinetic theory for short times the embryonic development of spherical shock waves can be studied.

CHAPTER V

NEARLY FREE-MOLECULE FLOW EXPANSIONS

In this chapter we formulate a solution for large Knudsen number expansions with collisions. We consider Case 1 of Chapter III with $m_1 = m_2$ and $T_{11} = T_{22}$. The governing kinetic equation for large Knudsen-number expansions is, as suggested by Kogan (1969),

$$\frac{Df}{Dt} = \bar{\varepsilon} J(f,f) \tag{5.1}$$

where $\bar{\varepsilon} = L/\lambda = Kn^{-1} << 1$. The characteristic length L can be either the initial radius of the sphere or the distance traveled by a molecule having a thermal speed $\beta^{-\frac{1}{2}}$ as discussed in Chapter I. The mean free path λ is assumed the same for all molecules. The left side of Equation (5.1) is given by Equation (2.11) without the subscript i.

The kinetic equation is called the Boltzmann equation when we let

$$J(f,f) = J_1 - fJ_2 \tag{5.2}$$

where

$$J_1 = \int f' f_1' g b db d\varepsilon d\vec{\xi}_1$$

and

$$J_2 = \int f_1 g b db d\varepsilon d\vec{\xi}_1 \ .$$

The integrations in J_1 and J_2 are five-fold, three on velocity space $\vec{\xi}_1$, one on the impact parameter plane b and one over all angles ε. These variables are shown in Figs. 5-1 and 5-2. Note that $d\vec{\xi}_1$ is the

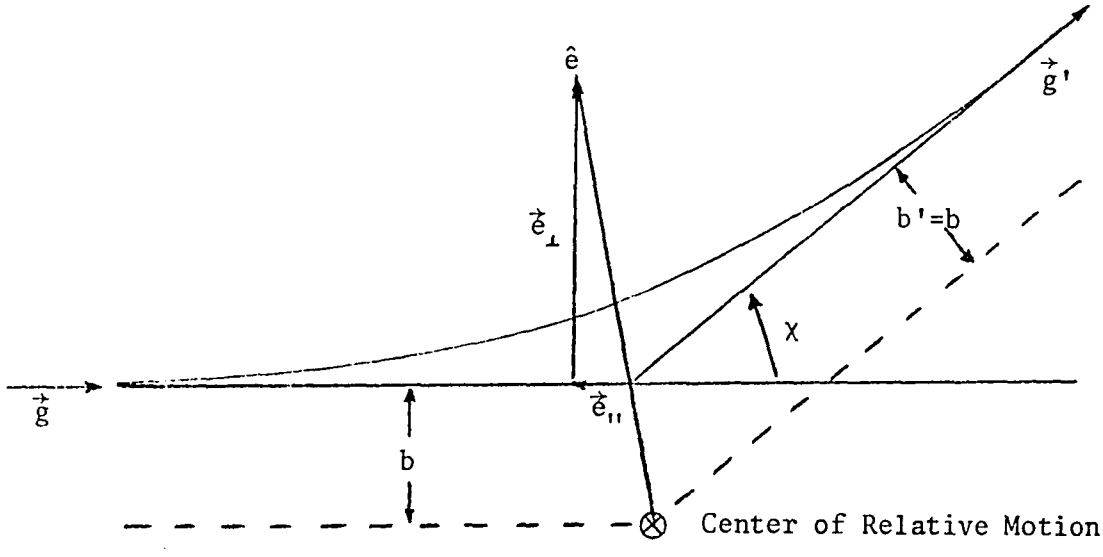


Figure 5-1. Collision Plane

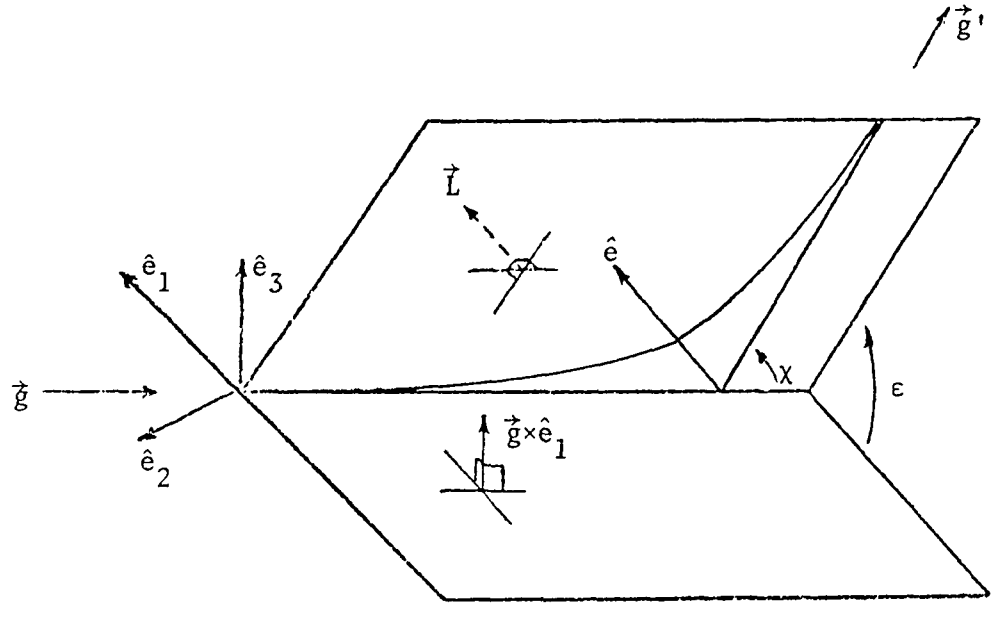


Figure 5-2. Orientation of Collision Plane.

volume element in $\vec{\xi}_1$ space and that J_2 for instance gives the total number of collisions experienced by ξ-molecules with all ξ_1-molecules. Furthermore,

$$\begin{aligned} f &= f(\vec{r},\vec{\xi},t) \\ f' &= f(\vec{r},\vec{\xi}',t) \\ f_1 &= f(\vec{r},\vec{\xi}_1,t) \\ f_1' &= f(r,\vec{\xi}_1',t) \end{aligned} \tag{5.3}$$

and the velocity vectors before a binary collision between ξ-molecules and ξ_1-molecules are unprimed and those after are primed. The relative velocity vector between the colliding molecules is given by $\vec{g} = \vec{\xi}_1 - \vec{\xi}$.

The initial condition for Equation (5.1) is Maxwellian and given by

$$f_o(\vec{r},\vec{\xi}) = n_{11}(\beta/\pi)^{3/2}\exp(-\beta\xi^2)[H(a-r)+\Delta H(r-a)] \ . \tag{5.4}$$

The differentiation of Equation (5.1) is carried out along the straight-line trajectory of a given molecule.

The form of the nearly free-molecule solution can thus be written as:

$$f(\vec{r},\vec{\xi},t) = f(\vec{r}-\vec{\xi}t,\vec{\xi},\ 0) + \bar{\varepsilon}\int_0^t J[\vec{r}-\vec{\xi}(t-\tau),\vec{\xi},\tau]d\tau \tag{5.5}$$

where τ is some time between zero and t. A physical interpretation of this solution can be deduced from Fig. 5-3.

Consider a packet of molecules with velocity $\vec{\xi}$ and a density given by the molecular distribution function $f(\vec{r},\vec{\xi},0)$ initially at A. The packet traverses the path AC and undergoes a change in density ending up with a distribution function $f(\vec{r},\vec{\xi},t)$. The net change in density is due to the integrated effect of inverse and direct collisions experienced

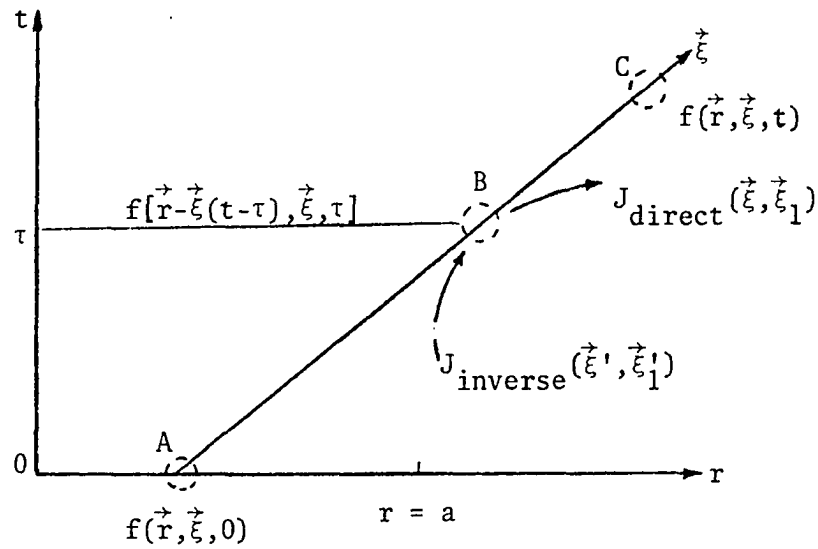


Figure 5-3. Graphic Interpretation of the Collisional Distribution Function.

by the packet. The inflow and outflow of molecules in the packet due to collisions as indicated at point B is typical. In general, collisions of ξ-molecules with ξ_1-molecules result in ξ'-molecules and ξ_1'-molecules respectively (and vice versa).

It is possible to seek the solution of Equation (5.1) as a series of $\bar{\varepsilon}$ such that

$$f = f^{(o)} + \bar{\varepsilon} f^{(1)} + O(\bar{\varepsilon}^2) \quad . \tag{5.6}$$

By substituting this series into (5.1) and equating like orders of $\bar{\varepsilon}$ we obtain a set of differential equations. For the purposes of this analysis we consider only the first-order approximation. The first-order differential equation is

$$\frac{Df^{(1)}}{Dt} = J[f^{(o)},f^{(o)}] \tag{5.7}$$

where $f^{(o)}$ is the zeroth order solution obtained previously for the collisionless problem, or

$$f^{(o)}(\vec{r},\vec{\xi},t) = n_{11}(\beta/\pi)^{3/2}\exp(-\beta\xi^2)[H(a-r_o)+\Delta H(r_o-a)] \qquad (5.8)$$

where r_o is given by Equation (3.8).

The solution to Equation (5.7) follows from (5.1), (5.2) and (5.5) and is written as

$$f^{(1)}(\vec{r},\vec{\xi},t) = \int_0^t J_1^{(o)}d\tau - f^{(o)}\int_0^t J_2^{(o)}d\tau \qquad (5.9)$$

since $f^{(1)}(\vec{r}-\vec{\xi}t,\vec{\xi},0) = 0$ to satisfy the initial conditions imposed.

To obtain the first-order solution the collision integrals $J_1^{(o)}$ and $J_2^{(o)}$ need to be evaluated. This will not be done in this study. Instead, the basic integrals will be set up and a discussion of the direct approach to finding the limits of integration will be presented.

In order to make the Boltzmann equation determinate an intermolecular force law must be assumed. For this study we shall assume psuedo-Maxwellian molecules [see Kogan (1969)]. Although this model does not particularly give an accurate representation of intermolecular forces in an actual gas it does afford a remarkable simplification of the collision integrals. This model allows us to write

$$gbdb = (16K/m)^{\frac{1}{2}}\rho d\rho$$

where K is a constant from the interaction force $F = 4K/r^{*5}$ with r^* being the distance between centers of the molecules. The replacement variable ρ is a parameter defined as

$$\rho = b(mg^2/16K)^{\frac{1}{4}} .$$

For these so-called pseudo-cutoff Maxwellian molecules we can

write the collision integrals of Equation (5.2) as:

$$J_1 = \left(\frac{16K}{m}\right)^{\frac{1}{2}} \int f^{(o)\prime} f_1^{(o)\prime} \rho d\rho d\varepsilon d\vec{\xi}_1 \tag{5.10}$$

and

$$J_2 = A \int f_1^{(o)} d\vec{\xi}_1 \tag{5.11}$$

where $A = (16K/m)^{\frac{1}{2}} \int_o^{\rho_o} \rho d\rho d\varepsilon$, a finite value.

From Equations (5.11), (5.8), and (2.2) the collision integral J_2 is easily evaluated to give

$$J_2 = An^{(o)}(\vec{r},\vec{\xi},t) \ . \tag{5.12}$$

The evaluation of J_1 is not as straightforward as J_2 owing to the term $f^{(o)\prime} f_1^{(o)\prime}$ in Equation (5.10). The molecular distribution functions of the ξ'-molecules and ξ_1'-molecules are written as

$$f^{(o)\prime} = n_{11}(\beta/\pi)^{3/2} \exp(-\beta\xi'^2)[H(a-r_o')+\Delta H(r_o'-a)] \tag{5.13}$$

and

$$f_1^{(o)\prime} = n_{11}(\beta/\pi)^{3/2} \exp(-\beta\xi_1'^2)[H(a-r_{o1}')+\Delta H(r_{o1}'-a)] \tag{5.14}$$

where r_o' and r_{o1}' are given as a $\text{fnc}(\vec{r},\vec{\xi},t,\vec{\xi}_1,\rho,\varepsilon)$. The constants of integration r_o' and r_{o1}' are written as

$$r_o'^2 = r^2 + 2r\xi_r't + \xi'^2t^2 \tag{5.15}$$

and

$$r_{o1}'^2 = r^2 + 2r\xi_{1r}'t + \xi_1'^2t^2 \tag{5.16}$$

with the relation between $\vec{\xi}'$, $\vec{\xi}_1'$ and $\vec{\xi}$, $\vec{\xi}_1$ given by

$$\vec{\xi}' = \vec{\xi} + (\vec{g}\cdot\hat{e})\hat{e} \tag{5.17}$$

and

$$\vec{\xi}_1' = \vec{\xi}_1 - (\vec{g}\cdot\hat{e})\hat{e} \tag{5.18}$$

where $(\vec{g}\cdot\hat{e})\hat{e}$ is the component of $\vec{g}$ parallel to the apse vector $\hat{e}$ shown in Fig. 5-1.

The substitution of Equations (5.13) and (5.14) into Equation (5.10) gives

$$J_1 = (\frac{16K}{m})^{\frac{1}{2}} n_{11}^2 (\frac{\beta}{\pi})^3 e^{-\beta\xi^2} \int e^{-\beta\xi_1^2} \tilde{H}\rho d\rho d\epsilon d\vec{\xi}_1 \ . \tag{5.19}$$

Considered in the writing of the exponent of Equation (5.19) is the conservation of energy of a collision which gives

$$\xi'^2 + \xi_1'^2 = \xi^2 + \xi_1^2 \ .$$

The function $\tilde{H}$ is a product of the Heaviside functions of Equations (5.13) and (5.14) and is written as

$$\tilde{H} = \Delta^2 + (1-\Delta)^2 H(a-r_o')H(a-r_{o1}') + (\Delta-\Delta^2)[H(a-r_o') + H(a-r_{o1}')] \ .$$

Thus Equation (5.19) can be written as the sum of four integrals:

$$J_1 = (16K/m)^{\frac{1}{2}} n_{11}^2 (\beta/\pi)^3 \exp(-\beta\xi^2)[\Delta^2 I_1 + (\Delta-\Delta^2)(I_2+I_3) + (1-\Delta)^2 I_4]$$

where

$$I_1 = \int \exp(-\beta\xi_1^2) d\vec{\xi}_1 \rho d\rho d\epsilon \tag{5.20}$$

$$I_2 = \int \exp(-\beta\xi_1^2) H(a-r_{o1}') d\vec{\xi}_1 \rho d\rho d\epsilon \tag{5.21}$$

$$I_3 = \int \exp(-\beta\xi_1^2) H(a-r_o') d\vec{\xi}_1 \rho d\rho d\epsilon \tag{5.22}$$

and

$$I_4 = \int \exp(-\beta\xi_1^2) H(a-r'_o) H(a-r'_{o1}) d\vec{\xi}_1 \rho d\rho d\varepsilon \ . \qquad (5.23)$$

The integrations of Equation (5.20) is straightforward, however, the evaluation of Equations (5.21) through (5.23) is much more complicated. This complication arises not because of the integrand but because of the limits of integration. The determination of these limits requires defining the spheres of integration $r'_{o1} < a$ and $r'_o < a$ in Equations (5.21) and (5.22) such that the limits are expressible as $\xi_1 = \xi_1(r,\xi,t,\rho,\varepsilon)$. The domain of integration of Equation (5.23) requires determining the intersection of the two spheres of integration given above.

In keeping with the purpose of this chapter we have formulated the collisional solution for nearly free-molecule flow expansions. The relation $(\vec{g}\cdot\hat{e})\hat{e}$ that is necessary to convert the primed molecular velocities to unprimed molecular velocities by means of Equations (5.17) and (5.18) is given in Appendix C.

CHAPTER VI

EXPANSIONS FOR SMALL KNUDSEN NUMBERS

For the last portion of this study we examine the viscous effects of spherical explosions by considering the continuum limit where the Knudsen number, based on the characteristic length $L = \beta^{-\frac{1}{2}}t$, goes to zero. The general characteristics of the short-time, weak explosion results are presented. For completeness of discussion the long-time solutions obtained by Rasmussen (1972) are included.

We consider the spherical expansion problem described by Case 1 in Chapter III where the gases inside and outside the sphere are the same and at the same initial temperature but have a density differential. As time progresses after the removal of the sphere boundary, for $Kn \to 0$, collisions increase in their importance until after a sufficient number of mean free times (average time between collisions) they become dominate. The proper equations, except in the region of the outward propagating shock wave present in sufficiently strong explosions, are the Navier-Stokes equations.

The exact general solution to the highly non-linear, viscous, heat conducting set of governing equations is indeed a difficult, if not impossible, problem. In this chapter a method is presented for obtaining an explicit viscous acoustic solution by linearizing the Navier-Stokes equations about a uniform ambient medium and applying

Laplace-transform techniques. This method has been used by Lick (1967) and Bienkowski (1965) to solve similar one-dimensional expansion problems.

By means of the viscous acoustic form of the Navier-Stokes equations we limit the application of the results to weak spherical explosions and must keep in mind that certain strictly non-linear phenomena will not be obtained in this way. The linearized analysis is, however, interesting not only from an analytical point of view but also can give important insight into the role of the non-linear and convective terms as well as the various wave and non-wave aspects of the problem.

The Viscous Acoustic Equation

We linearize the Navier-Stokes equations and combine them into a single equation for the velocity potential ϕ (see Appendix D for details) which is written as

$$\gamma\nabla^4\phi_t - \frac{1+\frac{4}{3}Pr}{\tilde{\mu}/\rho_{22}}\nabla^2\left[\phi_{tt} - \frac{a_o^2\nabla^2\phi}{\gamma+\frac{4}{3}Pr}\right] + \frac{\frac{4}{3}Pr}{(\tilde{\mu}/\rho_{22})^2}\left[\phi_{tt} - a_o^2\nabla^2\phi\right]_t = 0 \qquad (6.1)$$

where $Pr = C_p\mu/K$ is a Prandtl number

$\tilde{\mu} = \frac{4}{3}\mu$ is an effective viscosity coefficient

C_p is the specific heat at constant pressure

γ is the ratio of specific heats.

a_o is the isentropic speed of sound and

K the conductivity.

Both μ and K are considered the ambient values. Equation (6.1) is called the viscous acoustic equation. It is a linearized fifth-order

partial differential equation which is fourth-order in space derivatives and third-order in time derivatives.

The general features of the solution can be deduced directly from Equation (6.1) and verified by obtaining an explicit solution. Initially the motion is diffuse since for short times the highest order term dominates. Next a wave which travels at the speed $[a_o^2/(\gamma+\frac{4}{3}\,\mathrm{Pr})]^{\frac{1}{2}}$ tends to form as shown by the second term in Equation (6.1). This wave decays and the wave from the third term forms which propagates at the isentropic speed of sound. The isentropic wave decays as a result of the distribution of the energy of the disturbance over a larger spherical area as the perturbation propagates outward.

Equation (6.1) can be non-dimensionalized and rearranged to give a simpler expression. Owing to spherical symmetry the mean notion is in the radial direction so that independent variables of interest are r the radius and t the time. Their non-dimensional form is given by:

$$\tilde{t} = a_o^2 \rho_{22} t/\tilde{\mu} \quad \text{and} \quad \tilde{r} = a_o \rho_{22} r/\tilde{\mu} \ . \tag{6.2}$$

To simplify the problem we assume that Pr = 3/4 in Equation (6.1). The problem can be solved for an arbitrary Prandtl number but inversion of the Laplace transform would be greatly complicated. It has been founded by Bienkowski (1965) that the one-dimensional expansion solution is only weakly dependent on the Prandtl number and by assuming a value of 3/4 there is little loss in generality. This will be assumed true for the spherical problem as well. We have shown in Chapter III that the Prandtl number for Case 1 is 5/6. This is the same value

obtained by Yates and Karamcheti (1967) for their one-dimensional expansion problem. Also the assumed value does not vary significantly from the equilibrium value of 2/3.

The non-dimensional form of Equation (6.1) with Pr = 3/4 is given by:

$$\gamma\tilde{\nabla}^4\underset{\sim}{\phi}_t - (1+\gamma)\nabla^2\underset{\sim\sim}{\phi}_{tt} + \underset{\sim\sim\sim}{\phi}_{ttt} - \tilde{\nabla}^2\underset{\sim}{\phi}_t + \tilde{\nabla}^4\phi = 0 \ . \qquad (6.3)$$

The initial conditions for this equation of motion are given by:

$$\rho'(r,0) = \delta H(a-r)$$

$$u'(r,0) = 0$$

and

$$T'(r,0) = 0$$

where

$$\rho(r,t) = \rho_{22}(1+\rho')$$

$$u(r,t) = a_0 u' \text{ is the radial velocity}$$

$$T(r,t) = T_{22}(1+T')$$

and

$$\delta = (1-\Delta)/\Delta << 1$$

with the primed quantities much less than one. The boundary conditions are:

$$\text{for } r \to \infty : \ \rho' = T' = u' = 0$$

and

$$\text{for } r \to 0 : \ u' = 0 \text{ and } \rho', T' \text{ are finite, and at}$$

$r = a$ the continuity of u', ρ', T', and T'_r must be satisfied.

The Laplace Transform Solution

The solution to Equation (6.3) can be obtained by means of Laplace transforms. Those characteristics which suggest that it is worthwhile to try the Laplace transform technique are as follows: (1) the differential Equation (6.3) is linear, (2) at least one variable

(t) has the range zero to infinity and (3) there are appropriate initial conditions involving the variable in (2).

We let the Laplace transform be defined by

$$L\{\phi(\tilde{r},\tilde{t})\} = \bar{\phi}(\tilde{r},s) = \int_0^\infty e^{-s\tilde{t}}\phi(\tilde{r},\tilde{t})d\tilde{t}$$

in which $\tilde{r}$ is treated as a constant parameter in so far as the Laplace transform is concerned. The Laplace variable under the transform is s. We shall assume that the operations of differentiation with respect to r and Laplace transforms with respect to t are commutative.

The initial conditions derived in Appendix D, are written as:

$$\begin{aligned} \phi(r,0) &= 0 \\ \phi_t(r,0) &= -(\delta/\gamma)H(a-r) \\ \phi_{tt}(r,0) &= 0 \ . \end{aligned} \tag{6.4}$$

Applying standard Laplace transform techniques to Equation (6.3) and using the initial conditions given by Equation (6.4) we obtain the Laplace transform equation:

$$(\gamma s+1)\nabla^4\bar{\phi} - [(\gamma+1)s^2+s]\nabla^2\bar{\phi} + s^3\bar{\phi} = -s(\delta/\gamma)H(a-r) \tag{6.5}$$

with boundary conditions

$$\text{for } r \to \infty : \quad \bar{\phi}(r,s) = 0$$

$$\text{for } r \to 0 : \quad \bar{\phi}(r,s) = 0$$

and at r = a, $\bar{\phi}$ and its first three derivatives with respect to r are continuous functions. In Equation (6.5) and henceforth the tildas have been dropped.

The solution to Equation (6.5) has the form $\bar{\phi} = \bar{w}/r$. Substituting this relation into Equation (6.5) and evaluating the resulting fourth-order, linear differential equation we obtain

$$\bar{w} = \begin{cases} A_1 \sinh\lambda_1 r + B_1 \sinh\lambda_2 r - \dfrac{\delta r}{\gamma s^2}, & r < a \\ A_2 e^{-\lambda_1 r} + B_2 e^{-\lambda_2 r} & r > a \end{cases} \tag{6.6}$$

where $\lambda_1 = s^{\frac{1}{2}}$, $\lambda_2 = s/(\gamma s+1)^{\frac{1}{2}}$ and the coefficients $A_{1,2}$ and $B_{1,2}$ are unknown functions of s.

In order to solve for the unknown coefficients $A_{1,2}$ and $B_{1,2}$ the velocity, density, pressure and temperature relations are first found from:

$$\bar{u}' = \bar{\phi}_r , \tag{6.7}$$

$$\bar{\rho}' = \frac{1}{s} [\delta H(a-r) - \bar{w}_{rr}/r] \tag{6.8}$$

$$\bar{p}' = \frac{\gamma}{r} (-s\bar{w} + \bar{w}_{rr}) , \tag{6.9}$$

and

$$\bar{T}' = \bar{p}' - \bar{\rho}' , \tag{6.10}$$

perturbation flow quantities derived in Appendix D. The coefficients are then found by solving simultaneously the continuity relations at $r = a$ for $\bar{u}'$, ρ', $\bar{T}'$ and $\bar{T}'_r$.

The general transform solutions are:

$$\bar{u}' = \begin{cases} \dfrac{A_1\lambda_1 \cosh\lambda_1 r + B_1\lambda_2 \cosh\lambda_2 r}{r} - \dfrac{A_1 \sinh\lambda_1 r + B_1 \sinh\lambda_2 r}{r^2}, & r < a \\ -\dfrac{A_2\lambda_1 e^{-\lambda_1 r} + B_2\lambda_2 e^{-\lambda_2 r}}{r} - \dfrac{A_2 e^{-\lambda_1 r} + B_2 e^{-\lambda_2 r}}{r^2}, & r > a \end{cases} \tag{6.11}$$

$$\bar{\rho}' = \begin{cases} \frac{1}{s}\left[\delta - \frac{\lambda_1^2 A_1 \sinh\lambda_1 r + \lambda_2^2 B_1 \sinh\lambda_2 r}{r}\right], & r < a \\ -\frac{1}{s}\frac{\lambda_1^2 A_2 e^{-\lambda_1 r} + \lambda_2^2 B_2 e^{-\lambda_2 r}}{r}, & r > a \end{cases} \tag{6.12}$$

and

$$\bar{T}' = \begin{cases} \frac{A_1 \sinh\lambda_1 r - B_1\lambda_1^2(\gamma-1)\sinh\lambda_2 r}{r}, & r < a \\ \frac{A_2 e^{-\lambda_1 r} - B_2\lambda_1^2(\gamma-1)e^{-\lambda_2 r}}{r}, & r > a. \end{cases} \tag{6.13}$$

The pressure $\bar{p}'$ follows from Equation (6.10).

The expressions for $A_{1,2}$ and $B_{1,2}$ are:

$$A_1 = \frac{\delta(\gamma-1)\lambda_1(\lambda_1 a+1)}{\lambda_1 K(s)} e^{-\lambda_1 a} \tag{6.14}$$

$$B_1 = \frac{\delta(\lambda_2 a+1)}{\lambda_2 K(s)} e^{-\lambda_2 a} \tag{6.15}$$

$$A_2 = \frac{\delta\lambda_1(\gamma-1)}{2K(s)} [(\lambda_1 a-1)e^{\lambda_1 a}+(\lambda_1 a+1)e^{-\lambda_1 a}] \tag{6.16}$$

and

$$B_2 = -\frac{\delta}{2\lambda_2 K(s)} [(\lambda_2 a-1)e^{\lambda_2 a}+(\lambda_2 a+1)e^{-\lambda_2 a}] \tag{6.17}$$

where

$$K(s) = \lambda_2^2 + \lambda_1^4(\gamma-1) .$$

These transform solutions are complicated functions of s and the inversions cannot be done exactly. Analytical solutions for Equations (6.11) through (6.13) can be obtained by considering two limiting cases, long times ($s \to 0$) and short times ($s \to \infty$), (see Carslaw

and Jaeger (1963) for the mathematical notions involved). The short-time solutions have been obtained in this research work. Long-time solutions for T' and ρ' have been obtained by Professor M. L. Rasmussen and plotted from numerical results obtained by K. Frair on the IBM 1130 computer. These results are included in this chapter for completeness of discussion.

Analytical Short-Time Solutions

The short-time solutions are obtained by considering s large and expanding the terms of the transformed flow quantities in an asymptotic expansion of 1/s and keeping sufficient terms in order to satisfy the appropriate initial and boundary conditions of Equation (6.3). The velocity and density are determined by the A_1 coefficient for $r < a$, keeping terms to order $\frac{1}{s^{3/2}}(\lambda_1 a+1)$, and the A_2 coefficient for $r > a$ to order $\frac{1}{s^{3/2}}(\lambda_1 a\pm 1)$. To determine the temperature both the A_1 and B_1 coefficients for $r < a$ are needed, keeping terms to order $\frac{1}{s^{3/2}}(\lambda_1 a+1)$ and $\frac{1}{s^{3/2}}(\lambda_1 a+\gamma^{\frac{1}{2}})$, and for $r > a$ the A_2 and B_2 coefficients are needed, keeping terms of order $\frac{1}{s^{3/2}}(\lambda_1 a\pm 1)$ and $\frac{1}{s^{3/2}}(\lambda_1 a\pm\gamma^{\frac{1}{2}})$. The short-time results are found to be:

$$u' = \frac{\delta}{2\pi^{\frac{1}{2}}}\left\{\frac{a}{rt^{\frac{1}{2}}}\left[\exp(-R_1^2)-\exp(-R_2^2)\right]-\frac{2t^{\frac{1}{2}}}{r^2}\left[\exp(-R_1^2)-\exp(-R_2^2)\right]\right\} \quad (6.18)$$

$$\rho' = \frac{\delta}{2}\left\{\operatorname{erf}R_1 + \operatorname{erf}R_2 - \frac{2t^{\frac{1}{2}}}{r\pi^{\frac{1}{2}}}\left[\exp(-R_1^2)-\exp(-R_2^2)\right]\right\} \quad (6.19)$$

and

$$T' = -\frac{\delta}{2}\left\{\operatorname{erf}R_1 + \operatorname{erf}R_2 - \operatorname{erf}R_3 - \operatorname{erf}R_4 - \frac{2t^{\frac{1}{2}}}{r\pi^{\frac{1}{2}}}\left[\exp(-R_1^2)\right.\right.$$

$$\left.\left.-\exp(-R_2^2)-\gamma^{\frac{1}{2}}\left(\exp(-R_3^2)-\exp(-R_4^2)\right)\right]\right\} \quad (6.20)$$

where $R_1 = \frac{\tilde{a}-\tilde{r}}{2\tilde{t}^{\frac{1}{2}}}$, $R_2 = \frac{\tilde{a}+\tilde{r}}{2\tilde{t}^{\frac{1}{2}}}$, $R_3 = \frac{\tilde{a}-\tilde{r}}{2(\gamma\tilde{t})^{\frac{1}{2}}}$, and $R_4 = \frac{\tilde{a}-\tilde{r}}{2(\gamma\tilde{t})^{\frac{1}{2}}}$, and where t and r are the non-dimensional variables given by Equation (6.2).

The profiles of the flow quantities are given in Figs. 6-1 through 6-3 for $4\tilde{t}/\tilde{a}^2$, a non-dimensional time factor, equal to 0.01, 0.1, and 0.5. The profiles reflect the diffuse nature of the short-time solutions given by the highest order term of Equation (6.1) as discussed above. The qualitative form of the profiles compares with the diffuse results obtained in Chapters III and IV for Case 1 free-molecule explosions. A noticeable difference, however, exists between the analytical expressions obtained by free-molecule kinetic theory and the above short-time, viscous-acoustic results. The free-molecule solutions are functions of t in the form r/t whereas the short-time linearized solutions obtained herein are functions of $t^{\frac{1}{2}}$ in the form $r/t^{\frac{1}{2}}$. A comparison of applicable time scales is necessary to understand which of these two short-time solutions are valid.

In this chapter we assumed the governing characteristic length to be $L = \beta^{-\frac{1}{2}}t$. We then can write the Knudsen-number as

$$Kn = \frac{\lambda}{\beta^{-\frac{1}{2}}t} \quad . \tag{6.21}$$

The mean free path λ can be expressed as a function of initial sphere radius and a Reynolds number [see Vincenti and Kruger (1965)] or

$$\lambda = \left(\frac{2\pi}{\gamma}\right)^{\frac{1}{2}} \frac{a}{Rey} \quad . \tag{6.22}$$

For the large Knudsen number limit in Chapter III we defined a non-dimensional time $\tau = t/a\beta^{\frac{1}{2}}$ and for the small Knudsen number limit (the

inviscid acoustic solution) we defined the non-dimensional time as $\tau_c = ta_o/a$. In terms of the time factors and Reynolds number Equation (6.21) is written as

$$Kn = \frac{\pi^{\frac{1}{2}}}{Rey\,\tau_c} \to 0 \tag{6.23}$$

for the continuum limit and

$$Kn = \left(\frac{2\pi}{\gamma}\right)^{\frac{1}{2}} \frac{1}{Rey\tau} \to \infty \tag{6.24}$$

for the free-molecule limit.

The time scale appropriate for a valid application of the linearized Navier-Stokes solution is thus found to be

$$\tau_c >> \frac{\pi^{\frac{1}{2}}}{Rey} \quad . \tag{6.25}$$

The appropriate time scale for the validity of the free-molecule results is

$$\tau << \left(\frac{2\pi}{\gamma}\right)^{\frac{1}{2}} \frac{1}{Rey} \quad . \tag{6.26}$$

The Navier-Stokes equations are valid only after collisions become dominate. Thus the short-time diffusion solutions to the viscous-acoustic equation are of questionable value. The fact, however, that the short-time solutions obtained are diffusion solutions which compare qualitatively with the free-molecule results is of interest in understanding the development of the outward propagating shock wave as discussed in Chapter IV.

It is also of interest to note that the velocity function given by Fig. 6-2 is not normalized with the isentropic speed of sound but instead by an effective speed $\tilde{u}/\rho_{22}a$.

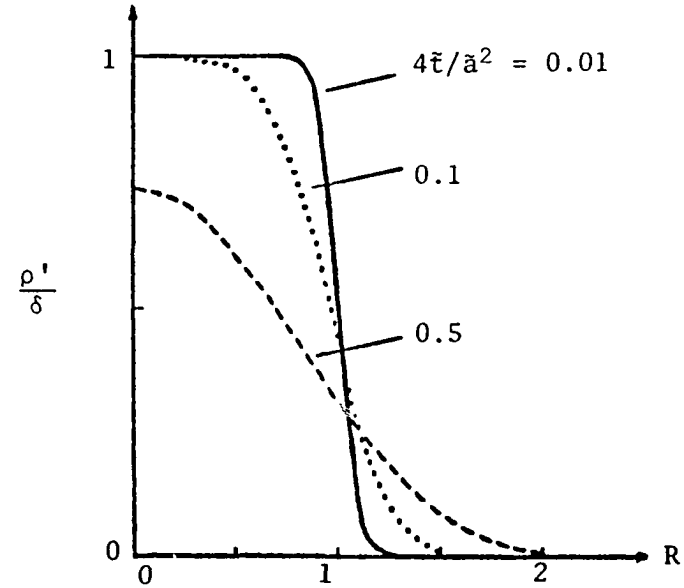


Fig. 6-1. Short-Time Density Profiles.

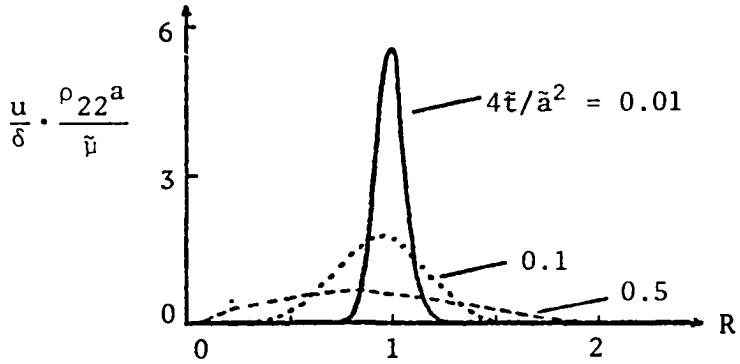


Fig. 6-2. Short-Time Velocity Profiles.

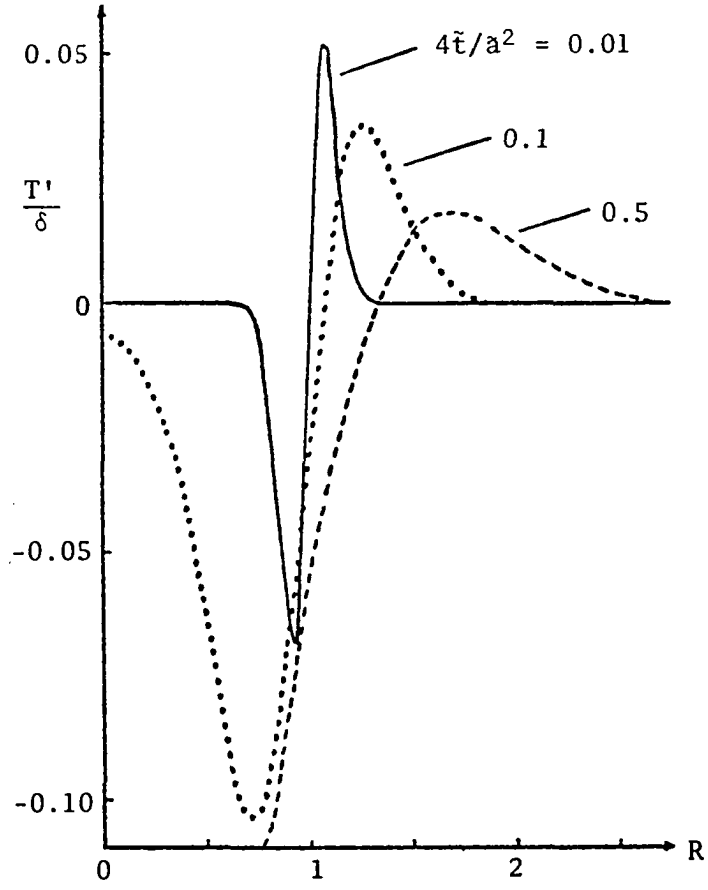


Fig. 6-3. Short-Time Temperature Profiles.

The Long Time Solution

The long time solutions for the temperature and density are shown in Figs. 6-4 and 6-5. These are wave-like solutions which correspond to the third term in Equation (6.1), the long-time wave solution. Actually the name given to this solution is a misnomer in that these solutions are valid for $\tilde{t} \to \infty$. The non-dimensional time given by Equation (6.2) can be recast as a product of a Reynolds number, $\text{Rey} = a_o \rho_{22} a/\tilde{\mu}$, and the non-dimensional time defined for the inviscid acoustic approximation in Chapter IV, $\tau_c = a_o t/a$, that is, $\tilde{t} = \text{Rey}\ \tau_c$ Thus for an arbitrary τ_c we can study the effects of $t \to \infty$ by letting the Reynolds number become large.

It is shown in Figs. 6-4 and 6-5 that for $\tau_c = 1.5$ and for increasing Reynolds number, or decreasing viscosity, the viscous acoustic long-time solution approaches the inviscid acoustic solution of Chapter IV. An observed difference in the viscous and inviscid acoustic solutions is that the inviscid solution has weak discontinuities at the wave fronts whereas the viscous result is a continuous function. The inclusion of the viscous terms cause the discontinuities to spread out yet still reflect the location of the wave fronts.

From Fig. 4-6 we can see that there is a secondary shock that propagates towards the origin behind the inward propagating expansion wave. After this secondary shock wave is reflected from the origin there are then two outward propagating shock waves. The linearized version of the reflected secondary shock is included in the viscous-acoustic long-time solution. As it propagates outward a residual temper-

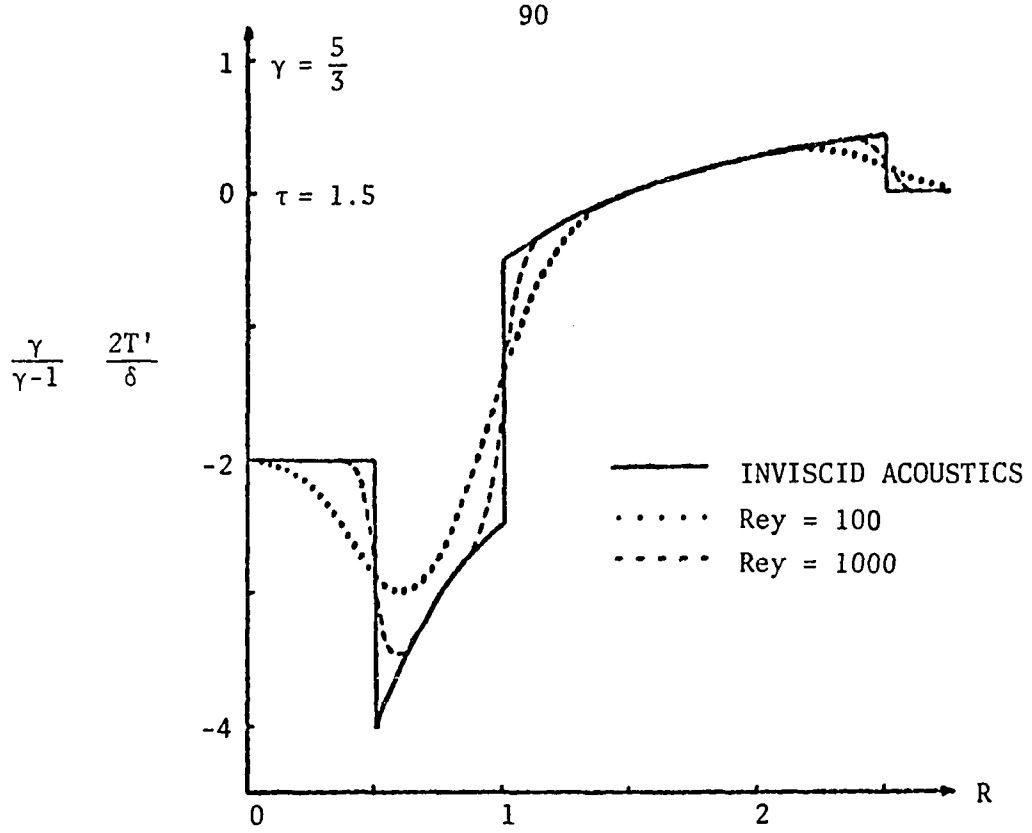


Fig. 6-4. Long-Time Viscous Acoustic Temperature Profiles for Varying Reynolds Number.

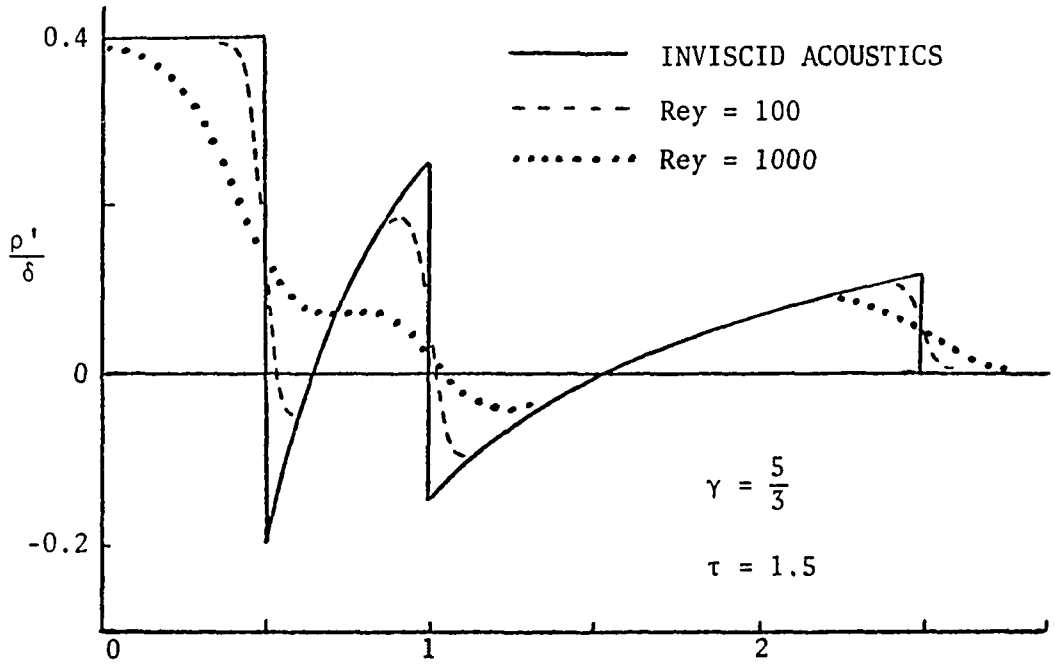


Fig. 6-5. Long-Time Viscous Acoustic Density Profiles for Varying Reynolds Number.

ature and density remain behind for $R \leq 1$. The residual temperature and density are a result of the initial entropy discontinuity given by Equation (4.8) not being dissipated by the neglected non-linear terms. These residual effect are reflected in the temperature and density profiles of Figs. 6-4 and 6-5. (For very large values of τ_c, on the order of the Reynolds number, this would not be true since the error function in the mathematical solution would then become important and affect the dissipation of this residual effect. That is the heat-flux terms of the linearized Navier-Stokes equations come into play.)

Another phenomenon that shows up in the linearized viscous solution which would not be present in the exact solution is the location of the contact surface at $R = 1$ for all times (less than times of the order of the Reynolds number). A solution that would include the non-linear terms would include a contact surface that would propagate outward from $R = 1$ as reflected in Fig. 4-6.

CHAPTER VII

CONCLUDING REMARKS

A comprehensive study has been presented on the propagation of an initial spherical uniform density discontinuity into a rarefied medium. Two limiting cases have been analyzed by means of two different theories of gas dynamics, the large Knudsen-number limit of kinetic theory and the small Knudsen-number limit of continuum theory.

Chapter II included a theoretical development of the expansion problem from the kinetic theory point of view. In Chapter III further knowledge of 2-species kinetic theory was obtained by considering three special cases: Case 1 assumed that the gas molecules initially inside and outside the sphere had the same mass and same temperature; Case 2 assumed that the gas initially inside the sphere was hydrogen and the gas outside the sphere was air, various initial temperature ratios were considered; Case 3 assumed a dissociated gas inside the sphere and a gas outside in its undissociated state. The effects of the transport properties for free-molecule expansions were discussed and the related transport coefficients were found. Case 1 was considered further in Chapter IV for large compression ratio explosions and implosions. A description of the embryonic formation of a spherical shock wave was presented. Also for large Knudsen numbers a solution of the Boltzmann equation was formulated in Chapter V in order to obtain first-order collision effects.

For the limit of small Knudsen numbers the spherical expansion problem was examined in Chapter VI by obtaining long-time and short-time viscous acoustic solutions from the linearization of the Navier-Stokes equations about a uniform ambient medium. The solutions were obtained by applying Laplace transform techniques.

The combined effect of the solutions presented in Chapters IV and VI give us a phenomenological description of the propagation of an initial spherical density discontinuity. For small times, prior to collisions, the free-molecule, diffusion solutions describe the embryonic formation of the outward propagating shock wave when $\rho_{11}>\rho_{22}$. The viscous-acoustic, long-time solutions gives insight into the wave solution after the shock has formed. The completion of the solution formulated in Chapter V for first-order collision effects would fill the gap between the short-time and long-time solutions presented. This first-order collision solution should also provide a description of the development of the secondary shock.

This spherical expansion problem has other interesting areas which remain to be studied. The work presented covers only a part of the full range of Knudsen-number regime, namely the two end limits. Further work should include the intermediate range of Knudsen numbers.

One approach would be to examine the problem by means of the 13-moment equations. This could be done by means of an exact solution or by linearizing the equations and obtaining an expression akin to that obtained in Chapter VI in terms of a velocity potential.

A solution could be sought by linearizing the Boltzmann equation or some other model of the collisional kinetic equation. This

would provide a description valid throughout the full range of Knudsen numbers.

REFERENCES

Bienkowski, G. "Propagation of an Initial Density Discontinuity," in *Advances in Applied Mechanics, Rarefied Gas Dynamics, Vol. 1,* edited by J. H. De Leeuw. New York: Academic Press, 1965.

Boltzmann, L. *Lectures on Gas Theory.* Translated by S. G. Brush. Berkley: University of California Press, 1964.

Burgers, J. M. *Flow Equations for Composite Gases.* Applied Mathematics and Mechanics, Vol. 11. New York: Academic Press, 1969.

Carslaw, H. S. and Jaeger, J. C. *Operational Methods in Applied Mathematics.* New York: Dover, 1963.

Freeman, N. C. "Solution of the Boltzmann Equation for Expanding Flows." *AIAA Journal,* 5 (Sept., 1969), 1696.

Friedman, M. P. "A Simplified Analysis of Spherical and Cylindrical Blast Waves." *Journal of Fluid Mechanics,* 11 (Aug., 1961), 1.

Keller, J. B. "Spherical, Cylindrical, and One-Dimensional Gas Flows." *Quarterly of Applied Mathematics,* 14 (July, 1956), 171.

Kogan, M. N. *Rarefied Gas Dynamics.* Translating Editor L. Trilling. New York: Plenum Press, 1969.

Krook, M. "Continuum Equations in the Dynamics of Rarefied Gases." *AIAA Journal,* 6 (Nov., 1959), 523.

Lamb, H. *The Dynamical Theory of Sound.* London: Arnold, 1910.

Landau, L. D. and Lifshitz, E. M. *Fluid Mechanics.* The Addison-Wesley Series in Advanced Physics, Vol. 6. London: Pergamon Press, 1959.

Liboff, R. L. *Introduction to the Theory of Kinetic Equations.* New York: Wiley, 1969.

Lick, W. "Wave Propagation in Real Gases," in *Advances in Applied Mechanics, Vol. 10* edited by G. Kuerti. New York: Academic Press, 1967.

Molmud, P. "Expansion of a Rarefied Gas Cloud into a Vacuum." *Physics of Fluids,* 3 (May, 1960), 362.

Narashima, R. "Collisionless Expansion of Gases into a Vacuum." *Journal of Fluid Mechanics*, 12 (Feb., 1962), 294.

Rasmussen, M. L. and Lake, J. G. "Viscous Acoustics and the Effects of Viscosity on Weak Explosions." Paper presented at Aerospace, Mechanical and Nuclear Engineering Department Seminar, University of Oklahoma, Norman, Oklahoma., Feb. 17, 1972.

Rayleigh, Lord. *Theory of Sound, Vol. II.* 2nd ed., London: MacMillan, 1896.

Sedov, L. I. *Similarity and Dimensional Methods in Mechanics.* Translating Editor M. Holt. New York: Academic Press, 1959.

Stanyukovich, K. P. *Unsteady Motion of Continuous Media.* London: Pergamon Press, 1960.

Truesdell, C. *Rational Thermodynamics.* New York: McGraw Hill, 1969.

Vincenti, W. G. and Kruger, C. H. Jr. *Introduction to Physical Gas Dynamics.* New York: Wiley, 1965.

Yates, J. E. and Karamcheti, K. *On the Kinetic Problem of Shock Tube Flow,* Stanford University Report No. 306, March 1967. Stanford, Calif.: Stanford University, 1967.

OTHER SOURCES

Cercignani, C. *Mathematical Methods in Kinetic Theory.* New York: Plenum Press, 1969.

Chapman, S. and Cowling, T. G. *The Mathematical Theory of Non-Uniform Gases.* 3rd ed. Cambridge: University Press, 1970.

Grad, H. "On the Kinetic Theory of Rarefied Gases." *Communications in Pure and Applied Mathematics,* 2 (Dec., 1949), 331.

Grundy, R. E. and Thomas, D. R. "Unsteady Spherically Symmetric Expansion of a Fixed Mass of Gas into a Vacuum." *AIAA Journal,* 7 (May, 1969), 967.

Hirschfelder, J. O., Curtiss, C. F., and Bird, R. B. *Molecular Theory of Gases and Liquids.* New York: Wiley, 1954.

Jeans, J. H. *The Dynamical Theory of Gases.* 4th ed. New York: Dover Publications, Inc., 1954.

Keller, J. B. "On the Solution of the Boltzmann Equation for Rarefied Gases." *Communication of Applied Mathematics,* 1 (Sept., 1948), 275.

Kreyszig, E. *Advanced Engineering Mathematics*. New York: Wiley, 1962.

Lake, J. G. "On the Propagation of a Spherical Density Discontinuity." *2nd Southwestern Graduate Research Conference in Applied Mechanics*, University of Houston, 1971, F.4/148.

Liepmann, H. W. and Roshko, A. *Element of Gasdynamics*. New York: Wiley, 1957.

Rainville, E. D. *The Laplace Transform*. New York: MacMillan, 1963.

Zel'davich, Ya. B. and Raizer, Uy. P. *Physics of Shock Waves and High Temperature Hydrodynamic Phenomena, Vol. I*. New York: Academic Press, 1966.

APPENDIX A

BASIC INTEGRAL RELATIONS

The two basic integral relations that must be evaluated in order to find the macroscopic flow field properties by means of Equation (2.3) are

$$I_m = \int_o^Y \xi^m [e^{-\beta(\frac{r}{t}-\xi)^2} - e^{-\beta(\frac{r}{t}+\xi)^2}] d\xi \qquad (A.1)$$

and

$$I_n = \int_o^Y \xi^n [e^{-\beta(\frac{r}{t}-\xi)^2} + e^{-\beta(\frac{r}{t}+\xi)^2}] d\xi \qquad (A.2)$$

where m = 1,2; n = 2,4 and Y is some upper limit. The first step is to transform Equations (A.1) and (A.2) by substituting the relation

$$x = \beta^{\frac{1}{2}}(\frac{r}{t} \pm \xi) \ .$$

We obtain a series of moment integrals of the form

$$J_n = \int_A^B x^n e^{-x^2} dx \qquad (A.3)$$

where n = 0,1,2,3; A = R/τ and B = (R±1)/τ. The first four moments of Equation (A.3) are of interest for this work. Their evaluation gives

$$J_o = \frac{\pi^{\frac{1}{2}}}{2} [\text{erfB-erfA}] \qquad (A.4)$$

$$J_1 = \tfrac{1}{2}[e^{-A^2} - e^{-B^2}] \qquad (A.5)$$

$$J_2 = \tfrac{1}{2}[Ae^{-A^2} - Be^{-B^2}] + \frac{\pi^{\frac{1}{2}}}{2}\,[\mathrm{erf}B - \mathrm{erf}A] \tag{A.6}$$

and

$$J_3 = \tfrac{1}{2}[(A^2+1)E^{-A^2} - (B^2+1)e^{-B^2}] \ . \tag{A.7}$$

The basic integral relations of (A.1) and (A.2) can then be evaluated to give: for $Y = a/\tau$:

$$I_1 = \frac{1}{2\beta}[e^{-R_1^2} - e^{-R_2^2}] + \frac{\pi^{\frac{1}{2}}R}{2\beta\tau}\,[\mathrm{erf}R_1 + \mathrm{erf}R_2] \ , \tag{A.8}$$

$$I_2 = -\frac{1}{2\beta^{3/2}}[R_2 e^{-R_1^2} + R_1 e^{-R_2^2}] + \frac{\pi^{\frac{1}{2}}}{2\beta^{3/2}}\,[\tfrac{1}{2} + \frac{R^2}{\tau^2}]\,[\mathrm{erf}R_1 + \mathrm{erf}R_2], \tag{A.9}$$

$$I_3 = \frac{1}{2\beta}\,[\frac{1}{\tau^2}\,(1-R+R^2+\tau^2)e^{-R_1^2} - \frac{1}{\tau^2}\,(1+R+R^2+\tau^2)e^{-R_2^2}$$

$$+ \frac{\pi^{\frac{1}{2}}}{\tau^3}\,(\frac{3}{2}\,R\tau^2 + R^3)\,(\mathrm{erf}R_1 + \mathrm{erf}R_2)] \ , \tag{A.10}$$

and

$$I_4 = \frac{1}{2\beta^{5/2}}\,[\frac{1}{\tau^3}\,(-1+R-R^2+R^3 - \frac{3}{2}\,\tau^2 + \frac{5}{2}\,R\tau^2)e^{-R_1^2}$$

$$- \frac{1}{\tau^3}(1+R+R^2+R^3 + \frac{3}{2}\,\tau^2 + \frac{5}{2}\,R\tau^2)e^{-R_2^2}$$

$$+ \frac{\pi^{\frac{1}{2}}}{\tau^4}\,(\frac{3}{4}\,\tau^4 + 3R^2\tau^2 + R^4)\,(\mathrm{erf}R_1 + \mathrm{erf}R_2)] \tag{A.11}$$

where $R_1 = (1+R)/\tau$ and $R_2 = (1-R)/\tau$;

for $Y = \infty$:

$$I_1 = \frac{\pi^{\frac{1}{2}}}{\beta}\,\frac{R}{\tau} \tag{A.12}$$

$$I_2 = \frac{\pi^{\frac{1}{2}}}{\beta^{3/2}}\,(\tfrac{1}{2} + \frac{R^2}{\tau^2}) \tag{A.13}$$

$$I_3 = \frac{\pi^{\frac{1}{2}}}{\beta^2}\,\frac{R}{\tau}\,(\tfrac{1}{2} + \frac{R^2}{\tau^2}) \tag{A.14}$$

and

$$I_4 = \frac{\pi^{\frac{1}{2}}}{\beta^{5/2}} \left(\frac{3}{4} + \frac{3R^2}{\tau^2} + \frac{R^4}{\tau^4}\right) . \qquad (A.15)$$

APPENDIX B

ASYMPTOTIC VALUES OF FLOW FIELD PROPERTIES

To more fully understand and appreciate the description of the flow field properties obtained in Chapters III and IV the asymptotic values for both large R and small R must be examined. This is accomplished by considering the asymptotic expansions of the solutions for each limit.

Asymptotic Behavior for Large R

First the asymptotic expansion of the two basic terms which appear throughout the solutions will be found. These are

$$E = e^{-R_1^2} - e^{-R_2^2} \tag{B.1}$$

and

$$F = \text{erf}R_1 + \text{erf}R_2 \tag{B.2}$$

where $R_1 = (1+R)/\tau$ and $R_2 = (1-R)/\tau$. For large R we can write Equation (B.1) as

$$E = -e^{-X^2}(1-e^{-4R/\tau^2}) \sim -e^{-X^2} \tag{B.3}$$

where $X = [(R-1)/\tau] >> 1$ and $[4R/\tau^2] >> 1$. Likewise we can write Equation (B.2) as

$$F = \text{erfc}X - \text{erfc}R_1 \sim \text{erfc}X$$

where

$$\text{erfc}X \sim \frac{e^{-X^2}}{\pi^{\frac{1}{2}}X}\left[1 - \frac{1}{2X^2} + \frac{3}{4X^4} + \ldots\right] . \tag{B.4}$$

By substituting the asymptotic expansion given by Equations (B.3) and (B.4) into the various solutions we obtain the following asymptotic limiting values for Cases 1 and 2 from Chapter III and for the special case of expansion into a vacuum:

Number Density

$$N \sim \begin{cases} \Delta \text{ for Case 1} \\ \Delta \dfrac{m_1}{m_2} \text{ for Case 2 } (\bar{\rho} \sim \Delta) \\ \dfrac{e^{-X^2}}{2\pi^{\frac{1}{2}} X} \left[\dfrac{1}{R} - \dfrac{1}{2X^2} + \dfrac{3}{4X^4} + \cdots\right] \quad \text{for } \Delta = 0; \end{cases} \tag{B.5}$$

Velocity

$$V \sim \begin{cases} 0 \text{ for } \Delta \neq 0 \\ X\left[1 + \dfrac{1}{X^2}\left(1 - \dfrac{1}{2R}\right) + \cdots\right] \quad \text{for } \Delta = 0; \end{cases} \tag{B.6}$$

Temperature

$$\bar{T} \sim \begin{cases} 1 \text{ for Case 1} \\ \dfrac{T_{22}}{T_{11}} \text{ for Case 2} \\ \dfrac{2}{3R} + O\left(\dfrac{1}{X^2}\right) \text{ for } \Delta = 0; \end{cases} \tag{B.7}$$

Stress Components

$$S_{JJ} \sim \begin{cases} -\Delta \quad \text{for Case 1} \\ -\Delta \dfrac{m_1 T_{22}}{m_2 T_{11}} \quad \text{for Case 2} \\ 0 \quad \text{for} \quad \Delta = 0 \end{cases} \tag{B.8}$$

where $J = R,\theta,\psi$;

Heat Flux

$$Q \sim 0 \text{ for all cases.} \tag{B.10}$$

Asymptotic Behavior for Small R

In order to investigate the flow field properties near $R = 0$ we expand the exponential terms as

$$\exp\left(-\frac{(1\pm R)^2}{\tau^2}\right) = e^{-1/\tau^2}\left[1 \pm \frac{2R}{\tau^2} + \left(-\frac{2}{\tau^2}+\frac{4}{\tau^4}\right)\frac{R^2}{2}\right.$$
$$\left.\left(-\frac{12}{\tau^4}+\frac{8}{\tau^6}\right)\frac{R^3}{6} + O(R^4)\right] \tag{B.11}$$

and obtain the asymptotic form of Equation (B.1) as

$$E \sim \begin{cases} -\frac{4R}{\tau^2}\left(1-\frac{1}{\tau^2}\right) & \text{for } \tau \gg 1 \\ -\frac{4R}{\tau^2} e^{-1/\tau^2} & \text{for } \tau > 0 \\ 0 \quad \text{for } \tau \ll 1\ . \end{cases} \tag{B.12}$$

The asymptotic forms of the error function are

$$\operatorname{erf}\left(\frac{(1\pm R)}{\tau}\right) \sim \begin{cases} \frac{2}{\pi^{\frac{1}{2}}}\left(\frac{1}{\tau}-\frac{1}{3\tau^3}\right) & \text{for } \tau \gg 1 \\ \operatorname{erf}(1/\tau) & \text{for } \tau > 0 \\ 2 \quad \text{for } \tau \ll 1\ . \end{cases} \tag{B.13}$$

By substituting the asymptotic expansions given by Equations (B.12) and (B.13) into the solutions from Chapter IV we obtain the following asymptotic values:

Number Density

$$N \sim \begin{cases} \Delta + \dfrac{4(1-\Delta)}{3\pi^{\frac{1}{2}}\tau^3} & \text{for } \tau \gg 1 \\ \Delta - \dfrac{2(1-\Delta)}{\pi^{\frac{1}{2}}\tau} e^{-1/\tau^2} + (1-\Delta)\operatorname{erf}(1/\tau) & \text{for } \tau > 0 \\ 1 & \text{for } \tau \ll 1 \end{cases} \tag{B.14}$$

Velocity

$$V \sim \begin{cases} 0 & \text{for } \tau \gg 1 \\ \dfrac{4(1-\Delta)Re^{-1/\tau^2}}{3\pi^{\frac{1}{2}}N(R\to 0,\tau)\tau^4} & \text{for } \tau > 0 \\ 0 & \text{for } \tau \ll 1 \end{cases} \tag{B.15}$$

Temperature

$$\bar{T} \sim \begin{cases} 1 & \text{for } \tau \gg 1 \\ 1 - \dfrac{4(1-\Delta)e^{-1/\tau^2}}{3\pi^{\frac{1}{2}}N(R\to 0,\tau)\tau^3} & \text{for } \tau > 0 \\ 1 & \text{for } \tau \ll 1 \ . \end{cases} \tag{B.16}$$

A further study of the temperature at R = 0 has been made to determine the time that the minimum temperature occurs at the origin and the minimum temperature itself. These values are shown in Figs. B-1 and B-2 as a function of the initial density ratio. The time that the minimum temperature occurs at R = 0 is found from the derivative of Equation (4.3) with respect to time set equal to zero. The transendental equation obtained is

$$(2-3\tau^2)[\Delta+(1-\Delta)\mathrm{erf}(1/\tau)] + \frac{6\tau(1-\Delta)}{\pi^{\frac{1}{2}}} e^{-1/\tau^2} = 0 \ . \qquad (B.17)$$

We can examine three significant cases, $\Delta = 1$, $\Delta \to 0$ and $\Delta \to \infty$, and obtain from Equation (B-17) the following:

for $\Delta = 1$;

$$2 - 3\tau^2 = 0 \qquad (B.18)$$

for $\Delta \to 0$;

$$(2-3\tau^2)\mathrm{erf}(1/\tau) + \frac{6\tau}{\pi^{\frac{1}{2}}} e^{-1/\tau^2} = 0 \qquad (B.19)$$

and

for $\Delta \to \infty$;

$$(2-3\tau^2)(1-\mathrm{erf}(1/\tau)) - \frac{6\tau}{\pi^{\frac{1}{2}}} e^{-1/\tau^2} = 0 \ . \qquad (B.20)$$

The results of these equations are shown in Figs. B-1 and B-2. There is a discontinuity in Fig. B-2 at $\tau = .816$ for $\Delta = 1$. From Equation (B-16) we find that $\bar{T} = 1$ when $\Delta = 1$ or the temperature is independent of τ when the initial density ratio is equal to unity. We can also observe that as $\Delta \to 0$ the minimum temperature goes asymptotically to zero but it takes an infinite time.

The behavior of the temperature at $R = 0$, as well as for all R, for increasing time, is observed in Fig. B-3. From Fig. B-2 we can obtain the time that the minimum temperature occurs (approximately τ=1.2) and from Fig. B-1 the minimum temperature at the origin (approximately $\bar{T} = .45$) can be obtained.

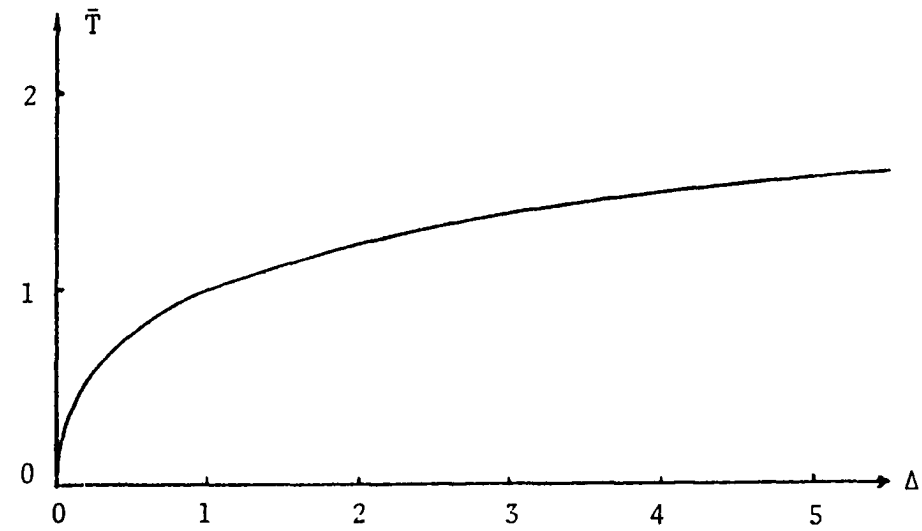


Fig. B-1. Minimum Temperature at R = 0 as a Function of the Initial Density Ratio.

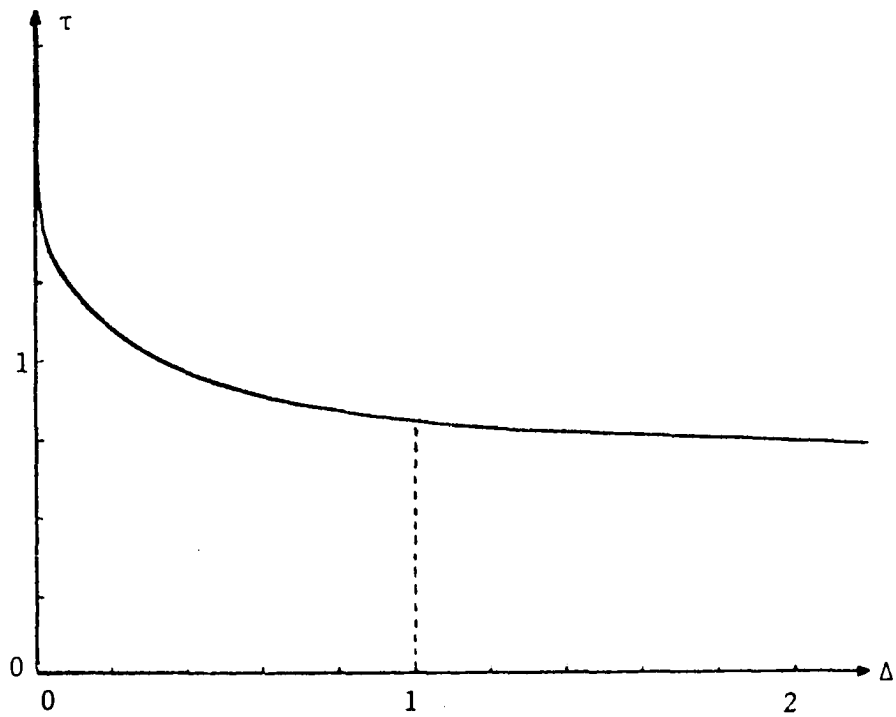


Fig. B-2. The Time for the Minimum Temperature to Occur at R = 0 as a Function of the Initial Density Ratio.

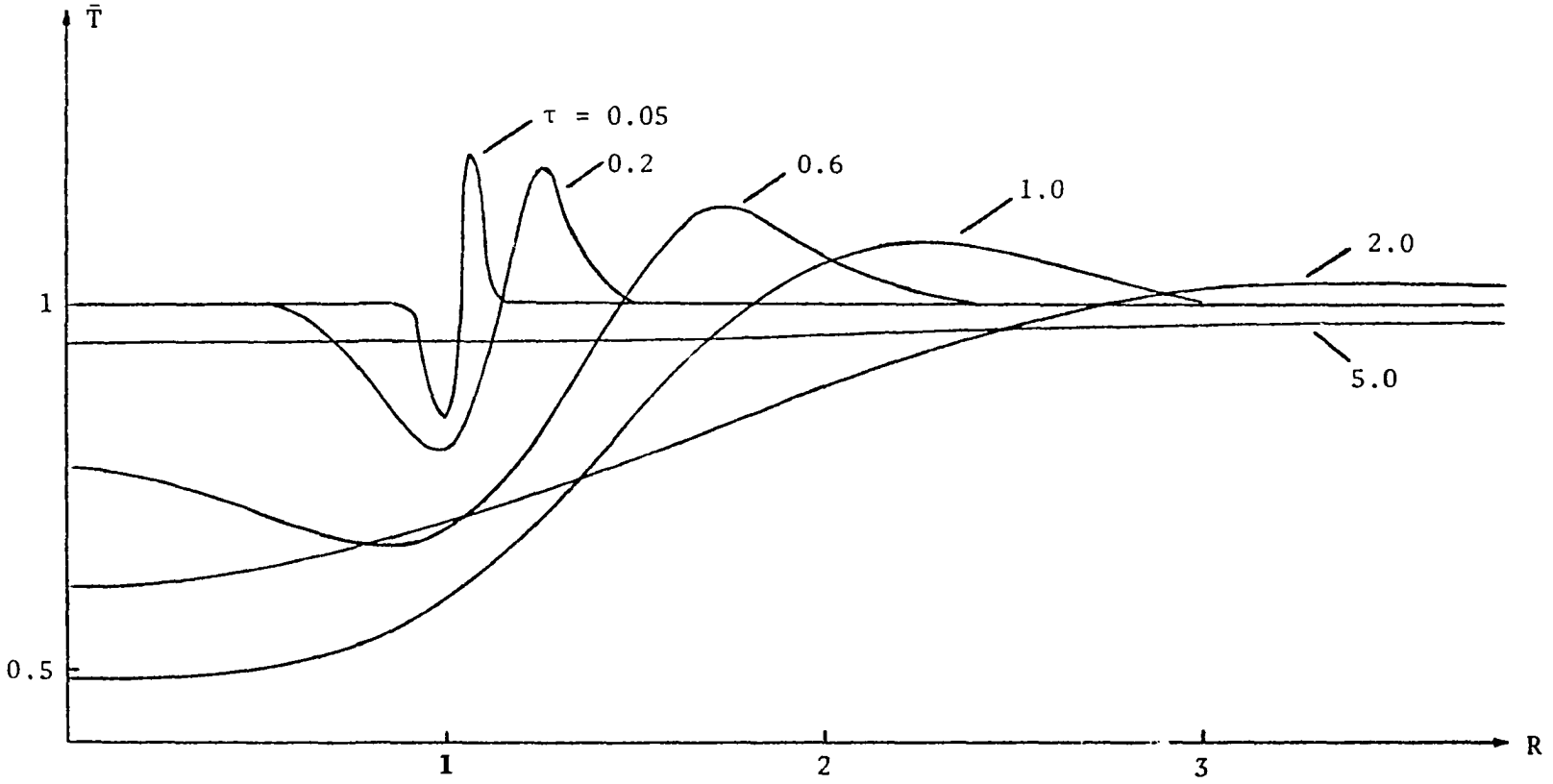


Fig. B-3. Temperature Profiles for Δ = 0.1 and Increasing Time

APPENDIX C

ANALYTICAL EVALUATION OF $(\vec{g}\cdot\vec{e})\vec{e}$

We refer to Figs. 5-1 and 5-2 for the evaluation of the quantity $(\vec{g}\cdot\hat{e})\hat{e}$. From Fig. 5-1 we can write the apse vector $\hat{e}$ as the sum of a parallel component and a perpendicular component with respect to $\vec{g}$. This is expressed as

$$\hat{e} = \vec{e}_{\parallel} + \vec{e}_{\perp}$$

where $\vec{e}_{\parallel}$ has the magnitude $|\vec{e}_{\parallel}| = \sin\frac{\chi}{2}$ and is in the direction $-\vec{g}$, and $\vec{e}_{\perp}$ has the magnitude $|e_{\perp}| = \cos\frac{\chi}{2}$ and is perpendicular to $\vec{g}$ with the unit direction vector given by

$$\hat{e}_{\perp} = - \frac{\vec{L}\times\vec{g}}{|\vec{L}\times\vec{g}|}$$

where $\vec{L}$ is the angular momentum. From the definition of a scalar product we have

$$\vec{g}\cdot\hat{e} = - g\sin\frac{\chi}{2} .$$

Thus we can write

$$(\vec{g}\cdot\hat{e})\hat{e} = - g\sin\frac{\chi}{2}[-\sin\frac{\chi}{2}\frac{\vec{g}}{g} - \cos\frac{\chi}{2}\frac{\vec{L}\times\vec{g}}{|\vec{L}\times\vec{g}|}] . \qquad (C.1)$$

In order to obtain a useable expression for Equation (C.1) we must evaluate $\hat{e}_{\perp}$. We write $\vec{L}$ and $\vec{g}$ in terms of the unit vectors shown in Fig. 5-2 as

$$\vec{L} = L_1\hat{e}_1 + L_2\hat{e}_2 + L_3\hat{e}_3$$

and

$$\vec{g} = g_1\hat{e}_1 + g_2\hat{e}_2 + g_3\hat{e}_3 \ .$$

The components of $\vec{g}$ are known from $\vec{g} = \vec{\xi}_1 - \vec{\xi}$. The components of $\vec{L}$ need to be determined.

From vector calculus we know that the cosine of the angle between two planes can be expressed as a relation of their normal vectors, or

$$\cos\varepsilon = \frac{\vec{L}\cdot(\vec{g}\times\hat{e}_1)}{|\vec{L}||\vec{g}\times\hat{e}_1|} \ . \qquad (C.2)$$

Since $\vec{g}$ lies in the collision plane and since $\vec{L}$ is perpendicular to $\vec{g}$ we have

$$\vec{L}\cdot\vec{g} = 0 \ . \qquad (C.3)$$

From the definition of $\vec{L}$ and knowing that the angular momentum is conserved we can show that

$$|\vec{L}| = L \qquad (C.4)$$

where $L = mgb$.

Equations (C.2) through (C.4) give three equations with which we can find the three unknown components of $\vec{L}$. In scalar form these equations are written as

$$L\cos\varepsilon(g_2^2+g_3^2)^{\frac{1}{2}} = g_3L_2 - g_2L_3 \qquad (C.5)$$

$$L_1g_1 + g_2L_2 + L_3g_3 = 0 \qquad (C.6)$$

and

$$L_1^2 + L_2^2 + L_3^2 = L^2. \qquad (C.7)$$

After solving the scalar equations we find

$$L_1 = \frac{L(g^2-g_1^2)^{\frac{1}{2}}}{g} \sin\varepsilon \tag{C.8}$$

$$L_2 = L\,\frac{gg_3\cos\varepsilon - g_1g_2\sin\varepsilon}{g(g^2-g_1^2)^{\frac{1}{2}}} \tag{C.9}$$

and

$$L_3 = L\,\frac{-gg_2\cos\varepsilon + g_1g_3\sin\varepsilon}{g(g^2-g_1^2)^{\frac{1}{2}}}\,. \tag{C.10}$$

The signs in the above results are chosen to match those of Vincenti and Kruger (1965) obtained by a geometrical analysis.

The unit vector $\hat{e}_\perp$ can then be evaluated to give

$$\hat{e}_\perp = -\frac{\vec{L}\times\vec{g}}{|\vec{L}\times\vec{g}|} = \frac{1}{g(g^2-g_1^2)}(g^2-g_1^2)\cos\varepsilon\hat{e}_1 - (g_1g_2\cos\varepsilon+gg_3\sin\varepsilon)\hat{e}_2$$

$$- (g_1g_2\cos\varepsilon-gg_2\sin\varepsilon)\hat{e}_3. \tag{C.11}$$

The substitution of Equation (C.11) into Equation (C.1) gives the necessary relation to obtain $\vec{\xi}_1'$ and $\vec{\xi}'$ in terms of unprimed variables from Equations (5.17) and (5.18).

The results given by Freeman (1967) for ξ_{1r}' can be obtained by letting $\hat{e}_1 = \hat{e}_r$ and taking the scalar product with Equation (5.18). For this relation to be useful in the integration limit of Equation (5.21) it will still be necessary to express the $\vec{\xi}_1$ components in terms of $\vec{\xi}$ components.

APPENDIX D

DERIVATION OF THE VISCOUS ACOUSTIC RELATIONS

The linearized version of the compressible viscous Navier-Stokes equations are

$$\frac{\partial \rho'}{\partial t} + a_o \mathrm{div}\vec{v}' = 0 \ , \tag{D.1}$$

$$\frac{\partial \vec{v}'}{\partial t} = - \frac{a_o}{\gamma} \nabla p' + \frac{\tilde{\mu}}{\rho_{22}} \nabla(\nabla \cdot \vec{v}') \ , \tag{D.2}$$

$$\frac{\partial s'}{\partial t} = \frac{K}{\rho_{22} C_v} \nabla^2 T' \ , \tag{D.3}$$

$$dp' = d\rho' + dT' \ , \tag{D.4}$$

and

$$dp' = \gamma d\rho' + ds' \tag{D.5}$$

where the primed quantities are given by the relations of (4.15) and the other terms are defined after Equation (6.1).

Owing to the spherical symmetry of the problem which is one-dimensional in r, we have $\mathrm{curl}\vec{v}' = 0$, or the flow is irrotational so that the velocity in Equations (D.1) and (D.2) can be expressed in terms of a velocity potential $\vec{v}' = \nabla\phi$. Substituting $\nabla\phi$ for $\vec{v}'$ we obtain for (D.1) and (D.2)

$$\frac{\partial \rho'}{\partial t} + a_o \nabla^2 \phi = 0 \tag{D.6}$$

and

$$\frac{\partial \phi}{\partial t} + \frac{a_o}{\gamma} p' - \frac{\tilde{\mu}}{\rho_{22}} \nabla^2 \phi = g(t) \tag{D.7}$$

where g(t) results from integrating over r. We let g(t) = 0.

Differentiation of Equation (D.7) gives

$$\phi_{tt} + \frac{a_o}{\gamma} p'_t - \frac{\tilde{\mu}}{\rho_{22}} \nabla^2 \phi_t = 0 \ . \tag{D.8}$$

Then by substituting the time derivative of (D.5) and the relations (D.3) and (D.1) into (D.8) we obtain

$$\nabla^2 T' = \frac{4\rho_{22} Pr}{3\tilde{\mu} a_o} \left[\frac{\tilde{\mu}}{\rho_{22}} \nabla^2 \phi_t + a_o^2 \nabla^2 \phi - \phi_{tt}\right] \ . \tag{D.9}$$

Combining the time derivatives of (D.4) and (D.5) with (D.3) and (D.9), and operating on the results with the operator ∇^2 we obtain

$$\nabla^2 T'_t = \frac{\gamma}{a_o} \nabla^2 \left[\frac{\tilde{\mu}}{\rho_{22}} \nabla^2 \phi_t - \phi_{tt}\right] + a_o \nabla^4 \phi \ . \tag{D.10}$$

We eliminate T' by taking the time derivative of (D.9) and setting the right hand side equal to the right hand side of (D.10). After rearrangement we obtain Equation (D.1), the viscous acoustic equation.

Other relations of interest in Chapter VI are the initial conditions for the Laplace transform of the viscous acoustic equation and the transforms of the flow variables.

We refer to the initial conditions of (6.3) and the conservation equations to find the relations given in (6.4). We assume that initially the potential function is zero. The first time derivative of the potential function is found from Equations (D.4) and (D.7)

From (D.4) we have

$$p'(\tilde{r},0) = \rho'(\tilde{r},0) = \delta H(a-r) \tag{D.11}$$

since initially T' = 0. From the non-dimensional form of (D.7) with g(t) = 0,

$$p' = \gamma[\tilde{\nabla}^2\phi - \phi_{\tilde{t}}] \tag{D.12}$$

which at time zero is

$$p'(\tilde{r},0) = -\gamma\phi_{\tilde{t}}(\tilde{r},0) \ . \tag{D.13}$$

Thus by substitution of (D.11) into (D.13) we obtain (6.4). It immediately follows that $\phi_{\tilde{t}\tilde{t}}(\tilde{r},0) = 0$.

The relations given by (6.7), the Laplace transform of the perturbation quantities, are easily obtained. The radial component of the velocity perturbation follows from the definition of the velocity potential. The density relation (6.8) follows from the Laplace transform of the non-dimentional form of (D.6), or

$$L\{\rho'_t\} = s\bar{\rho}' = -\tilde{\nabla}^2\bar{\phi} + \rho'(\tilde{r},0) \tag{D.14}$$

where $\rho'(\tilde{r},0)$ is given by Equation (6.3). We can write the first term on the right hand side of (D.14) as

$$\tilde{\nabla}^2\bar{\phi} = \frac{1}{\tilde{r}}\,(2\bar{\phi}_{\tilde{r}} + \tilde{r}\bar{\phi}_{\tilde{r}\tilde{r}}) \ .$$

From the definition of $\bar{w} = \tilde{r}\bar{\phi}$ we write the second derivative of $\bar{w}$ as

$$\bar{w}_{\tilde{r}\tilde{r}} = \tilde{r}\bar{\phi}_{\tilde{r}\tilde{r}} + 2\bar{\phi}_{\tilde{r}} \ .$$

Thus we obtain the density relation

$$s\bar{\rho}' = \delta H(a-r) - \frac{\bar{w}_{\tilde{r}\tilde{r}}}{\tilde{r}}$$

The transform temperature (6.10) is obtained from the Laplace transform of the time derivative of (D.4) which gives

$$\bar{T}' = - \bar{\rho}' + \bar{p}' \tag{D.16}$$

where $\bar{p}'$ follows from the Laplace transform of the non-dimensional form of (D.7). The density $\bar{\rho}'$ is given above. From (D.7) we obtain

$$s\bar{\phi} + \frac{1}{\gamma} \bar{p}' - \tilde{\nabla}^2\bar{\phi} = 0$$

or

$$\bar{p}' = \gamma[\frac{\bar{w}_{\tilde{r}\tilde{r}}}{\tilde{r}} - s \frac{\bar{w}}{\tilde{r}}] \ . \tag{D.17}$$